WITTECK DEVELOPMENT INC.

Open File Report 88-18

MINERALOGICAL STUDIES OF MOUNT PLEASANT TUNGSTEN ORE

(Project 5295)

by

J.G. Davison,
Head, Mineralogical Services
Witteck Development Inc.

Canada-New Brunswick Mineral Development Agreement
Entente Canada-Nouveau-Brunswick L'Exploitation Minérale

Natural Resources and Energy New Brunswick
Ressources Naturelles et Énergie Nouveau-Brunswick
Energy, Mines and Resources Canada
Énergie, Mines et Ressources Canada

Price $8.05

88-06221/

This report has been reproduced by:

Minerals and Energy Division
Department of Natural Resources and Energy
New Brunswick

Hon. Morris Green, Minister

1988

MINERALOGICAL STUDIES OF MOUNT PLEASANT TUNGSTEN ORE

(Project 5295)

This project was funded under the Canada-New Brunswick Mineral Development Agreement, a subsidiary agreement under the Economic and Regional Development Agreement.

Copies available by contacting:

Minerals and Energy Division
Department of Natural Resources
and Energy
P. O. Box 6000, Fredericton
New Brunswick E3B 5H1

1988

Report No.: Open File Report
88-18

Author: J.G. Davison, Witteck
Development Inc.

Catalogue No.: ISSN 0712-4562

This report should be referenced in the following manner:

DAVISON, J.G. 1988. A survey of mineral industry attitudes toward mineral exploration and development in New Brunswick and Nova Scotia. New Brunswick Department of Natural Resources and Energy, Minerals and Energy Division, Open File Report 88-18, 147 p.

WITTECK DEVELOPMENT INC.
2640 South Sheridan Way, Mississauga, Ontario, Canada L5J 2M4
Telephone: (416) 823-7381 Telex: 06-982328

MINERALOGICAL STUDIES OF MOUNT PLEASANT TUNGSTEN ORE

Witteck Project No. 5295

for

New Brunswick Dept. of Natural Resources and Energy
Mineral Resources Division
P.O. Box 6000
Fredericton, New Brunswick
E3B 5H1

J.G. Davison
Head, Mineralogical Services

TABLE OF CONTENTS

		Page No.
1.0	INTRODUCTION	1
2.0	PROCEDURES	3
2.1	Sample Preparation	3
2.2	Sample Examination	7
3.0	RESULTS	8
3.1	Mineral Assemblage	8
3.2	Mineral Liberation	37
3.2.1	Gravity Concentrate	37
3.2.2	Flotation Concentrate	39
3.2.3	Ore	60
4.0	DISCUSSION OF MINERAL BENEFICIATION	74
4.1	Copper-Lead-Zinc	81
4.2	Molybdenum-Bismuth	82
4.3	Tungsten	83
4.4	Fluorite	84
4.5	Rare Earths and Yttrium	84
5.0	CONCLUSIONS AND RECOMMENDATIONS	86
APPENDIX I	- Photomicrographs and EDXA Spectral Plots	89

NOTE: Colour photomicrographs are available for viewing at the Minerals and Energy Division office, Fredericton, N.B.

LIST OF TABLES

Table 1 - Microscopy Samples

Table 2 - Microscopy Mounts and Thin Sections

Table 3 - Screen Analyses of Gravity and Flotation Concentrates

Table 4 - Mineral Assemblage

Table 5 - Minerals and Metals

Table 6 - Mineral Liberation Data - MP1,6

Table 7 - Mineral Liberation Data - MP2,7

Table 8 - Mineral Liberation Data - MP3,8

Table 9 - Mineral Liberation Data - MP4,9

Table 10 - Mineral Liberation Data - MP5,10

Table 11 - Mineral Liberation Data - Gravity Concentrate

Table 12 - Mineral Liberation Data - Flotation Concentrate

Table 13 - Mineral Liberation by Screen Fraction and Product Type

Table 14 - Binary Particles - Gravity Concentrate

Table 15 - Binary and Middling Associations - Fluorite

Table 16 - Binary Particles - Flotation Concentrate

Table 17 - Cumulative Liberation Yield Diagram - Gravity Concentrate - Wolframite

Table 18 - Cumulative Liberation Yield Diagaram - Gravity Concentrate - Fluorite

Table 19 - Cumulative Liberation Yield Diagaram - Gravity Concentrate - Arsenopyrite

Table 20 - Cumulative Liberation Yield Diagram - Gravity Concentrate - Bismuth

Table 21 - Cumulative Liberation Yield Diagaram - Gravity Concentrate - Molybdenite

Table 22 - Cumulative Liberation Yield Diagaram - Gravity Concentrate - Sphalerite

LIST OF TABLES (Cont'd)

Table 23 - Cumulative Liberation Yield Diagram - Gravity Concentrate - Galena

Table 24 - Cumulative Liberation Yield Diagaram - Gravity Concentrate - Chalcopyrite

Table 25 - Cumulative Liberation Yield Diagaram - Gravity Concentrate - Pyrite

Table 26 - Cumulative Liberation Yield Diagram - Flotation Concentrate - Wolframite

Table 27 - Cumulative Liberation Yield Diagram - Flotation Concentrate - Fluorite

Table 28 - Cumulative Liberation Yield Diagram - Flotation Concentrate - Arsenopyrite

Table 29 - Cumulative Liberation Yield Diagram - Ore - Wolframite

Table 30 - Cumulative Liberation Yield Diagram - Ore - Fluorite

Table 31 - Cumulative Liberation Yield Diagram - Ore - Arsenopyrite

Table 32 - Cumulative Liberation Yield Diagram - Ore - Molybdenite

Table 33 - Cumulative Liberation Yield Diagram - Ore - Sphalerite

Table 34 - Cumulative Liberation Yield Diagram - Ore - Galena

Table 35 - Cumulative Liberation Yield Diagram - Ore - Chalcopyrite

Table 36 - Cumulative Liberation Yield Diagram - Ore - Pyrite

Table 37 - Liberation Curves - Complete Liberation - Sulphides

Table 38 - Liberation Curves - Complete Liberation - Wofframite, Fluorite

Table 39 - Liberation Curves - +75% Liberation - Sulphides

Table 40 - Liberation Curves - +75% Liberation - Wofframite, Fluorite

1187A

LIST OF PHOTOMICROGRAPHS

1. Overview displaying numerous liberated grains of arsenopyrite, pyrite,wolframite, fluorite, galena, silicates and sphalerite-chalcopyrite. High degree of liberation with few binary particles of arsenopyrite-wolframite, arsenopyrite-bismuth and wolframite-silicates

2. Coarse binary particle of wolframite-molybdenite with grey molybdenite flakes occupying interstitial porosity and fracture/cleavage surfacesin wolframite. Liberated grains include galena, arsenopyrite, fluorite and wolframite

3. Coarse binary particle of wolframite enclosing minute subrounded grain of bismuth; also several fully liberated wolframite particles

4. Coarse aggregate of deformed molybdenite flakes exhibiting complete liberation. Note wide variation in flake size to a maximum length of 55 microns. Also liberated pyrite, arsenopyrite, wolframite and binary galena-silicates particle

5. Coarse polymineralic intergrowth of sphalerite with lenticular to elongate to subrounded inclusions of chalcopyrite and extensively disseminated minute particles of stannite-kesterite. The latter also occur as irregular ribbon lamellae. Also, liberated and binary particles of wolframite with silicates

6. Coarse polymineralic intergrowth of chalcopyrite and pyrrhotite with sphalerite. At right, sphalerite with chalcopyrite-kesterite inclusions along crystallographic planes

7. Binary association of galena-pyrite. Galena infills interstitial-intercrystal porosity and crystallographic planes, also coarse galena aggregate crystals cement the pyrite

8. Binary associations of bismuthinite-pyrite (above) and (below) arsenopyrite cemented by bismuthinite (grey) and native bismuth (yellow-orange)

9. Binary associations of native bismuth-chalcopyrite, tennantite-sphalerite (at far right) and arsenopyrite subhedra cemented by native bismuth.

10. Typical binary association exhibiting simple intergrowth of bismuthinite and native bismuth. Particle reports as liberated for bismuth beneficiation. Also liberated galena, arsenopyrite, wolframite, pyrite and sphalerite

11. Overview of flotation concentrate exhibits abundant liberated wolframite, arsenopyrite and minor base metal sulphides. Also several binary particles of fluorite-wolframite, wolframite-silicates. Note abundance of minus 10 micron fines

12. Liberated coarse particles of fluorite (dark, at center), grey-brown wolframite and arsenopyrite. Also, liberated particles in the minus 10 micron fraction

13. Complex polymineralic intergrowth of sphalerite (dark grey), chalcopyrite, tennantite (light grey), kesterite (brown) and galena (white). Also numerous liberated particles of wolframite. Note wolframite-silicate binary (center)

14. Coarse binary sulphide particle of arsenopyrite replaced by tennantite. Also liberated wolframite; ternary wolframite-cassiterite-silicate(left)

15. Smooth liberated native bismuth, also wolframite and arsenopyrite

16. Coarse binary type association of fluorite (dark grey) with sphalerite. The latter forms porous aggregates containing interstitial silicates, wolframite, cassiterite, fluorite and galena. Minute droplets of chalcopyrite are disseminated within the sphalerite

17. Coarse aggregate particle of sphalerite-chlorite-chalcopyrite (inclusions) - silicates cemented by fine galena and cassiterite along interstitial-intercrystal porosity; also coarse galena enclosing earlier silicates and sphalerite

18. Abundant equant crystals of sphalerite with extensive exsolution textures, also minor interstitial galena, pyrite, chalcopyrite, enclosed by silicates (light grey) and fluorite (dark grey). Liberation at less than 150 - 200 mesh

19. Coarse sulphide intergrowth with euhedral to anhedral arsenopyrite cemented by molybdenite followed by sphalerite-chalcopyrite-galena. The coarse grained galena and chalcopyrite fill interstices with fluorite and minor cassiterite

20. EDXA Spectral plot of sphalerite-chalcopyrite intergrowth

21. Coarse sphalerite exhibits strong crystallographic control over inclusions of pyrrhotite, chalcopyrite, stannite-kesterite. Liberation of inclusions poor with expected dilution of zinc grade

22. Coarse ternary sulphide intergrowth of galena with sphalerite (dark grey) and stannite-kesterite (light grey-brown)

23. EDXA Spectral plot of gahnite $ZnAl_2O_4$; zinc rich spinel located as inclusion within interstices of aggregate quartz

24. EDXA Spectral plot of sphalerite (Zn, Fe) S containing polymineralic inclusion of cassiterite (SnO_2), chalcopyrite ($CuFeS_2$) and galena (PbS)

25. Liberated sulphide particle comprising sphalerite with disseminated subsequent blebs to ribbons of chalcopyrite (yellow), galena-galenobismutite (white), galena (white) and stannite-kesterite (grey-brown)

26. EDXA Spectral plot of lead-bismuth sulphosalt, galenobismutite, ($PbBi_2S_4$) inclusion within sphalerite-chalcopyrite

27. EDXA Spectral plot of galena, PbS, inclusion within sphalerite-chalcopyrite

28. Fine unliberated spalerite-chalcopyrite and pyrite disseminated within quartz-topaz-silicate microbreccia. Liberation difficult to impossible at expected grinds

29. Effective binary association of fluorite-sphalerite with minor interstitial pyrite and pyrrhotite. Sphalerite intergrown with fine acicular crystals of cassiterite. The latter is finely developed withinthe fluorite

30. As previous, with fine aggregates of euhedral cassiterite needles disseminated within fluorite adjacent to honey-brown sphalerite

1187A

31. EDXA Spectral plot of stannite-kesterite series tentatively identified as kesterite Cu_2ZnSnS_4 with excess iron content (as described by Petruk, 1973)

32. EDXA Spectral plot of fine cassiterite enclosed by sphalerite-chalcopyrite aggregate

33. Coarse binary association of galena and sphalerite exhibits near complete liberation from silicates and fluorite

34. Unliberated subhedra to anhedra of tarnished pyrite exhibits cementation by galena. The latter also occurs as separate grains all of which are enclosed by silicate gangue. Effective liberation of galena from pyrite requires fine grinds of less than 325-400 mesh

35. Coarsely liberated aggregate particle of chalcopyrite with minor interstitial sphalerite and galena

36. Polymineralic aggregate of chalcopyrite replacing sphalerite (note cleavage control at left) and replaced by irregular ribbon lamellae of bornite followed by dark blue covellite, which rims the entire sulphide particle

37. EDXA Spectral plot of chalcopyrite, $CuFeS_2$

38. EDXA Spectral plot of Bornite, Cu_5FeS_4

39. Aggregate particle exhibiting subhedral to euhedral arsenopyrite (containing minute grains of bismuth), wolframite (enclosing sphalerite-covellite-chalcopyrite) along fractures of quartz. Liberation potential high at 150 - 200 mesh

40. Complex sulphide intergrowth with extremely fine crystal dimensions comprising dark grey sphalerite, chalcopyrite, pyrite (white), galena (grey-blue) and tetrahedrite-tennantite (green-grey) with dark fluorite and minor silicates. Bulk sulphide liberation potential high with separation from fluorite at 200 - 270 mesh

41. EDXA Spectral plot of typical tennantite mineral composition $(Cu, Fe)_{12}\ As_4\ S_{13}$

42. Coarse silicate aggregate with patchy to disseminated fluorite(dark grey) and microfracture controlled sulphide mineralization by minute to coarse flakes of molybdenite typically in association with minute crystals of bismuth and prismatic wolframite. Partial liberation, by exposure, very typical molybdenite texture.

1187A

WD1

43. Fine intergrowth of native bismuth-molybdenite interstitial to wolframite-fluorite-silicates. Liberation at fine grinds with molybdenite-bismuth and molybdenite-wolframite binaries expected

44. Numerous molybdenite flakes disseminated through fluorite-silicate microbreccia interstitial to coarse subhedral to anhedral quartz. Minor native bismuth occurs within microbreccia matrix

45. Finely disseminated flakes of molybdenite and grains of native bismuth within quartz-topaz-chlorite microbreccia. Fluorite (dark grey-gre n) also encloses minute sulphides. Liberation potential of sulphides generally poor

46. Fine warped flakes of molybdenite occur within fluorite hosted by silicates, primarily quartz. Liberation of both molybdenite and fluorite only at very fine grinds

47. Fine flakes of molybdenite, irregular grains of native bismuth, locally in association with molybdenite and coarse prismatic wolframite enclosed within silicates

48. Coarse liberated aggregate of molybdenite flakes exhibiting euhedral form and also fine granular aggregate crystals. Minute particles of bismuth occur with the molybdenite.

49. EDXA Spectral plot of molybdenite, MoS_2

50. Bismuth mineralization occurs as fine ribbon-type and irregular bleb lamellae within complex polymineralic sulphide aggregate of sphalerite followed by chalcopyrite, galena, tetrahedrite-tennantite and minor wolframite with fluorite-silicate matrix. Mineral liberation poor with bismuth probably reporting to bulk sulphide or lead concentrate

51. Coarse aggregate crystals of loellingite, $FeAs_2$, with abundant intercrystal crystallographically controlled inclusions of native bismuth. Molybdenite cements the loellingite and hosts bismuth within intercrystal dilation porosity

52. As above, close-up view of dendritic cleavage controlled bismuth and bimineralic bismuthinite-native bismuth; also monomineralic bismuthinite. Loellingite cemented at lower right by wolframite

1187A

53. Coarse loellingite associated with large elongate grains of bismuth cement and minute inclusions of native bismuth. The loellingite is liberated at coarse particle size with bismuth exposed to potential leach solutions

54. Coarse aggregate crystals of loellingite exhibiting graphic texture with dendritic inclusions of native bismuth. Liberation of bismuth poor to impossible with potential recovery by leach solution

55. EDXA Spectral plot of loellingite, $FeAs_2$

56. Isolated irregular grains of native bismuth occur interstitial to coarse quartz. Bismuth typically less than 20 microns in diameter

57. EDXA Spectral plot of native bismuth, Bi

58. EDXA Spectral plot of bismuthinite, Bi_2S_3

59. EDXA Spectral plot of lead-bismuth sulphosalt, tentatively identified as cosalite, $Pb_2\ Bi_2\ S_5$.

60. Coarse aggregate particle exhibiting large crystals of wolframite intergrown with fluorite and several types of silicate minerals. Minor molybdenite and native bismuth associated with wolframite

61. Prismatic wolframite enclosed within silicate minerals and spatially associated with coarse arsenopyrite-loellingite-bismuth cemented by minor sphalerite-chalcopyrite

62. EDXA Spectral plot of wolframite, variety ferberite $(Fe,Mn)\ WO_4$

63. Fine grained fluorite, primarily mauve coloration, and cloudy iron carbonates interstitial to quartz and topaz

64. Fine grained, clear to weakly mauve coloration, fluorite with carbonates in silica-topaz-chlorite greisen breccia

65. Fine grained mauve fluorite intergrown with kaolinite, chlorite and lesser carbonates interstitial to quartz aggregate grains. The quartz contains myriad inclusions of zircon, clays and apatite.

66. Ternary association comprising clear and mauve varieties of fluorite with brown chlorite, minor cassiterite and carbonates

67. Fully liberated crystal fragment of mauve fluorite with well developed cleavage pattern and few inclusions

68. Aggregate particle comprising clear and mauve varieties of fluorite with lesser yellow clays and minute subsequent yellowish to brownish yellow inclusions comprising cassiterite, rutile and monazite-xenotime. Minor ferroan carbonates also occur along cleavages of fluorite

69. EDXA Spectral plot of fluorite exhibiting minor to trace quantities of yttrium, possibly in solid solution as yttrofluorite (Ca,Y) (F, O_2)

70. Binary intergrowth particle of clear and mauve fluorite with radial arrays of fibrous green chlorite. Cassiterite occurred as subsequent inclusions, within both fluorite and chlorite, as individual and aggregate crystals

71. Coarse fragment primarily comprised of clear to locally mauve, fluorite with acicular green chlorite, pale brown subequant cassiterite, subsequent rhombs of ferroan-manganese carbonates and cerium-lanthanum fluocarbonates ranging in composition from bastnaesite to synchysite

72. Fluorite, clear variety, associated with opaque sphalerite, cloudy brown ferroan carbonates and fine inclusions including acicular rutile, subsequent monazite and cerium fluocarbonates of the bastnaesite-synchysite series

73. EDXA Spectral plot of monazite, cerium-lanthanum phosphate containing calcium-thorium substitution for REE, with formula (Ce,La,Th,Ca) PO_4

74. EDXA Spectral plot of monazite (Ce,La,Ca,Th) PO_4 noting variations in REE:Ca:Th ratios

75. EDXA Spectra plot of monazite (Ce,La,Ca,Th) PO_4 and xenotime, Y PO_4 or a substitution series between the yttrium and REE end members

76. EDXA Spectral plot of thorian synchysite $(Ce,Ca,Th)(CO_3)_2F$, associated with Fe-Mn carbonates and/or oxides

77. EDXA Spectral plot of Ce-La-Ca fluocarbonate, probably ranging in composition from parisite to roentgenite

78. EDXA Spectral plot of Ce-La fluocarbonate, tentatively identified as bastnaesite, $(Ce,La)(CO_3)F$

79. Euhedral crystal of zircon, interstitial to quartz grains; also infilling interstices are ferroan and magnesium-calcium carbonates with minor clear fluorite

80. Aggregate particle comprising hydrothermal brown biotite retrograded to chlorite and clay minerals hosted by quartz and minor carbonates

81. EDXA Spectral plot of rutile, TiO_2, containing minor Ta,Nb and Fe possibly microscopic intergrowths of columbite, $Fe(Nb,Ta)_2O_6$

82. Aggregate silicate gangue particle comprised of clear fluorite, pale brown biotite, chlorite, rutile and yellowish clays or micaceous sheet silicates

83. Euhedral topaz prism partially enclosed by clear fluorite and quartz. Note abundance of fine ferroan carbonate inclusions in fluorite

84. Overview of silicate and fluorite mineral liberation exhibits quartz, clear fluorite, mauve fluorite, topaz and minor carbonates and clay minerals

1.0 INTRODUCTION

At the request of Mr. Dean Thibault of New Brunswick Department of Natural Resources and Energy, Mineral Resources Division, three samples were submitted to Witteck Development Inc. for mineralogical investigation.

The samples represented ore feed material, flotation concentrates and gravity concentrates from the Mount Pleasant Tin Mine, Charlotte County, New Brunswick. Of particular importance in this study was the amenability of the Mt. Pleasant ore to gravity and/or flotation recovery of tungsten, fluorite, bulk sulphides (Mo, Bi, Zn, Cu, Pb) and yttrium-rare earths. As such, the following topics were addressed:

1. Identification of all mineral types to compare flotation and gravity processing routes

2. Examination of mineral chemistries, associations and textures with reference to mineral beneficiation

3. Investigation of mineral liberation size, by semi-quantitative mineralogical point and area counts, to provide preliminary data to establish optimum grind parameters

4. Preliminary study of yttrium and rare earth associations to provide insight on poor recoveries from previous testwork

5. Comment upon possible extraction techniques for yttrium-rare earths, base metal sulphides, fluorite and tungsten minerals.

Data presentation in tables, histograms and semi-log plots were utilized to summarize the semi-quantitative mineralogy in a useful format. In addition, photomicrographs and energy-dispersive x-ray analyses (SEM-EDXA spectral plots) were supplied to visually qualify and quantify mineralogical data.

2.0 PROCEDURES

2.1 Sample Preparation

Three samples, representing ore feed material, oxide flotation concentrates and gravity concentrates, were received.

The ore feed material was screened at 10 mesh and the oversize reduced by stage crushing to pass 10 mesh. The minus 10 mesh material was then screened through 20, 48, 100, 200 and 400 mesh. Representative samples of each screen fraction were riffled and collected into 20 gram charges.

The screen fractions, listed in Table 1, and flotation and gravity concentrates were prepared into 25 mm diameter epoxy base polished ore mounts and 27 x 46 mm polished thin sections.

All samples for microscopy are listed in Table 1 and 2.

Table 1

MICROSCOPY SAMPLES

Ore Feed (1939 grams)

SCREEN FRACTIONS

MESH SIZE SAMPLE #	(MICRONS)	WEIGHT (g)	WEIGHT (%)	MICROSCOPY
-10 +20	(833-1650)	765.0	40.75	MP1,6
-20 +48	(295-833)	492.6	26.24	MP2,7
-48 +100	(147-295)	181.8	9.68	MP3,8
-100 +200	(74-147)	164.8	8.78	MP4,9
-200 +400	(37-74)	86.4	4.60	MP5,10
-400	(LT37)	186.9	9.95	-

METALLURGICAL PRODUCTS:

Gravity Concentrate (as received)	GC1,2,3,4
Flotation Concentrate (as received)	FC1,2,3,4

1187A

Table 2

MICROSCOPY MOUNTS AND THIN SECTIONS

Sample No.	Polished Mount	Polished Thin Section
MP1		X
MP2		X
MP3		X
MP4		X
MP5		X
MP6	X	
MP7	X	
MP8	X	
MP9	X	
MP10	X	
GC1		X
GC2		X
GC3	X	
GC4	X	
PC1		X
PC2		X
PC3	X	
PC4	X	

The gravity and flotation concentrate products, from an 80% minus 200 mesh feed material, were screened as received, to assess particle size distribution. The results are given in Table 3.

1187A

Table 3

SCREEN ANALYSES OF GRAVITY AND FLOTATION CONCENTRATES

SAMPLE TYPE	MESH SIZE (MICRONS)		WEIGHT (%)	P_{80}
Flotation Concentrate				
	+200	(+74)	7.29	
	+270	(52-74)	11.59	
				approx. 50 microns
	+325	(45-52)	5.07	
	+400	(37-45)	11.95	
	-400	(LT37)	64.10	
Gravity Concentrate				
	+200	(+74)	1.86	
	+400	(37-74)	17.53	
	-400	(LT37)	80.61	
				approx. 35 microns

1187A

2.2 Sample Examination

Each polished mount and polished thin section was examined under reflected and transmitted light using a Leitz polarizing microscope equipped with magnifications of 50x, 100x, 200x, 500x and 1250x; the later using oil immersion. Each sample was scanned along parallel traverses to cover the entire surface of the slide/mount. Each field was observed for mineral identification, average and minimum/maximum dimensions, liberation, textures and associations. Quantitative mineralogical data was calculated by surface area of individual mineral grains and binary to polymineralic associations were noted. Qualitative analytical chemistry of mineral species was performed on a Hitachi scanning electron microscope equipped with a Tracor Northern 2000 EDS system.

Mineral chemistry is displayed on log frequency/keV spectral plot of elemental peaks. Photomicrographs of interesting associations display the variability of mineral types, textures and associations and to visually observe the degree of liberation from diluent minerals.

The liberation studies were calculated from surface area data from numerous fields for each screen fraction and for the metallurgical product. Binary and polymineralic unliberated particles were assessed by mineral proportions using arbitrary ranges of 0-25%, 25 - 50%, 50 - 75%, and 75 - 100% wanted mineral. Liberation was calculated from the midpoint of each percentile range with the proportion of fully liberated mineral grains. The data is displayed in Tables 6, 7, 8, 9, 10, 11, 12 and 13.

3.0 RESULTS

3.1 MINERAL ASSEMBLAGE

The Mount Pleasant polymetallic ore deposit, situated in Charlotte County, New Brunswick, occurs primarily within and along the exocontact of a highly brecciated and greisenized feldspathic porphyry suprajacent to a microgranitic stock.

The deposit comprised a complex mineral assemblage of potential ore minerals, opaque and non-opaque alteration and replacement minerals. The opaque minerals included sulphides, oxides, sulphosalts, sulpharsenides, arsenides and native metals. Alteration minerals comprised silicates, fluorides, carbonates, fluocarbonates, and minor borosilicates.

Ore mineralization comprised a complicated mineral paragenesis (Petruk, 1973) including copper, lead, zinc, indium, molybdenum, bismuth, niobium, silver, tungsten, tin, and yttrium - rare earth elements, the latter chiefly comprising the light lanthanides, cerium, lanthanum, with minor thorium.

The mineral assemblage described in the present study is given in Table 4. By metal type, the observed phases are listed in Table 5.

Table 4

MINERAL ASSEMBLAGE

Sphalerite	$(Zn,Fe)S$
Chalcopyrite	$CuFeS_2$
Stannite	Cu_2FeSnS_4
Kesterite	Cu_2ZnSnS_4
Tetrahedrite	$(Cu,Fe)_{12}Sb_4S_{13}$
Tennantite	$(Cu,Fe)_{12}As_4S_{13}$
Galena	PbS
Arsenopyrite	$FeAsS$
Loellingite	$FeAs_2$
Pyrite	FeS_2
Pyrrhotite	$Fe_{1-x}S$
Molybdenite	MoS_2
Bismuth	Bi
Bismuthinite	Bi_2S_3
Galenobismutite	$PbBi_2S_4$
Cosalite	$Pb_2Bi_2S_5$
Cassiterite	SnO_2
Gahnite	$ZnAl_2O_4$
Wolframite	$(Fe,Mn)WO_4$
Rutile	$(Ti,Nb,Ta)O_2$
Bornite	Cu_5FeS_4
Covellite	CuS
Marcasite	FeS_2
Graphite	C
Magnetite	Fe_3O_4
Hematite	Fe_2O_3
Apatite	$Ca_2(PO_4)F$

1187A

Table 4 Cont'd

Quartz	SiO_2
Fluorite	CaF_2
Topaz	$AlSiO_4(F,OH)_2$
Alkali feldspar	$(K,Na)AlSi_3O_8$
Chlorite	$(Mg,Fe)_6Al_2Si_4O_{10}(OH)_8$
Kaolinite	$Al_2Si_2O_72H_2O$
Muscovite-Sericite	$KAl_3Si_3O_{10}(OH)_2$
Serpentine	$(Mg,Fe)_3(Si_2O_5)(OH)_4$
Calcite	$CaCO_3$
Dolomite	$(Ca,Mg)(CO_3)_2$
Siderite	$(Fe,Mn)CO_3$
Biotite	$K(Mg,Fe)_3(Si_3O_{10})(OH)_2$
Zircon	$Zr\ SiO_4$
Monazite	$(Ce,La,Th)\ PO_4$
Xenotime	$Y\ PO_4$
Bastnaesite	$CeCO_3F$
Synchysite	$CeCa(CO_3)_2F$
Parisite	$Ce_2Ca(CO_3)_2F_2$
Roentgenite	$Ce_3Ca_2(CO_3)_5F_3$
Yttrofluorite	$(Ca,Y)(F,O_2)$

Table 5

MINERALS AND METALS

MINERALIZATION TYPE	MINERALS*
Zinc	Sphalerite, stannite, kesterite, gahnite, stannoidite*, mawsonite*
Copper	Chalcopyrite, stannite, kesterite, mawsonite*, tetrahederite, tennantite, bornite, covellite, sphalerite, wittichenite*, roquesite*, aikinite*
Lead	Galena, galenobismutite, cosalite, aikinite*
Silver	Tetrahedrite - tennantite, galena, native silver*
Molybdenum	Molybdenite
Bismuth	Bismuthinite, native bismuth, cosalite, galenobismutite, aikinite*, wittichenite*
Indium	Roquesite*
Tungsten	Wolframite, rutile*
Tin	Cassiterite, Stannite, Kesterite, Stannoidite*, Mawsonite*
Yttrium	Xenotime, yttrofluorite
Rare earths	Monazite, Bastnaesite, Synchysite, Parisite, Roentgenite, Yb-Er phosphate*
Fluorine	Fluorite
Niobium	Rutile, Columbite*

* See Petruk, 1973

1187A

Table 6

LIBERATION DATA - MP1,6

MINERAL	LIBERATED #	1	2	3	4	VOL.%	LIBERATION %
Bismuth		352				0.79	-
Pyrite		80			9200	20.88	-
Arsenopyrite/ Loellingite		4996		8000	10000	51.73	-
Molybdenite		1322				2.97	-
Bismuthinite		4				0.01	-
Wolframite		117	7200			16.45	-
Chalcopyrite		1891				4.25	-
Sphalerite		1163				2.61	-
Galena		129				0.29	-
Total Grains - 44,454							
Fluorite		NC					-

1187A

Table 7

LIBERATION DATA - MP2,7

MINERAL	LIBERATED #	1	2	3	4	VOL.%	LIBERATION %
Bismuth		65				0.21	-
Pyrite	2	335	650			3.2	-
Arsenopyrite/ Loellingite		1069	1800	176	80	10.5	-
Molybdenite		1185		1		3.9	-
Bismuthinite		1			1	.01	-
Wolframite	72	106	96	1610		6.2	3.82
Chalcopyrite		704	5	3	1750	8.1	-
Sphalerite	548	1021	8033	738	7084	57.1	3.14
Galena		627	1627	900	96	10.6	
Total Grains - 30,485							
Fluorite	16	4.1	9.2	3.5	3.6		43.9
	9	9.1	6.2	0.7	4.5		(Avg. 37.9) 30.5

1187A

Table 8

LIBERATION DATA - MP3,8

MINERAL	LIBERATED #	1	2	3	4	VOL.%	LIBERATION %
Bismuth		115				0.32	-
Pyrite	964	156	193	89	192	4.5	60.4
Arsenopyrite/ Loellingite	3245	232	813	583	1136	17.15	54.0
Molybdenite	1699	904	485	7	3	8.8	54.8
Bismuthinite		1				.01	-
Wolframite	1116	239	704	882	530	9.9	32.15
Chalcopyrite	123	461	382	7	284	358	9.7
Sphalerite	8454	416	1184	2696	3187	45.5	53.05
Galena	2231	298	557	294	161	10.1	63.0
Total Grains - 35,023							
Fluorite	137	3.0	11.2	14.7	36.9		67.5

1187A

Table 9

LIBERATION DATA - MP4,9

MINERAL	LIBERATED #	1	2	3	4	VOL.%	LIBERATION %
Bismuth		2.9			0.9	0.63	-
Pyrite	18	0.6	1.6	0.7	0.9	3.64	82.57
Arsenopyrite/ Loellingite	90	0.6	2.8	4.9	7.2	17.65	85.3
Molybdenite	71	4.2	6.4	4.2	4.5	15.11	78.6
Bismuthinite	1	0.7	0.8			0.41	40.0
Wolframite	36	0.5	3.6	4.9	3.6	8.13	74.07
Chalcopyrite	11	1.6	6.8	2.8		3.71	49.55
Sphalerite	191	1.0	8.4	2.8	19.8	39.4	81.06
Galena	57	1.0	4.4	2.1	2.7	11.2	84.8
Total Grains - 597.5							
Fluorite	388	2.6	12.0	23.8	47.7		81.8

1187A

Table 10

LIBERATION DATA - MP5,10

MINERAL	LIBERATED #	1	2	3	4	VOL.%	LIBERATION %
Bismuth	27	2.3	1.6	1.4	1.8	0.20	79.18
Pyrite	97		3.2	4.2	1.8	6.2	91.34
Arsenopyrite/ Loellingite	242	0.2	2.0	5.6	8.1	15.06	93.83
Molybdenite	295	4	10.2	8.4	4.5	18.8	91.58
Bismuthinite	1	0.7	0.8			0.14	40.0
Wolframite	147		1.6	3.5	0.9	8.9	96.08
Chalcopyrite	82	1.7	4.4	7.7	1.8	5.7	84.02
Sphalerite	494	0.4	6.0	17.5	86.4	35.3	81.74
Galena	114	0.8	4.8	11.9	3.6	7.88	84.4
Total Grains - 1712.8							
Fluorite	518	0.8	8.0	14.0	20.7		92.2

1187A

SULPHIDE MINERALS

The sulphide minerals comprised sphalerite, stannite, kesterite, galena, pyrite, pyrrhotite, marcasite, chalcopyrite, molybdenite, bismuthinite, covellite, and bornite.

Sphalerite, Stannite, Kesterite

Sphalerite, the most common sulphide mineralization, occurred as minute disseminated, anhedral to subhedral crystals and crystal aggregates within silicates (Photomicrograph 18), to coarse pods and masses of monomineralic to polymineralic aggregates up to 1200 microns in diameter (Photomicrographs 16, 17 and 19). Coarsely liberated sphalerite aggregates up to 1000 microns in diameter were observed in the coarse ore screen fractions.

The sphalerite ranges in composition from iron-poor to iron rich with coloration from black to honey brown. Marked variations in grain coloration, and intensity and coloration of internal reflections, the latter from white to orange to yellow to red-brown was observed. Both compositional and point analysis by EDXA (Photomicrographs 20 and 24), indicated variable quantities of iron, copper and tin, in part due to minute inclusions and solid solution impurities.

Fine grained sphalerite, occurring within the greisenized breccia matrix of quartz - chlorite - topaz - biotite - clays, typically occur interstitial to coarse fractured quartz crystals (vein material and fine grained subhedral topaz microlites (Photomicrograph 18). The fine sphalerite ranged in size from less than 15 to 200 microns in diameter. Fracture filling of silicates also occurred with sphalerite - galena - chalcopyrite - pyrrhotite associations. Sphalerite breccias with silicate cements were also present.

Complex polymineralic aggregates, with core grains of sphalerite, commonly comprised simple linear growth patterns. However, very fine, interlocking series of cementations comprising galena, (Photomicrograph 22), chalcopyrite, tetrahedrite - tennantite, native bismuth, molybdenite, pyrite and pyrrhotite were also observed. In addition, sphalerite occurred in association with cassiterite, as inclusions cemented by sphalerite, and commonly with fluorite, (Photomicrographs 16, 29 and 30), of clear and mauve varieties.

The sphalerite also contained myriad inclusions of chalcopyrite, stannite, kesterite and to lesser degree pyrrhotite, galena, pyrite, wolframite and cassiterite (Photomicrographs 17, 19 and 21). The inclusions ranged primarily from less than one micron to fifty microns in diameter forming subsequent to ribbon lamellae controlled by crystallographic orientation.

Sphalerite also contained grains of silicates, primarily chlorite and bismuth. However, many of the occluded particles occur later in the paragenetic sequence (see also Petruk, 1973), and infill porosity interstitial to sphalerite crystals and also along crystallographic planes. Sphalerite may be partially replaced by chalcopyrite, bornite and covellite (Photomicrograph 36).

Stannite - kesterite and possibly stannoidite were identified primarily as minute droplets and inclusions within the sphalerite (Photomicrographs 13, 21 and 25), and to lesser degree with tetrahedrite-tennantite. The inclusions ranged in size from submicron to a maximum of approximately 40 microns. Numerous grains ranging up to 250 microns in diameter, exhibit marked tarnishing and strong anisotropism, similar to the optical properties of stannite-kesterite.

Bulk chemical analysis by SEM-EDXA indicate the mineral compositions. The grains occurred as brownish colored droplets and lamellae within sphalerite associated with tennantite (Photomicrograph 31). All of the above minerals were included with the prodominant mineral, sphalerite, in the mineral liberation studies. More detailed research is required to fully assess the sphalerite-stannite-kesterite-stannoidite mineralization.

Galena

Galena occurred as coarse masses up to 800 microns in diameter comprising anhedral to subhedral crystals and aggregates exhibiting well developed cleavages. The galena also occurred as discrete subhedral crystals ranging from less than fifty to 250 microns enclosed by silicates, occurring interstitial to the coarse quartz-topaz breccia fragments.

1187A

In addition, the galena formed interstitial cements to sulphides (Photomicrograph 19), and locally replaced sulphides including sphalerite (Photromicrograph 33), chalcopyrite, pyrite, arsenopyrite and molybdenite, with grains ranging from less than 10 to 200 microns, though primarily less than 50 microns. Coarse aggregates of galena, up to several hundred microns, also enclosed acicular blades of chlorite, silica, sphalerite (Photomicrograph 22), and minor cassiterite and wolframite.

Galena also occurred as fine subequant to bleb or ribbon inclusions within sphalerite, commonly as monomineralic or polymineralic grains associated with bismuthinite, bismuth, galenobismutite, chalcopyrite or pyrrhotite (Photomicrograph 25).

Fine to coarse galena grains were also cemented by later tetrahedrite-tennantite, molybdenite, silicates, carbonates and fluorite. The galena inclusions were typically less than 20 microns in diameter and range to approximately 100 microns. The minute inclusions locally occur in association with galenobismutite (Photomicrograph 25), and cosalite enclosed by sphalerite-stannite-kesterite grains.

X-ray analysis by SEM-EDXA (Photomicrograph 27) indicated that the galena contained trace quantities of silver in solid solution as no argentiferous mineral inclusions were identified.

Pyrite, Pyrrhotite, Marcasite

Pyrite, pyrrhotite and marcasite formed the iron sulphide assemblage. Pyrite occurred as euhedral to subhedral crystals and crystal aggregates, ranging up to 450 microns in diameter, with single crystals in the 20 to 125 micron range.

Fine grained pyrite crystals, in euhedral and also as extremely fine sooty textured grain aggregates, ranged from less than one micron to approximately 10 microns in complex polymetallic aggregates.

Intergrowths with bismuth, bismuthinite, chalcopyrite, galena, (Photomicrograph 7), sphalerite (Photomicrograph 28), tetrahedrite-tennanite, arsenopyrite and loellingite were observed. The sulphides commonly formed within crystallographic planes and along internal porosity (Photomicrograph 34). The inclusions, primarily comprising galena, ranged from less than five microns to fifty microns. The pyrite is locally mixed with fine grained marcasite which replaced the pyrite along grain margins and fractures.

Pyrrhotite occurred as ragged subhedral to anhedral grains, ranging up to 300 microns in length, and occurred as isolated grains in silicate gangue, lamellae to interstitial cement within sphalerite-stannite-kesterite (Photomicrograph 21), and minute intergrowths with galena or chalcopyrite, typically of less than 40 microns in diameter.

Chalcopyrite

Chalcopyrite occurred as coarse aggregates up to 800 microns in length with abundant to rare inclusions of sphalerite (Photomicrograph 35), stannite-kesterite, galena, pyrite, wolframite, tetrahedrite-tennantite and arsenopyrite/loellingite. The chalcopyrite also occurred as inclusions, commonly along crystallographic planes within sphalerite and stannite-kesterite (Photomicrographs 5, 18, 19, 21 and 25).

The inclusions ranged from submicron to 100 microns with an average size of less than 10 microns. Inclusion dimensions within sphalerite were either random along cleavages, radially decreasing toward the core of sphalerite or of irregular distribution. Locally, the inclusions are polymetallic with molybdenite, bismuthinite, and bismuth.

The chalcopyrite may cement earlier arsenopyrite, chalcopyrite and/or sphalerite. Coarse polymetallic intergrowths of chalocpyrite with any or all of galena, pyrite, arsenopyrite, pyrrhotite (Photomicrograph 6), sphalerite, tetrahedrite, tennantite, bismuth and rutile were observed. The chalcopyrite ranged from less than five microns to a maximum of 100 microns. Very fine intergrowths with poor liberation characteristics, particularly with sphalerite, bismuth, stannite and silicates, were common.

Coarse grained chalcopyrite, up to 250 by 800 microns, occurred within brecciated silica - topaz - chlorite. In addition, finely disseminated chalcopyrite, of 5 to 30 microns, also formed this association. The finely disseminated chalcopyrite within silicates may occur with one or several sulphide minerals.

The chalcopyrite was locally replaced by irregular lamellae of bornite and blades of covellite which may form rims on coarse grained chalcopyrite with incipient to pervasive replacement of smaller grains (Photomicrographs 35 and 39).

Qualitative analysis of the chalcopyrite indicated the typical spectral plot (Photomicrograph 37).

Bornite, Covellite

Bornite and covellite occur together as replacements and exsolution lamellae within chalcopyrite. The bornite and covellite occur together as replacements and exsolution lamellae within chalcopyrite. The bornite formed irregular lamellae from less that 10 microns to 50 microns in length (Photomicrograph 36) and both chalcopyrite and bornite exhibit peripheral replacement by covellite. The covellite formed along hairline fractures with minute blades and also as matted fibrous grains up to 150 microns after chalcopyrite. Qualitative analysis of the bornite by SEM-EDXA is given in Photomicrograph 38.

Molybdenite

Molybdenite occurred primarily as thin veinlet mineralization interstitial to quartz-topaz fragments within the fine grained quartz-chlorite-clay matrix. The elongate molybdenite flakes were commonly exposed along the margin of the coarsely ground ore ranging in size from less than 20 microns to lengths of 300 microns (Photomicrograph 42). Fine grained flakes, of less than 10 to 40 microns were commonly enclosed by chlorite, fluorite, clays and quartz. The fine molybdenite commonly exhibited extensive warping and contorted flakes (Photomicrograph 46) and ranged in size from less than five microns to 400 microns, commonly occurring up to 75 microns in length.

Intergrowths of molybdenite with bismuth, bismuthinite, and wolframite, typically being silicate hosted, were common (Photomicrographs 43, 44, 45 and 47).

The molybdenite was typically of fine grain size with aggregates to 175 microns. Intergrowths, after arsenopyrite and loellingite, with sphalerite and galena were observed.

The molybdenite locally occurred as inclusions, probably controlled by crystallographic planes and fractures, within stannite, arsenopyrite, sphalerite and wolframite (Photomicrograph 2).

Coarse liberated grains up to 200 by 350 microns were observed and typically included both the hexagonal (coarse blades) and rhombohedral (very fine grains) polytypes (Photomicrographs 4 and 48). Qualitative X-ray analyses (SEM-EDXA) indicated the composition shown in Photomicrograph 49.

Bismuthinite

Bismuthinite was typically associated with native bismuth, commonly as simple rectilinear intergrowths, of less that 75 microns diameter (Photomicrograph 10). Coarse bismuthinite locally contained relicts of native bismuth, of less than 10 microns, and formed grains up to 80 microns.

Bismuthinite formed minute inclusions, locally monomineralic or bimineralic with bismuth, within molybdenite, arsenopyrite, loellingite, galena, sphalerite, covellite, chalcopyrite, tetrahedrite-tennantite and silicates, ranging in size from less than 5 microns to 30 microns (Photomicrograph 8). Bismuthinite occurred along grain boundaries of quartz-topaz with fluorite, clays and fine quartz in grains up to 50 microns diameter. Qualitative x-ray analyses by SEM-EDXA indicated the composition given in Photomicrograph 58.

OXIDE MINERALS

The oxide minerals comprised wolframite, cassiterite, gahnite, rutile, magnetite, ilmenite and hematite.

Wolframite

Wolframite formed coarse grained aggregates of up to 1500 microns within the breccia matrix with silicates. The wolframite also formed euhedral to anhedral grains ranging from 50 to 500 microns within silicate-sulphide-oxide aggregates. The wolframite crystals occurred as disseminated euhedra to subhedra within the brecciated silicates. Individual or clustered grains ranged from less than 10 to greater than 200 microns in length.

The wolframite formed intergrowths and middling type associations with arsenopyrite, chalcopyrite, loellingite, galena, cassiterite, rutile, silica, chlorite, sphalerite, fluorite, molybdenite, and bismuth. Several examples are given in Photomicrographs 60 and 61. The wolframite was locally cemented by the sulphides and native metals, particularly with molybdenite and bismuth.

The latter two minerals commonly occurred within the wolframite cleavage planes (Photomicrograph 2) or fully enclosed within massive wolframite (Photomicrograph 3). Wolframite crystals from 100 - 200 microns were common with crystals up to 700 by 900 microns. Liberated grains up to 460 by 520 microns were observed in the coarse screen fractions.

Qualitative SEM-EDXA analyses of the wolframite indicated an iron-rich composition, ferberite, with a variable content of the Mn-rich huebnerite component. A typical compositional analysis is given in Photomicrograph 62.

1187A

WD1

Cassiterite

Cassiterite typically occurred as fine subequant to acicular crystals, commonly as aggregrates and locally as disseminated individual needles. The grains ranged in size from less than 10 microns to 150 microns, the latter dimension for elongate crystals and also for aggregates of granular cassiterite.

The cassiterite was typically observed within fluorite, iron carbonates, wolframite, chlorite, sphalerite and rutile-bearing particles, (Photomicrographs 16, 29 and 30). Average dimensions of the cassiterite crystals were approximately 20 to 25 microns. Qualitative SEM-EDXA analyses indicated typical SnO_2 compositions (Photomicrograph 32).

Gahnite

The zinc spinel, gahnite, occurred as rare green subequant grains, of less than approximately 30 to 40 microns diameter. The gahnite formed minute inclusions within or interstitial to quartz. SEM-EDXA analysis of the gahnite is given in Photomicrograph 23.

Magnetite, Hematite, Ilmenite, Rutile

Magnetite, hematite, ilmenite and rutile occurred a disseminated grains ranging in size from less than five microns to a maximum of approximately fifty microns. The magnetite and ilmenite exhibited lamellae to octahedral solid solution-exsolution twinning and were partially replaced by hematite. The oxides typically occurred within the silicate breccia or were enclosed by various sulphide minerals.

Rutile grains were common and occurred in association with sphalerite, wolframite, cassiterite and the silicate breccia matrix of quartz, chlorite and clay minerals. The grains typically ranged in size from less than 10 microns to less than 50 microns. SEM-EDXA analysis of a rutile grain indicated the presence of niobium, tantalum and iron and may indicate finely disseminated intergrowths of rutile with columbite (Photomicrograph 81).

SULPHOSALTS

The sulphosalts were comprised of tetrahedrite, tennantite, cosalite and galenobismutite.

Tetrahedrite-tennantite

The tetrahedrite and tennantite occurred as intergrowths with and replacements after arsenopyrite (Photomicrograph 14), loellingite, sphalerite (Photomicrograph 13), chalcopyrite, and galena. The particles ranged in size from less than 10 microns in polymetallic intergrowths to coarse grains of 120 microns in diameter.

The finely intergrown tetrahedrite-tennantite occurred in association with native bismuth, galena and earlier sulphides including pyrite, arsenopyrite and sphalerite (Photomicrographs 40 and 50). Tennantite also occurred as isolated masses or veinlits within quartz, chlorite and serpentine, as coatings or cements after galena, sphalerite, stannite and chalcopyrite.

Qualitative analysis by SEM-EDXA indicated compositions of the arsenic end member, tennantite and less commonly, the antimony-rich tetrahedrite. An example of the tennantite composition is given in Photomicrograph 41.

Galenobismutite

Galenobismutite occurred as minute inclusions of less than 15 microns in diameter, locally associated with galena in bimineralic inclusions, within sphalerite-stannite-kesterite. Qualitative analysis by SEM-EDXA indicated the bulk composition given in Photomicrograph 26.

Cosalite

Cosalite occurred as fine grained, subequant inclusions within galena and sphalerite with diameters of less than 15 microns, and also occurred as rare coarse particles up to 60 by 80 microns. The latter particles were liberated in sample MP-4 such that mineral associations were not available. The bulk composition, obtained by qualitative SEM-EDXA is given Photomicrograph 59.

SULPHARSENIDES, ARSENIDES

Arsenopyrite, Loellingite

The sulpharsenides and arsenides were comprised of arsenopyrite and loellingite. The two minerals exhibit similar optical properties and, for purposes of this report, are described as such. Both minerals combine to comprise one of the major opaque phases in the deposit. The minerals occurred as euhedral to anhedral crystals and crystal aggregates with intergrowths of both minerals being common. The crystals ranged in size from less that 30 microns to a maximum of 350 microns with coarse aggregates to 500 by 1500 microns.

Euhedral crystals enclosed by silicate gangue commonly range from 20 to 50 microns.

The arsenopyrite and loellingite were typically fractured and contained crystallographically controlled inclusions of native bismuth (Photomicrographs 51 and 52), locally exhibiting graphic textures (Photomicrograph 54), ranging from submicron to 30 by 130 microns. Locally, the arsenopyrite and loellingite were cemented by coarse particles of native bismuth (Photomicrograph 53). In addition, the arsenopyrite/loellingite contained inclusions of sulphides and oxides including molybdenite, sphalerite, galena, tetrahedrite-tennantite, wolframite and chalcopyrite. Also, intergrowths with silicates, particularly within fractured quartz (Photomicrograph 39) were common.

Qualitative analysis by SEM-EDXA of typical loellingite compositions are given in Photomicrograph 55.

NATIVE ELEMENTS

The native elements occurring in the samples were comprised of native bismuth and graphite (carbon). No inclusions of native silver were observed (see Petruk, 1973).

Native Bismuth

The native bismuth primarily occurred in spatial association with arsenopyrite, loellingite, molybdenite, wolframite, fluorite and silicates.

The overall textures are very similar to native gold, exhibiting ragged tendrils to smooth equant to elongate grains (Photomicrograph 15) ranging in size from less that one micron to a maximum of 130 microns. The particles were typically of less than 50 microns in diameter.

Bismuth, a late paragenetic mineral, occurred as minute disseminated grains, interstitial to quartz within the greisenized breccia matrix, as elongate to subequant, crystallographically controlled inclusions within arsenopyrite, loellingite (Photomicrographs 51, 52, 53 and 54) and wolframite (Photomicrograph 3), and as finely disseminated intergrowths (Photomicrograph 50) after chalcopyrite, pyrrhotite, tetrahedrite-tennantite, galena, bismuthinite and pyrite, typically ranging from less than one micron to a maximum of 30 microns.

Bismuth was commonly associated with bismuthinite as graphic intergrowth, simple linear binary particles and bimineralic inclusions within sulphides. Binary particles commonly exhibited bismuthinite cements around bismuth and vice versa. Bismuth commonly cemented fine grained arsenopyrite (Photomicrograph 9), loellingite, pyrite (Photomicrograph 8), chalcopyrite (Photomicrograph 9) and pyrrhotite. Associations with molybdenite were very common and bismuth occurred as grains, ranging from less than two microns to 50 microns in diameter, within dilation zones of kinked molybdenite (Photomicrographs 43, 45 and 47). Qualitative analysis of native bismuth by SEM-EDXA is given in Photomicrograph 57.

Graphite

Graphite was observed as minute elongate flakes, locally associated with molybdenite, or within the brecciated matrix interstitial to coarse grained quartz-topaz-chlorite. The graphite ranged in size from less than 20 microns to a maximum of 150 microns in length.

SILICATE MINERALS

The silicate minerals were comprised of quartz, topaz, alkali feldspar, chlorite, serpentine, kaolinitic clay minerals, muscovite-sericite-hydromica, biotite and zircon.

Quartz

Quartz was the primary component of the greisenization-silicification replacement mineralization and occurred as coarse to fine grained, euhedral to equant, interlocking crystal aggregates. The quartz exhibited variable degrees of fracturing with a brecciated matrix comprising fine quartz and subordinate silicate minerals. Inclusions of topaz, chlorite, zircon, white mica, biotite, fluorite, carbonate and apatite were common.

Topaz

Topaz was also very common in the greisenized breccia and ranged from coarse, fractured euhedral to subhedral crystals to

fine crystals, commonly less than 50 microns in length. The topaz exhibited stubby prismatic forms (Photomicrograph 53) and also formed fine microlites or crystallites, locally forming metacrysts. Isolated crystals were intergrown with quartz, clays, chlorite and fluorite.

Alkali Feldspar

Alkali feldspar, of albitic composition, was intergrown with quartz and topaz, commonly fractured and may represent relicts of early feldspar porphyry mineralogy. The feldspars commonly exhibited cloudy replacement by white mica and clay minerals.

Chlorite

Chlorite, a dark green variety, occurred as irregular masses commonly associated with quartz, fluorite, white mica-sericite and serpentine, and formed interstitial intergrowths to coarse quartz-topaz grains (Photomicrographs 66, 70 and 71). The chlorite contained numerous inclusions of quartz, rutile, cassiterite, molybdenite, bismuth, wolframite and base metal sulphides in addition to biotite, minor ferroan carbonates and rare earth fluocarbonates (Photomicrographs 70 and 71).

Serpentine

Serpentine, a pale green variety, was observed as very fine grained aggregates associated with chlorite in interstices of quartz-topaz, and within the breccia matrix adjacent to coarse crystals of quartz-topaz. The serpentine also occurred adjacent to fine grained sulphides within the breccia matrix.

Kaolinite, Muscovite, Biotite

Kaolinitic clays occur throughout the quartz greisen as coarse patches within the breccia as replacements of topaz, and commonly, formed fine intergrowths with fluorite interstitial to quartz (Photomicrographs 64 and 65). Muscovite-sericite-hydromica occurred as fine grained replacements after feldspars, topaz, and biotite with fluorite and fine grained quartz in the breccia matrix. Biotite formed partially corroded metacrysts replaced by chlorite and ferroan carbonates within brecciated quartz and subordinate silicates (Photomicrograph 66, 80 and 82).

Zircon

Zircons occurred as simple to zoned, euhedral to subhedral crystals and crystal aggregates interstitial to brecciated quartz and within the fine grained silicate matrix. The crystals, as exhibited in Photomicrograph 79, ranged in size from less than 5 to a maximum of 40 microns.

CARBONATES

Carbonate minerals were comprised of calcite, dolomite, and siderite. The carbonates occurred in fine grained to coarse grained aggregates of euhedral rhombic crystals to anhedral granular masses ranging up to 200 by 600 microns in size. Interstitial to quartz, fluorite, chlorite and topaz, the carbonates typically contained a myriad of extremely fine inclusions and exhibited clear to cloudy brown coloration (Photomicrographs 66, 68, 72 and 80).

The carbonates were spatially associated with cassiterite, rutile, rare earth fluocarbonates and phosphates commonly within fluorite-biotite-chlorite-quartz. Qualitative analysis of the carbonates indicated compositions of Fe-Mn, Ca-Mg, and Ca only, comprising siderite, dolomite and calcite, respectively.

FLUOCARBONATES

The rare earth fluocarbonates occurred as disseminated grains and clustered grains within fluorite and to a lesser degree, with chlorite, biotite, and quartz and were commonly associated with cassiterite, rutile and ferroan carbonates. The fluocarbonates occurred with rutile and ferroan carbonates. The fluocarbonates occurred as grains of elongate tabular to equant forms, ranging in size from less than 5 to a maximum of 45 microns.

Qualitative compositional analysis by SEM-EDXA indicated several possible minerals, based on cerium-lanthanum-calcium and thorium contents. The minerals comprised a range of cerium fluocarbonates from bastnaesite through parisite, roentgenite and synchysite (Photomicrographs 76, 77 and 78). The effects of the cheralite component (Ca, Th) are well exhibited by the spectral plots given in Photomicrograph 76.

BOROSILICATES

Borosilicates comprised tourmaline of various compositions with coloration ranging from blue to orange-brown to bright green to yellow in subhedral to euhedral prismatic crystals ranging in size up to 70 by 95 microns.

1187A

WD1

The tourmaline was disseminated within the fine grained breccia matrix and within fractured quartz grains.

PHOSPHATES

The phosphate minerals comprised apatite, monazite and tentatively, xenotime. The apatite occurred as minute, subequant to prismatic grains within brecciated quartz and the silicate matrix. The monazite and tentatively, xenotime, occurred as disseminated, tabular, euhedral to anhedral crystals and crystal aggregates within brecciated quartz and also within fluorite and/or chlorite (Photomicrographs 68, 70, 71 and 72). The phosphates ranged in size from less than 5 microns to a maximum of 45 microns, locally occurring as liberated grains within the finely ground concentrate product.

The grains were identified primarily by SEM-EDXA analyses with compositions of monazite, cerium-lanthanum-thorium phosphate, and possible xenotime, yttrium phosphate, associated with cerium fluocarbonates and/or monazite. Examples of the chemical compositions are given in Photomicrographs 73, 74 and 75.

FLUORIDES

The fluorides were comprised chiefly of fluorite with minor fluorine incorporated within tourmaline, topaz and possibly apatite. The fluorite was pervasive throughout the mineralized samples in veins interstitial to quartz-topaz-biotite-chlorite, coarse euhedral to anhedral crystals commonly in masses with arrays of chlorite. Finely disseminated fracture and breccia matrix fillings were associated with kaolinite, white mica, fine grained quartz, carbonates, phosphates, cassiterite, wolframite, rutile and numerous sulphide minerals.

Several textures of the fluorite, exhibited in Photomicrographs 63, 64, 65, 66, 67, 68, 70, 71 and 72, illustrate the size range and mineralogical associations. The fluorite ranged in coloration from clear to mauve, commonly exhibiting homogeneous discoloration or local mauve patches adjacent to ferroan or radioactive (Ce-La-Th) minerals (Photomicrographs 68 and 71).

Fine interstitial fluorite ranged in size from 5 to 150 microns intergrown with chlorite, kaolinite and quartz. Coarse grained fluorite crystals ranged in size up to 350 by 1300 microns. Inclusions within fluorite, partially controlled by cleavages and interstitial crystal porosity, included bismuth, molybdenite, rare earth fluocarbonates, sphalerite, chalcopyrite, zircon, cassiterite and wolframite.

The bulk composition of the fluorite, as determined by SEM-EDXA (Photomicrograph 69), indicated typical CaF_2 although analyses of dark coloured purple to black fluorite indicated the presence of yttrium, either occurring as yttrofluorite (rare earth bearing fluorite described by Petruk, 1964) or possibly yttrium fluoride, YF_3.

3.2 MINERAL LIBERATION

3.2.1 Gravity Concentrate

The results of mineral liberation studies on the gravity concentrate are given in Tables 11 and 13. The liberation data was calculated using particles ranging in size from 20 to 74 microns. Screen analysis of the gravity concentrate, given in Table 3, indicated that only 1.86 weight percent of the particles exceeded diameters of 74 microns (200 mesh). Particle size distribution indicated that 80.6% by weight of the gravity concentrate passed 400 mesh (37 microns). Average particle size for the liberation study was estimated at 30 - 35 microns with most particles of 20 - 55 microns diameter.

Table 11 indicated the relative proportions of minerals of interest (oxides - sulphides only). The concentrate product was primarily comprised of arsenopyrite/loellingite, wolframite, galena and silicates with lesser pyrite, fluorite and sphalerite. Bismuth, bismuthinite, chalcopyrite and molybdenite formed minor components. Based on relative proportions, the sulphides-oxides, silicates and fluorite contributed, by volume, 49.5%, 47.5% and 3.0% respectively.

Also indicated by Tables 11 and 13 were the degree of liberation of the major mineral species. Liberation of pyrite, arsenopyrite, loellingite, wolframite, sphalerite, galena, fluorite and silicates exceeded 90% (complete liberation). Wolframite, arsenopyrite/loellingite, galena and fluorite, with liberations near or exceeding 95% by volume, indicated excellent grades by mineral type. Cumulative liberation yield calculations indicated that a significant proportion of the arsenopyrite/loellingite, pyrite, wolframite, galena, sphalerite and native bismuth particles comprise greater than 75% of the particle volume (Tables 17 through 25).

Table 11

LIBERATION DATA - GRAVITY CONCENTRATE

(20 - 75 MICRONS)

MINERAL	LIBERATED #	1	2	3	4	VOL.%	LIBERATION %
Bismuth	(72)	10.6	12.8	23.4	49.5	3.3	42.0 (70.8)
Pyrite	220	0.2	4.4	7.2	9	7.8	91.4 (95.1)
Arsenopyrite/ Loellingite	940	0.1	0.4	7.2	33.3	31.9	95.8 (99.2)
Molybdenite	(39)	0.3	4.8	1.2	5.4	0.81	76.9 (87.5)
Bismuthinite	(2)	2.0	13.2	6.0	1.8	0.61	8.0
Wolframite	819	0.4	1.6	6	20.7	29.9	96.9 (99.3)
Chalcopyrite	(66)	2.7	8.4	3.0	8.1	1.6	74.8 (88.0)
Sphalerite	218	0.4	4.2	7.8	7.2	7.7	91.8 (94.8)
Galena	464	0.5	7.2	10.8	10.8	16.08	94.1 (96.2)
Total Grains - 3018							
Fluorite	189	0.5	2.8	3	2.7		95.5 (96.8)
Silicates	2652						92.4

1187A

Those particles containing less than 50% by volume of wanted mineral generally appear to be rejected to the tailings product. Exceptions are bismuth and bismuthinite, which, due to fine average particle size, occur in association with arsenopyrite/loellingite across a wide range of relative mineral proportions.

The types of binary and polymetallic associations, which comprise the unliberated particles in the gravity concentrate, are given in Tables 14 and 15. Examples of bimineralic to polymineralic associations observed in the gravity concentrate, are shown in Photomicrographs 2, 3, 5, 6, 7, 8, 9 and 10. Clearly, the textures of the binary associations, the fine particle and intergrowth size indicate that complete liberation of each specific mineral type will not be achieved with gravity feeds of 80% passing 200 mesh. However, excellent grade recovery based on the cumulative optimum yield curves for major sulphides, wolframite and fluorite suggests that subsequent treatment by flotation and/or magnetic separation to produce separate wolframite, fluorite and bulk sulphide products may provide viable processing routes.

3.2.2 Flotation Concentrate

The results of mineral liberation studies on the flotation concentrate are given in Tables 12 and 13. The liberation data were calculated using particles ranging from 20 to 100 microns. Average particle size of the particles under liberation study was approximately 55 - 75 microns. Screen analysis of the flotation concentrate, given in Table 3, indicated a significant difference in particle size distribution to the gravity concentrate with 7.29 wt % exceeding 200 mesh (74 microns).

Table 12

LIBERATION DATA - FLOTATION CONCENTRATE

(20 - 75 MICRONS)

MINERAL	LIBERATED #	1	2	3	4	VOL.%	LIBERATION %
Bismuth							
Pyrite	12		0.8	1.4		0.51	84.5
Arsenopyrite/ Loellingite	675	0.7	1.4	0.6	21.6	28.79	96.5
Molybdenite	5	0.3	1.2	0.6		0.22	70.4
Bismuthinite							
Wolframite	1647	0.7	10.2	7.2	17.1	70.26	97.9
Chalcopyrite							
Sphalerite	5	0.1	0.8		1.8	0.22	64.9
Galena							
Total Grains - 2344							
Fluorite	43	0.7	4.4	7.7	7.2		68.2
Silicates	655						97.9

Table 13

MINERAL LIBERATION BY SCREEN FRACTION AND PRODUCT TYPE

MINERAL	SCREEN FRACTION (MESH) +28	+48	+100	+200	+400	GRAVITY CONC.	FLOTATION CONC.
Bismuth	-	-	-	-	79.18	42.0 (70.8)	NC
Pyrite	-	-	60.4	82.57	91.34	91.4 (95.1)	81.5
Arsenopyrite/ Loellingite	-	-	54.0	85.30	93.83	95.8 (99.2)	96.5
Molybdenite	-	-	54.8	78.6	91.58	76.9 (87.5)	70.4
Bismuthinite	-	-	-	40	40	8.0	NC
Wolframite	-	3.82	32.15	74.07	96.08	96.9 (99.3)	97.9
Chalcopyrite	-	-	9.7	49.55	84.02	74.8 (88.0)	NC
Sphalerite/ Stannite/ Kesterite	-	3.14 (43.8)	53.05 (73.04)	81.06 (89.47)	81.74 (96.0)	91.8 (94.8)	64.9
Galena	-	-	63.0	84.8	84.4	94.1 (96.2)	NC
Fluorite	-	37.9	67.5	81.8	92.2	95.5 (96.8)	68.2
Silicates	NC	NC	NC	NC	NC	NC	NC

NC - Not Calculated

(70.8) - includes particles containing +75% wanted mineral

Table 14

BINARY PARTICLES - GRAVITY CONCENTRATE

MINERAL	BINARY ASSOCIATION
Sphalerite:	Pyrite
	Pyrite, Galena
	Galena
	Arsenopyrite
	Loellingite
	Galena, Chaleopyrite
	Chalcopyrite
Galena:	Sphalerite
	Sphalerite, Pyrite
	Pyrite
	Pyrrhotite
	Chalcopyrite
	Bismuth
	Arsenopyrite
	Tetrahedrite - tennantite
	Covellite
	Fluorite
	Silicates
Arsenopyrite/Loellingite:	Bismuth
	Chalcopyrite
	Chalcopyrite, Bismuth, Bismuthinite
	Sphalerite, stannite
	Molybdenite
	Galena
	Sphalerite, Chalcopyrite
	Chalcopyrite, Bismuth
Molybdenite:	Pyrite
	Sphalerite - stannite
	Arsenopyrite
	Silicates
Pyrite:	Molybdenite
	Galena
	Galena, Silicates
	Galena, Chalcopyrite
	Bismuth, Bismuthinite
	Bismuth
	Silicates
	Sphalerite - stannite
	Galena, Sphalerite

1187A

Table 14

BINARY PARTICLES - GRAVITY CONCENTRATE

MINERAL	BINARY ASSOCIATION
Wolframite:	Fluorite
	Pyrite
	Silicates
	Molybdenite
	Bismuth
Chalcopyrite:	Galena
	Pyrite, Galena
	Sphalerite, Silicates
	Silicates
	Arsenopyrite/Loellingite
	Sphalerite
	Sphalerite, Arsenopyrite
	Bismuth
	Pyrite
	Tetrahedrite - tennantite
Bismuth:	Bismuthinite
	Fluorite
	Arsenopyrite/Loellingite
	Molybdenite
	Silicates
	Pyrrhotite, Silicates
	Pyrite
	Sphalerite - stannite
	Bismuthinite, Sphalerite
	Wolframite
Bismuthinite:	Bismuth
	Tetrahedrite - tennantite
	Arsenopyrite, Chalcopyrite, Bismuth
	Arsenopyrite, Chalcopyrite
	Pyrrhotite, Bismuth
	Bismuth, Stannite, Sphalerite
Tetrahedrite - tennanite:	Bismuthinite
	Chalcopyrite
	Galena
	Sphalerite
	Chalcopyrite, Silicates

1187A

Table 15

BINARY AND MIDDLING ASSOCIATIONS - FLUORITE

Gravity Concentrate:	Wolframite
	Bismuth
	Pyrrhotite, Bismuth
	Bismuthinite
	Molybdenite
	Chalcopyrite
	Galena
	Silicates
Flotation Concentrate:	Wolframite
	Arsenopyrite, Bismuth, Chalcopyrite
	Sphalerite
	Sphalerite, Galena
	Sphalerite, Chalcopyrite
	Silicates
MP5,10 (-200, +400):	Silicates (58)
	Molybdenite (5)
	Arsenopyrite, Silicates (4)
	Sphalerite, Cassiterite, Rutile
	Wolframite, Silicates
MP4,9 (-100, +200):	Arsenopyrite (11)
	Wolframite (9)
	Molybdenite (8)
	Sphalerite (5)
	Molybdenite, Silicates
	Chalcopyrite, Silicates
	Wolframite, Silicates
	Pyrite, Sphalerite, Silicates
	Bismuth
	Arsenopyrite, Silicates
	Sphalerite, Chalcopyrite

1187A

Table 15 Cont'd

BINARY AND MIDDLING ASSOCIATIONS - FLUORITE

MP3,8 (-48, +100):	Chalcopyrite
	Pyrite, Sphalerite
	Pyrite
	Arsenopyrite
	Wolframite
	Sphalerite, Rutile, Cassiterite
	Sphalerite, Silicates
	Sphalerite, Pyrite, Arsenopyrite
	Silicates, Arsenopyrite, Sphalerite, Pyrrhotite
	Tetrahedrite
	Pyrite, Silicates
	Bismuth, Bismuthinite
	Sphalerite, Chalcopyrite
	Galena, Silicates
	Sphalerite
	Molybdenite
	Molybdenite, Silicates
	Bismuth, Silicates
	Bismuth, Cassiterite, Silicates

Table 16

BINARY PARTICLES - FLOTATION CONCENTRATE

MINERAL	BINARY ASSOCIATION
Sphalerite:	Fluorite Silicates Galena
Galena:	Pyrite Bismuth, Wolframite Arsenopyrite, Loellingite Rutile, Cassiterite Sphalerite Silicates
Arsenopyrite/Loellingite:	Fluorite, Silicates Sphalerite, Bismuth, Fluorite Silicates Bismuth, Silicates
Molybdenite:	Fluorite Silicates Pyrite
Pyrite:	Galena Molybdenite Sphalerite, Silicates
Wolframite:	Fluorite, Chalcopyrite, Fluorite Silicates Bismuth
Chalcopyrite:	Wolframite Silicates
Bismuth:	Fluorite, Wolframite Arsenopyrite, Loellingite Fluorite, Arsenopyrite Bismuthinite
Bismuthinite:	Fluorite, Arsenopyrite Silicates, Wolframite

1187A

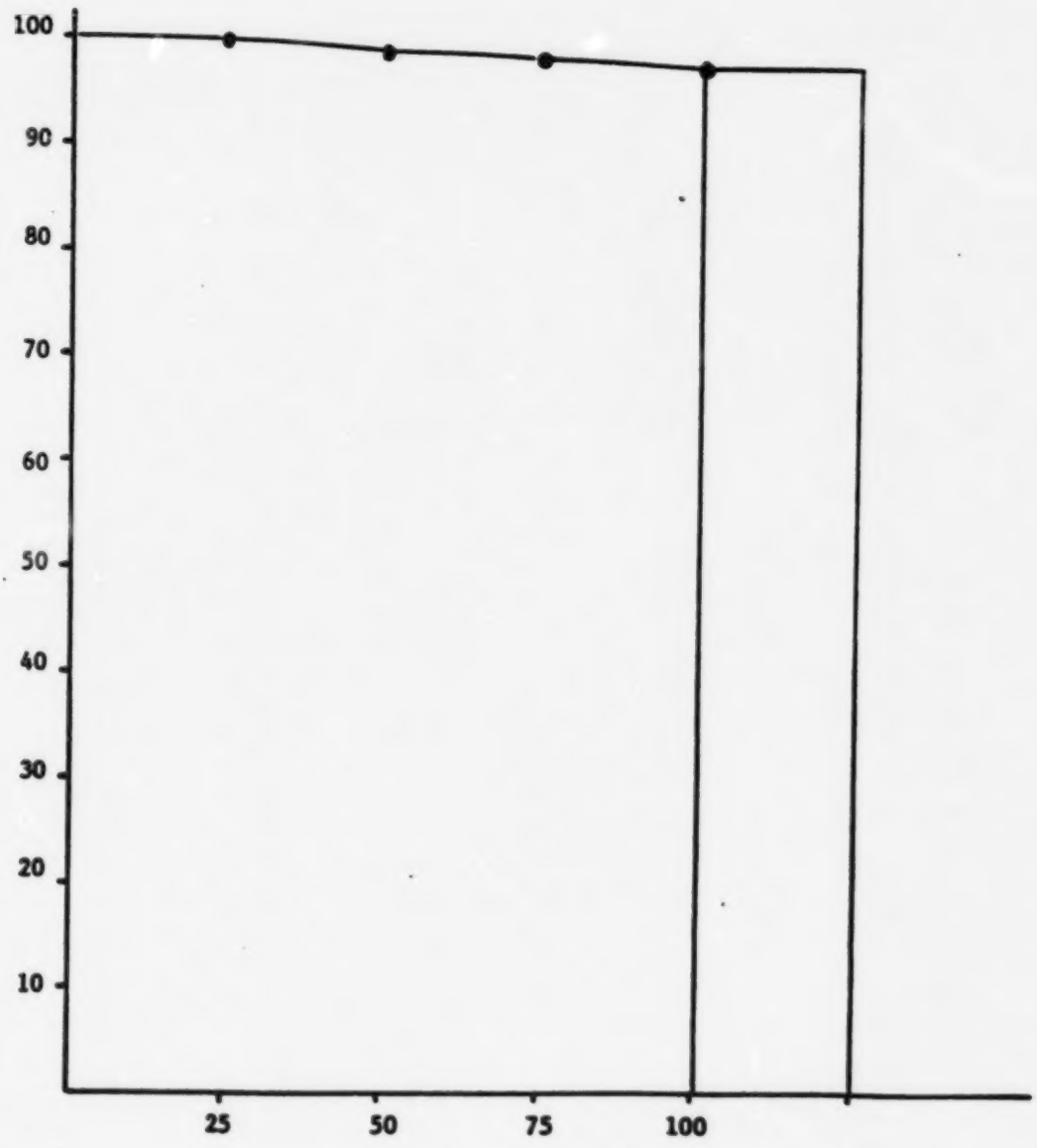

Table 17 - Cumulative Liberation Yield Diagram - Gravity Concentrate - Wolframite

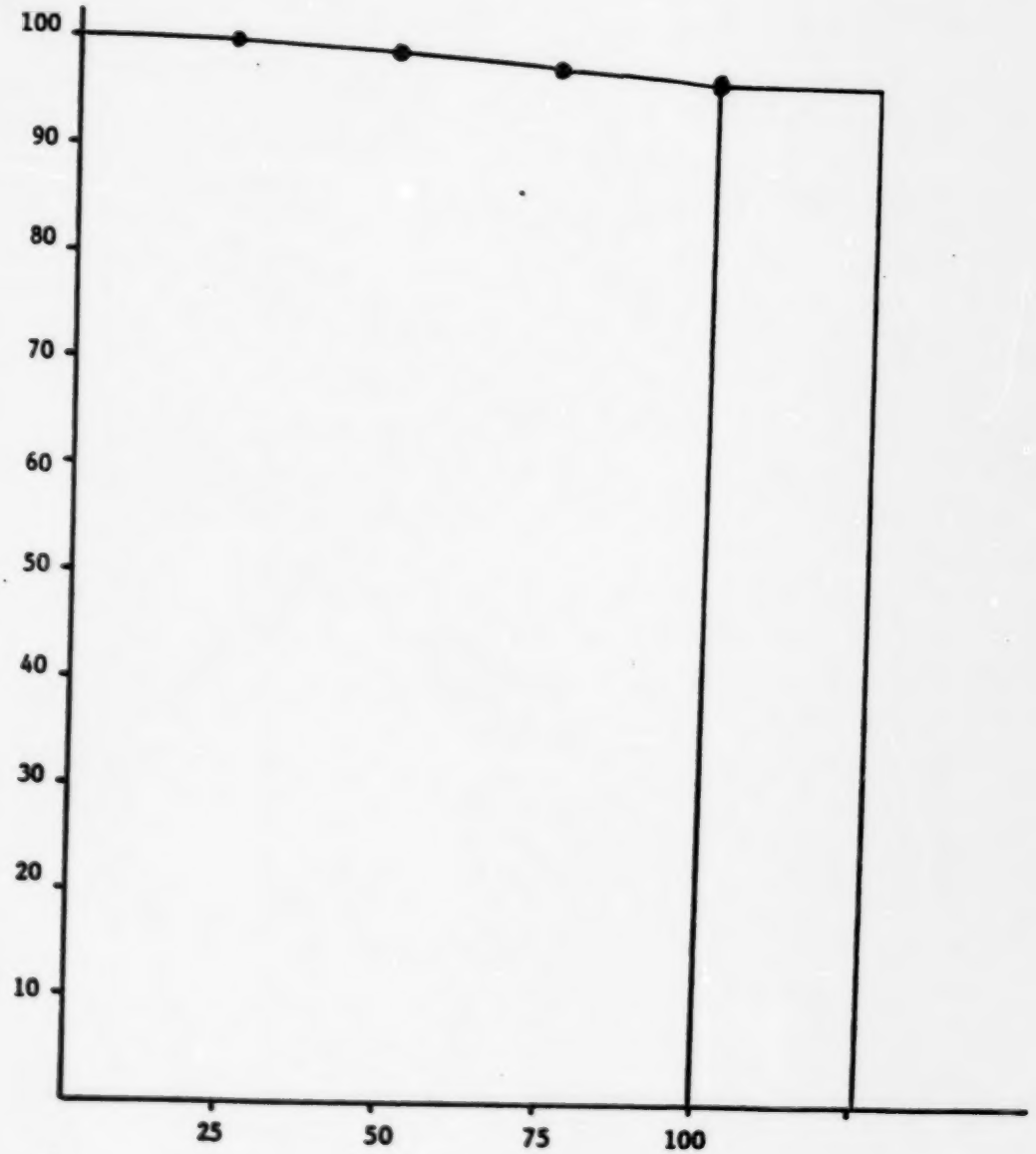

Table 18 - Cumulative Liberation Yield Diagaram - Gravity Concentrate - Fluorite

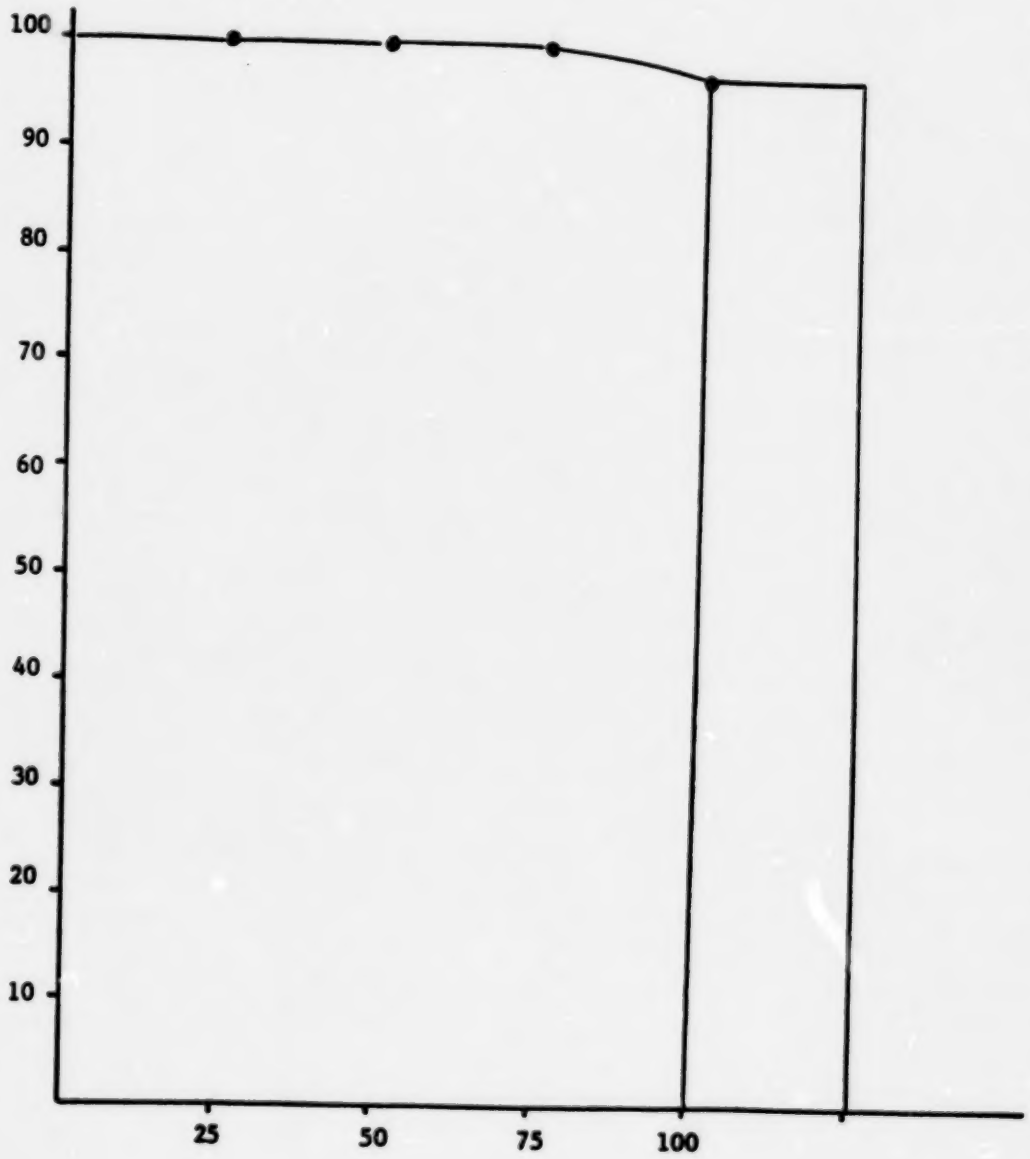

Table 19 - Cumulative Liberation Yield Diagaram - Gravity Concentrate - Arsenopyrite

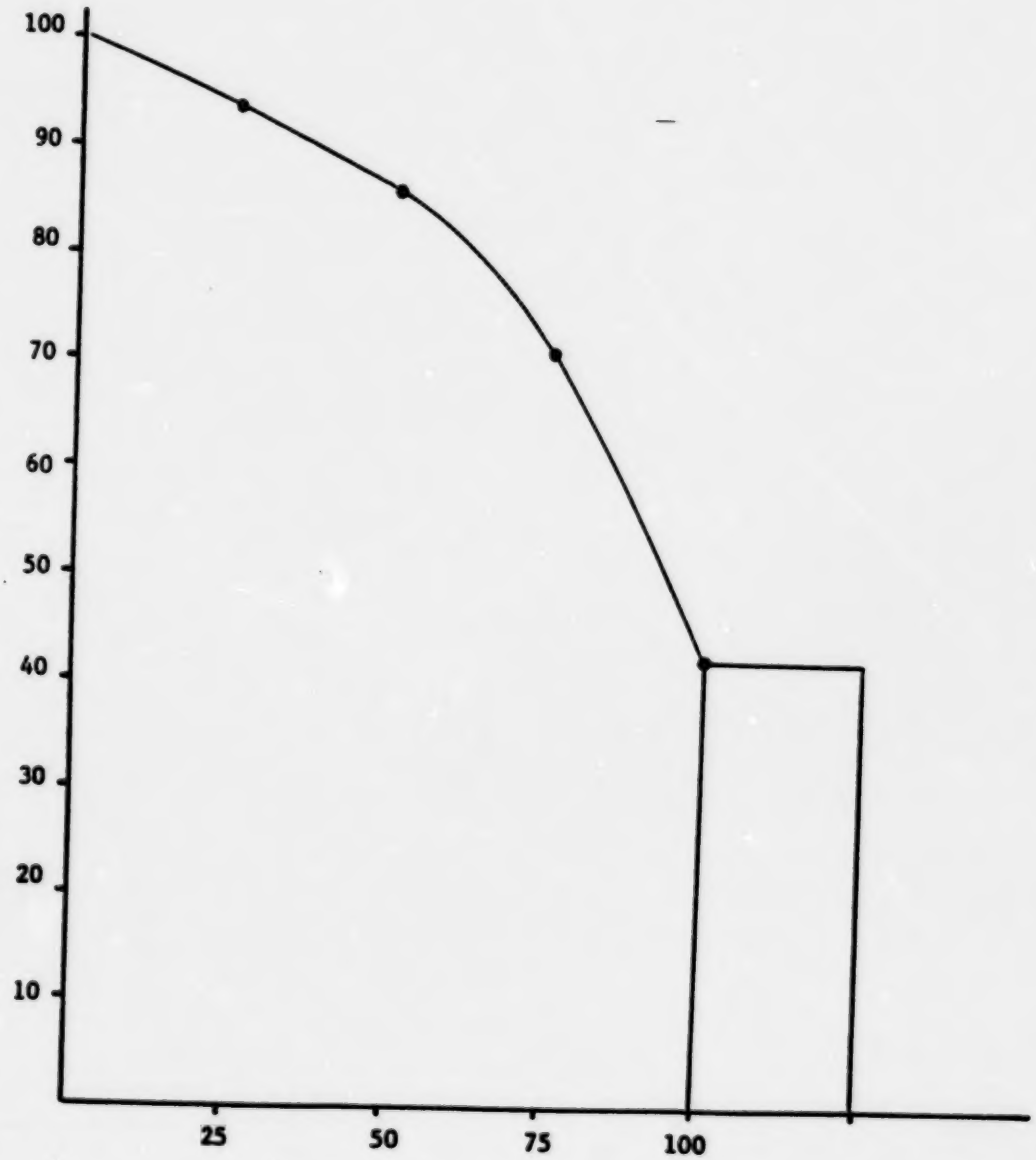

Table 20 - Cumulative Liberation Yield Diagram - Gravity Concentrate - Bismuth

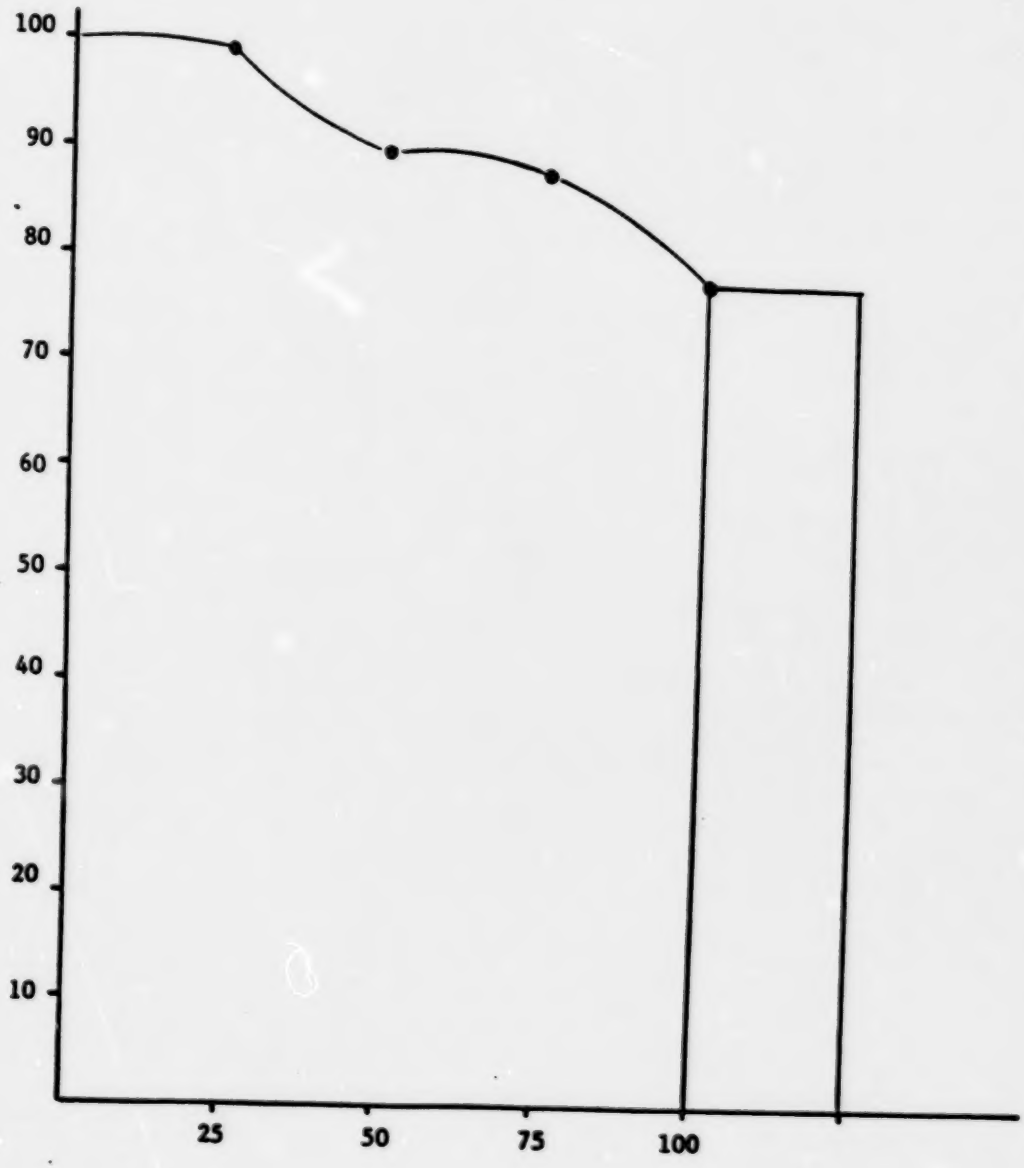

Table 21 - Cumulative Liberation Yield Diagaram - Gravity Concentrate - Molybdenite

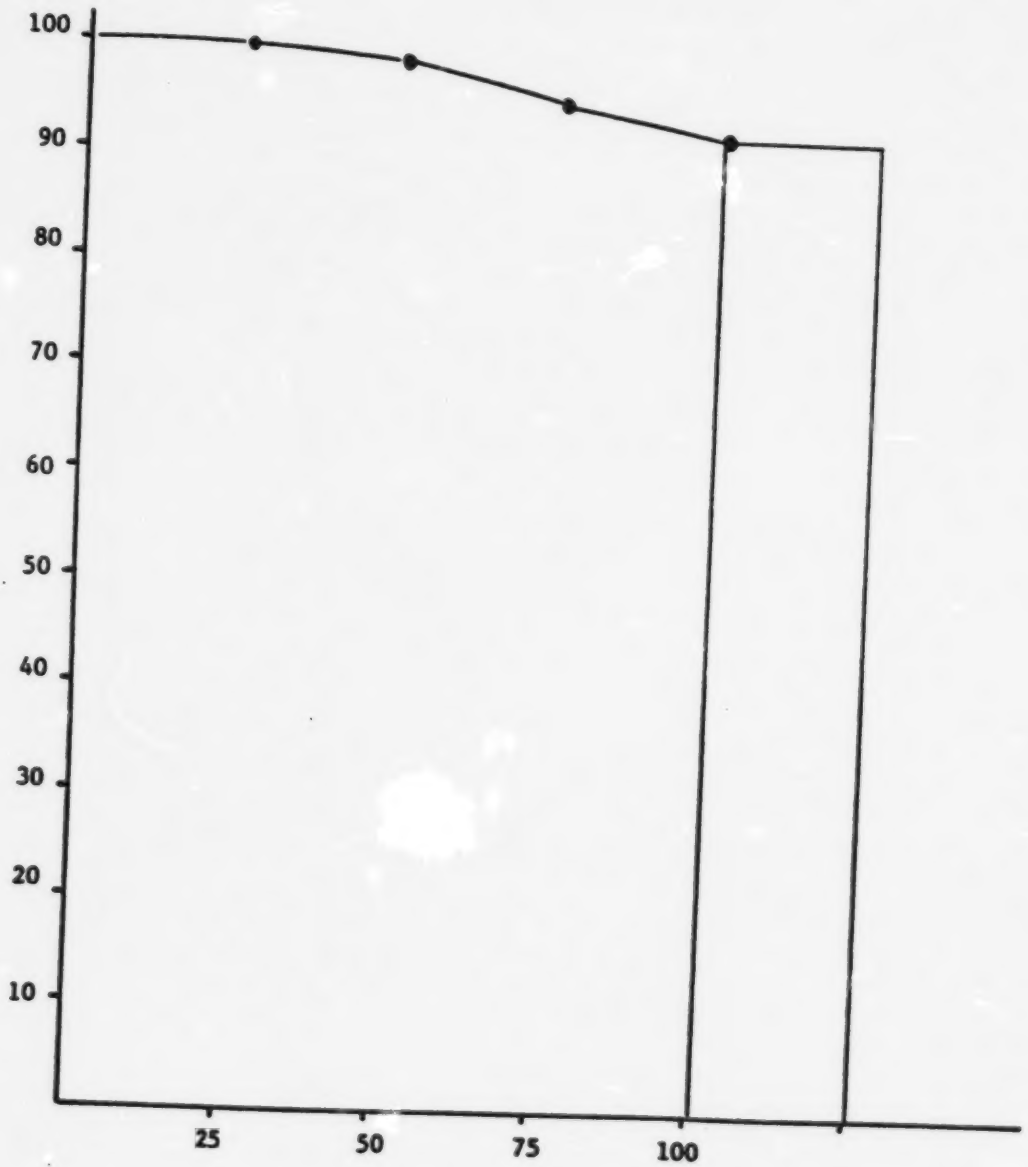

Table 22 - Cumulative Liberation Yield Diagaram - Gravity Concentrate - Sphalerite

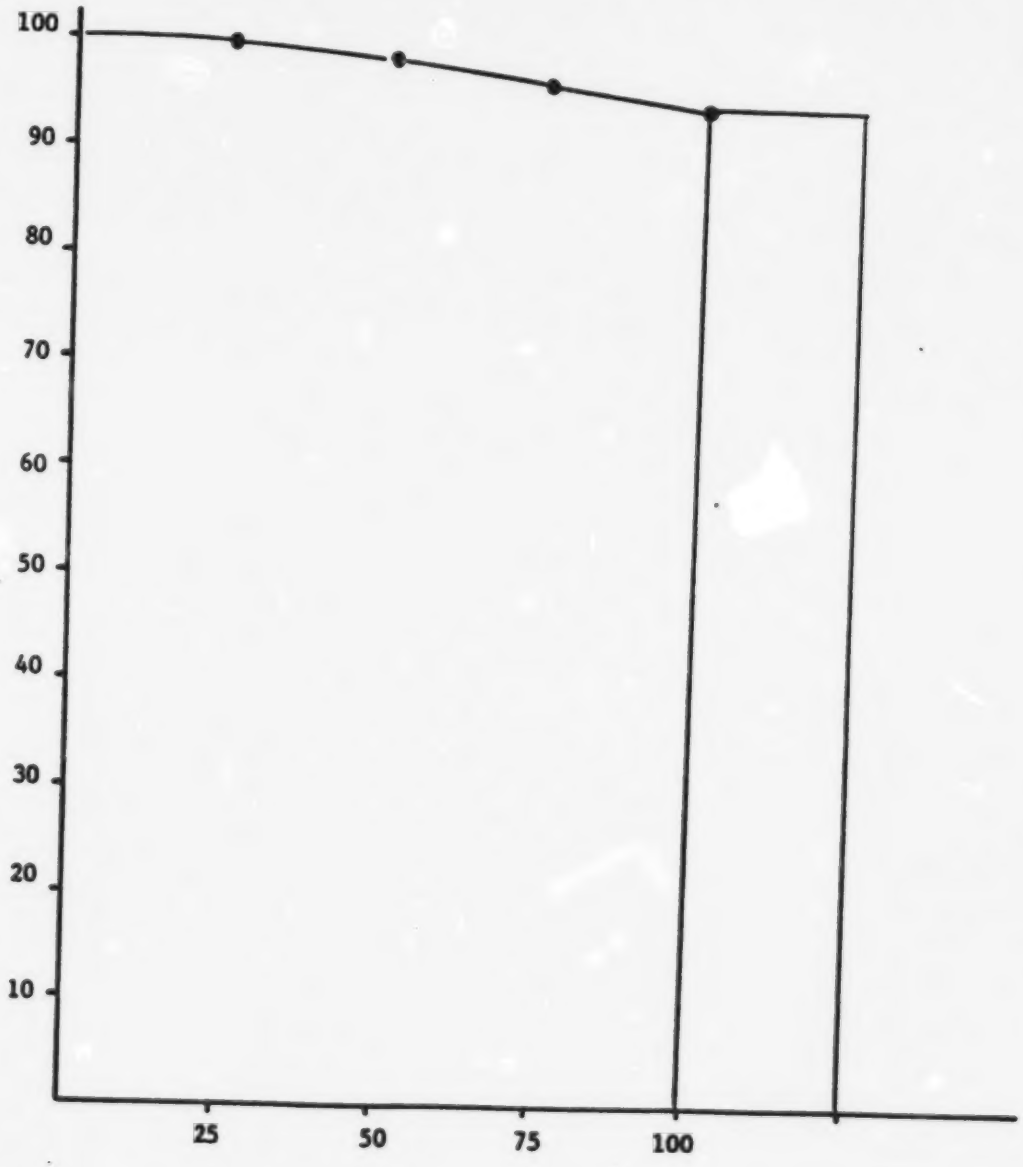

Table 23 - Cumulative Liberation Yield Diagram - Gravity Concentrate - Galena

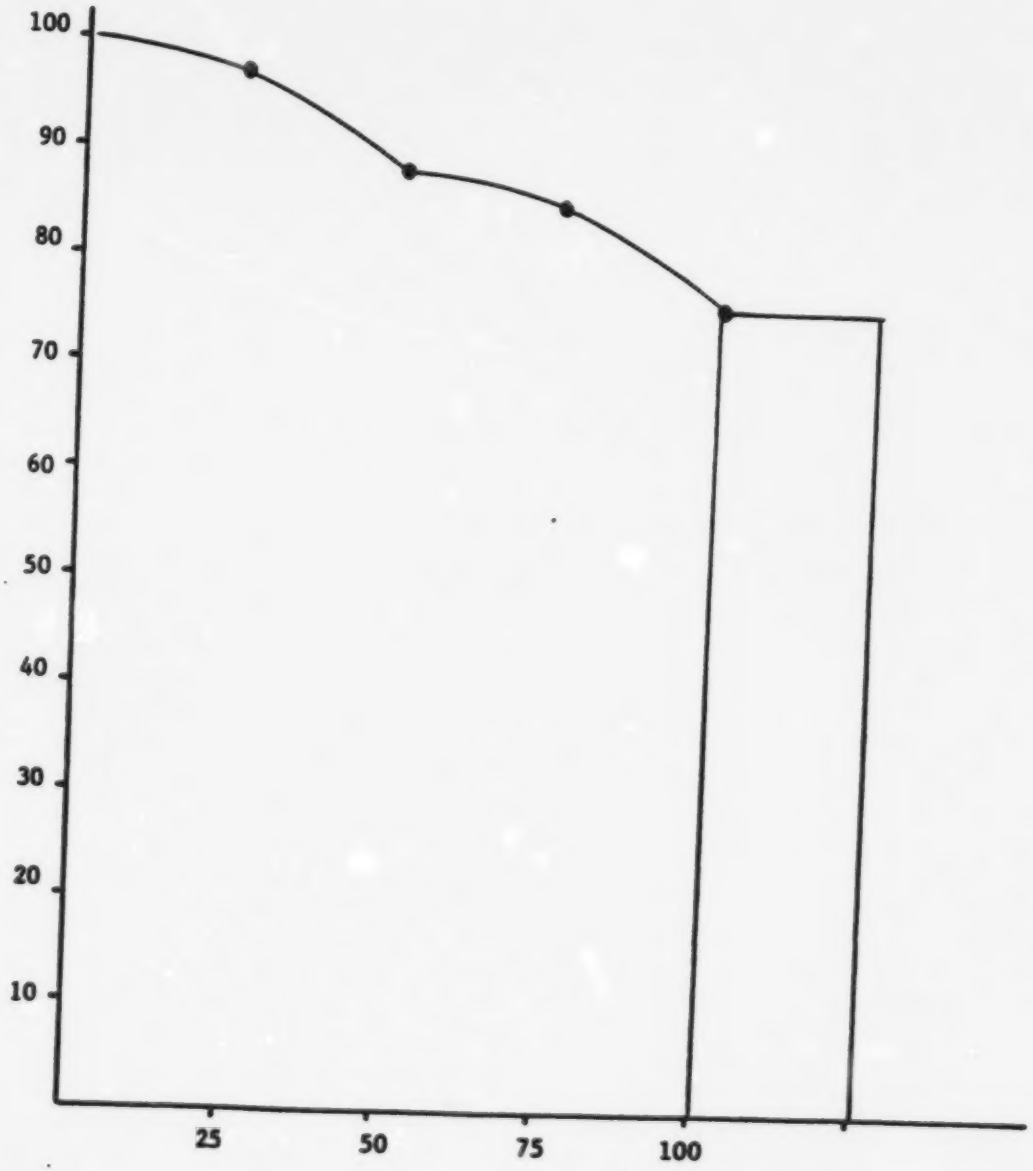

Table 24 - Cumulative Liberation Yield Diagaram - Gravity Concentrate - Chalcopyrite

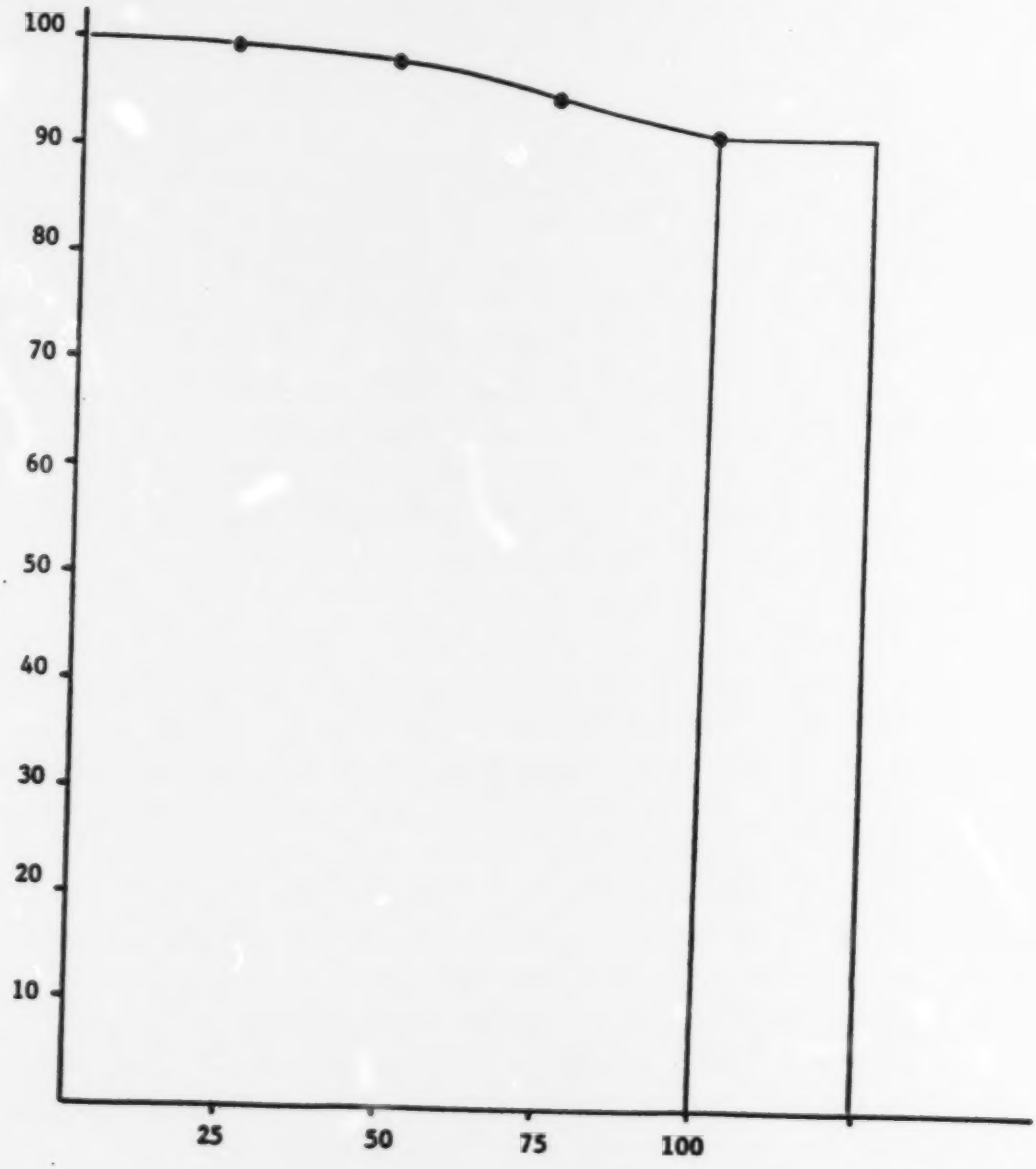

Table 25 - Cumulative Liberation Yield Diagaram - Gravity Concentrate - Pyrite

Table 12 indicates the relative proportion of minerals of interest (oxides-sulphides only). The concentrate product was predominently comprised of arsenopyrite, loellingite, wolframite and silicates with minor to trace quantities of fluorite, native bismuth, pyrite, molybdenite, bismuthinite, sphalerite and chalcopyrite. Based on relative proportions, the oxides-sulphides, silicates and fluorite contributed by volume, 77.9%, 20.04% and 2.05%, respectively.

Also indicated by Tables 12 and 13 were the degree of liberation of the major mineral species. Arsenopyrite/loellingite and wolframite exhibited liberation values of 96.5% and 97.9%, respectively. Inclusion of particles containing greater than 75% of wanted mineral illustrated enhanced liberation recovery levels for arsenopyrite/loellingite and wolframite of 99.6% and 99.05% respectively. Overviews of the degree of liberation of the primary mineral species, arsenopyrite/loellingite, wolframite and fluorite, are displayed in Photomicrographs 11 and 12.

The binary and polymineralic associations observed in the flotation concentrates are exhibited in Tables 15 and 16. Examples of bimineralic and polymineralic sulphide particles are given in Photomicrographs 13 and 14. The photomicrographs clearly exhibit the prismatic to angular particles of liberated wolframite.

As noted previously, calculations of cumulative liberation yields (Tables 26, 27 and 28) indicated a predominence of grains with high proportions of wanted mineral particularly for wolframite (Table 26). Fluorite also displayed similar, though less acute, trends (Table 27) to occur as greater than 50% volume of wanted mineral within specific particles.

1187A

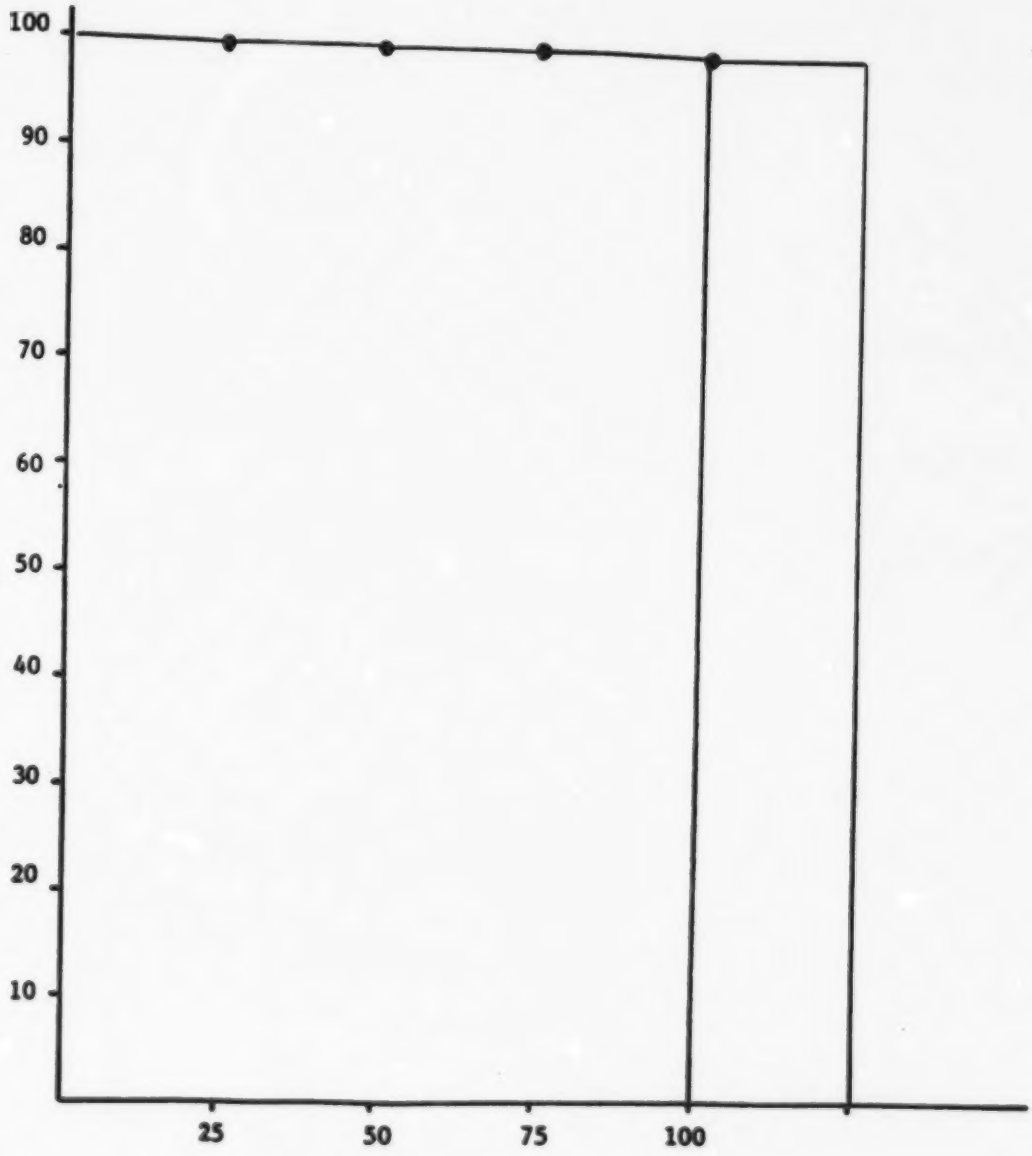

Table 26 - Cumulative Liberation Yield Diagram - Flotation Concentrate - Wolframite

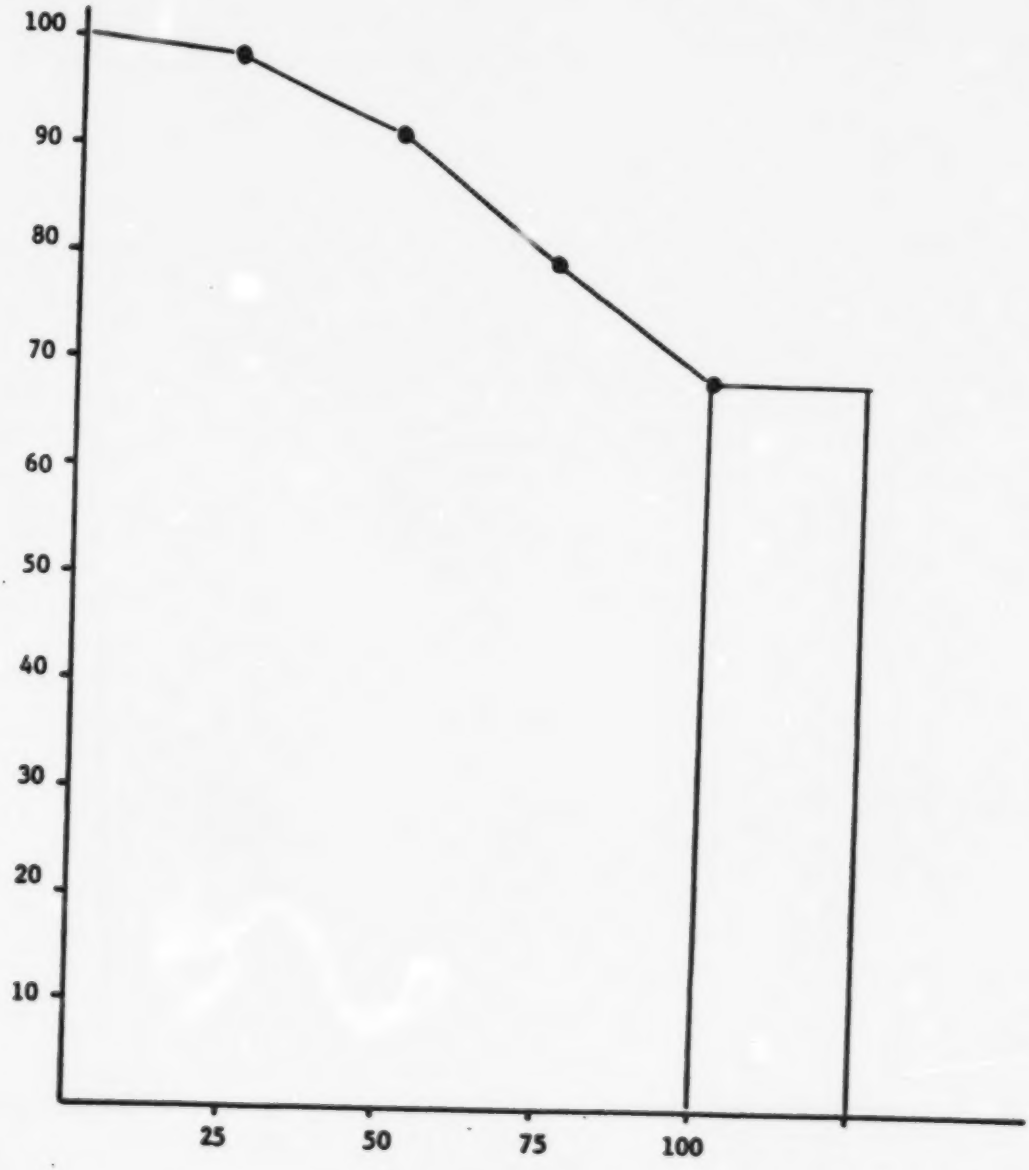

Table 27 - Cumulative Liberation Yield Diagram - Flotation Concentrate - Fluorite

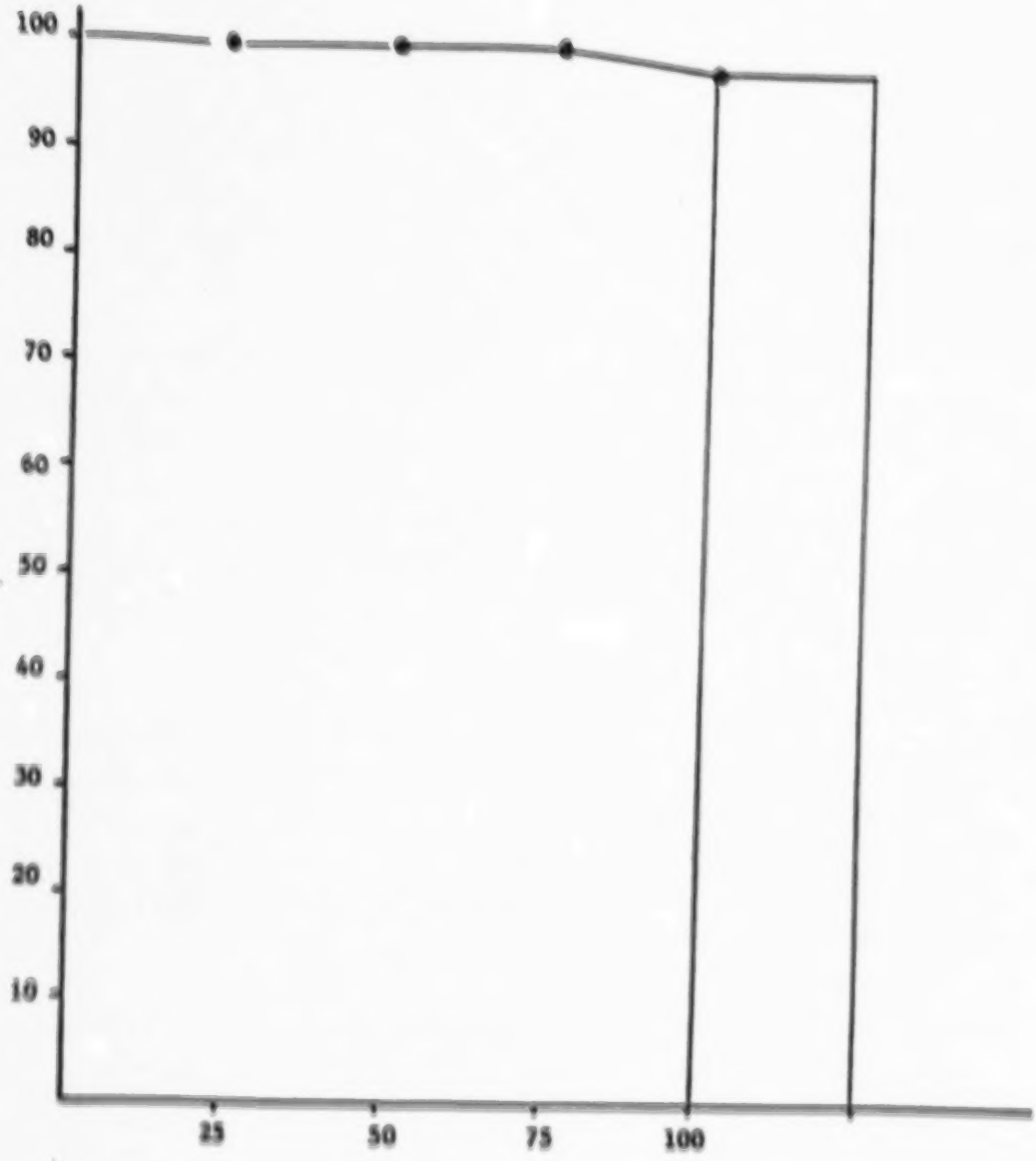

Table 28 - Cumulative Liberation Yield Diagram - Flotation Concentrate - Arsenopyrite

The binary particles, which occur with fluorite, are listed in Table 15, and are comprised primarily of sulphides and wolframite with minor silicates.

3.2.3 Ore

MP1,6 (+20 mesh)

The results of mineral liberation studies on the coarse ore screen fractions are given in Tables 6 and 13. All liberation data was calculated by surface area counting of mineral grains. Average particle size of the MP1,6 sample was approximately 1200 microns.

Table 6 illustrates the relative distribution of mineral species of interest (oxides-sulphides only). The presence of coarse masses of sphalerite, galena, pyrite, arsenopyrite, loellingite and fluorite within the ore body result in widely variable mineral proportions in coarse screen fractions. As such, few coarse particles of pyrite, arsenopyrite/loellingite and wolframite contribute heavily to the mineral balance for MP1,6.

Also indicated by Tables 6 and 13 were the degree of liberation for the major mineral species. The data indicated that isolated coarse particles of arsenopyrite and pyrite locally comprised greater than 75% of particle volume, however, overall liberation of oxides, sulphides and fluorite was effectively absent.

The minerals of interest typically comprised less than 25% of individual particle volumes in the coarse screen fraction.

Binary and polymineralic associations were ubiquitous with several specific groupings including arsenopyrite with loellingite, bismuth and molybdenite; sphalerite with galena, stannite, chalcopyrite, and tennantite; wolframite with bismuth and molybdenite; and wolframite with fluorite and silicates. All of the above groupings typically occurred as fine to coarse patches, of up to 1100 microns, within fractured quartz, a breccia matrix comprising quartz, topaz, chlorite, biotite, kaolinite and serpentine, or as disseminated crystals within quartz, topaz, chlorite and commonly fluorite.

MP2,7 (+48 mesh)

The results of mineral liberation studies, based upon surface area data, in the +48 mesh screen fraction, are given in Table 7. Average particle size of the sample was approximately 600 microns.

Table 7 illustrates the relative distribution of the mineral species of interest (oxides-sulphides only). As noted in the previous section, the presence of coarse masses of sulphide minerals were common in the Mount Pleasant ore body. The liberation data indicated the presence of coarse particles of sphalerite, galena, chalcopyrite, wolframite and arsenopyrite/loellingite. The particles ranged in degree of liberation from free to quantities of less than 25% volume within the silicate-dominant particles. Cumulative liberation calculations indicated widely variable results. High proportion of wanted minerals commonly comprised a minor fraction of the coarsely ground particles. The effects of coarse sulphide (sphalerite, galena, chalcopyrite) and oxide (wolframite) masses are clearly evident.

1187A

Liberation of sphalerite and wolframite was observed. In sphalerite, 3.14% was fully liberated with 43.0% liberated with particle volumes of greater than 75% sphalerite. The liberation of fluorite reflected the presence of coarse aggregates with values of 30.5% and 43.9% (average 37.9%) liberation from gangue.

Binary and polymineralic associations were similar to those groupings described in the previous section and by Petruk (1973) in the mineral assemblage and paragenesis section. Binary associations with fluorite are described in Table 15. The associations include all of the major sulphide minerals, oxides including wolframite and cassiterite and silicates, the latter occurring only in polymineralic aggregate particles.

MP3,8 (+100 mesh)

The results of the mineral liberation studies, based on surface area counts, in the +100 mesh fraction, are given in Table 8. Average particle size was estimated at 200 microns.

Table 8 illustrates the relative distribution of the minerals of interest (oxides-sulphides only). The influence of coarse masses of sulphide and oxide minerals was less obvious with the liberation data compared to the coarser screen fractions. The liberation abundance data indicated that the sample was comprised of abundant sphalerite and arsenopyrite/loellingite with lesser galena, molybdenite and wolframite and minor to trace quantities of chalcopyrite, pyrite, bismuthinite and bismuth.

The particles ranged in degree of liberation from those completely free of diluent minerals to those comprising less than 25 volume % of wanted mineral hosted by silicates, oxides-sulphides and/or fluorite. The results of cumulative liberation yield data are summarized in Tables 29 through 36. Wolframite, fluorite, arsenopyrite/loellingite, sphalerite, chalcopyrite, and pyrite display steep curves indicative of numerous middlings and insufficient particle size attrition. Galena exhibited a less acute trend while molybdenite was comprised of liberated particles and those grains containing less than 50% by volume of molybdenite. Clearly, addtional comminution is required to increase overall liberation and decrease the percentage of middling particles for all mineral species.

Liberation in the MP3,8 screen fraction ranged from only 32 to 63% for the major sulphide-oxide assemblage. Poor liberation of chalcopyrite, bismuth and bismuthinite are typical of these minerals which primarily occur as fine inclusions, cements and intergrowths with sulphide host particles.

Liberation of fluorite, displayed in Table 8, at 67.5 volume %, exceeded the sulphide and oxide liberation, and the middling particles comprised a variety of binary and polymineralic associations (Table 15).

MP4,9 (+200 mesh)

The results of the liberation studies are summarized in Table 9. Average particle size of the sample was estimated at 90 microns.

1187A

Table 9 indicates the relative distribution of the mineral species of interest. The data indicated that the sample was primarily comprised of sphalerite with lesser arsenopyrite/loellingite, molybdenite, galena and wolframite with minor to trace pyrite, chalcopyrite, bismuth and bismuthinite.

Cumulative liberation yield calculations, summarized in Tables 29 through 36, display sharp increases in overall liberation of all mineral species. The curves indicate that numerous middling associations occur within each mineral species and the slope of the curves, particularly for chalcopyrite indicate a wide scope of frequency distribution within each volume % fraction. Clearly, the liberation has increased, yet further attrition was required to optimize the mineral liberation.

Overall mineral liberation ranged from 78 - 85 volume % for the major sulphides with only 74 volume % for wolframite. Chalcopyrite, bismuth and bismuthinite occur in low populations and typically display poor to moderate liberation. Numerous binary and polymineralic associations were observed between two or several sulphides, oxides, silicates or fluorite.

Fluorite liberation was calculated at 81.8 volume % with a steep cumulative yield curve of particles comprising high proportions of fluorite. Binary and polymineralic associations with fluorite were common and are summarized in Table 15.

MP5,10 (+400 mesh)

The results of the liberation studies are given in Table 10. Average particle size was estimated at between 45 and 50 microns.

1187A

Table 10 also indicated the relative mineral frequency distribution of the sulphides - oxides group. The data indicated that the sample was primarily comprised of sphalerite with lesser molybdenite, arsenopyrite/loellingite, wolframite, galena and pyrite and minor chalcopyrite, bismuth and bismuthinite.

Cumulative liberation yield calculations, summarized in Tables 29 through 36, indicated increased particle liberation for most species. Wolframite, fluorite, arsenopyrite, molybdenite, and pyrite exhibit moderate increases with distinct optimization of the cumulative liberation curve. Chalcopyrite displayed a marked increase in overall liberation to 84 volume % with a considerable optimization of the cumulative liberation yield curve. Sphalerite and galena particle liberation yield data indicates that optimization of mineral liberation has been achieved in the interval between average particle sizes of 50 - 90 microns. The continued particle attrition to 50 microns, however, enhanced the scope of the liberation yield with attrition of middling particles.

Overall mineral liberation increased to 81 to 94 volume % for sulphide species, 96.1 volume % for wolframite and 79.2 volume % for native bismuth. The data indicated the much improved liberation of native bismuth at particle sizes below 200 mesh liberation of fluorite, increasing to 92.2 volume %, occurred with numerous binary and polymineralic associations (see Table 15). The binary occurrances, as displayed by the steep liberation yield curve, primarily contain greater than 75 volume % fluorite.

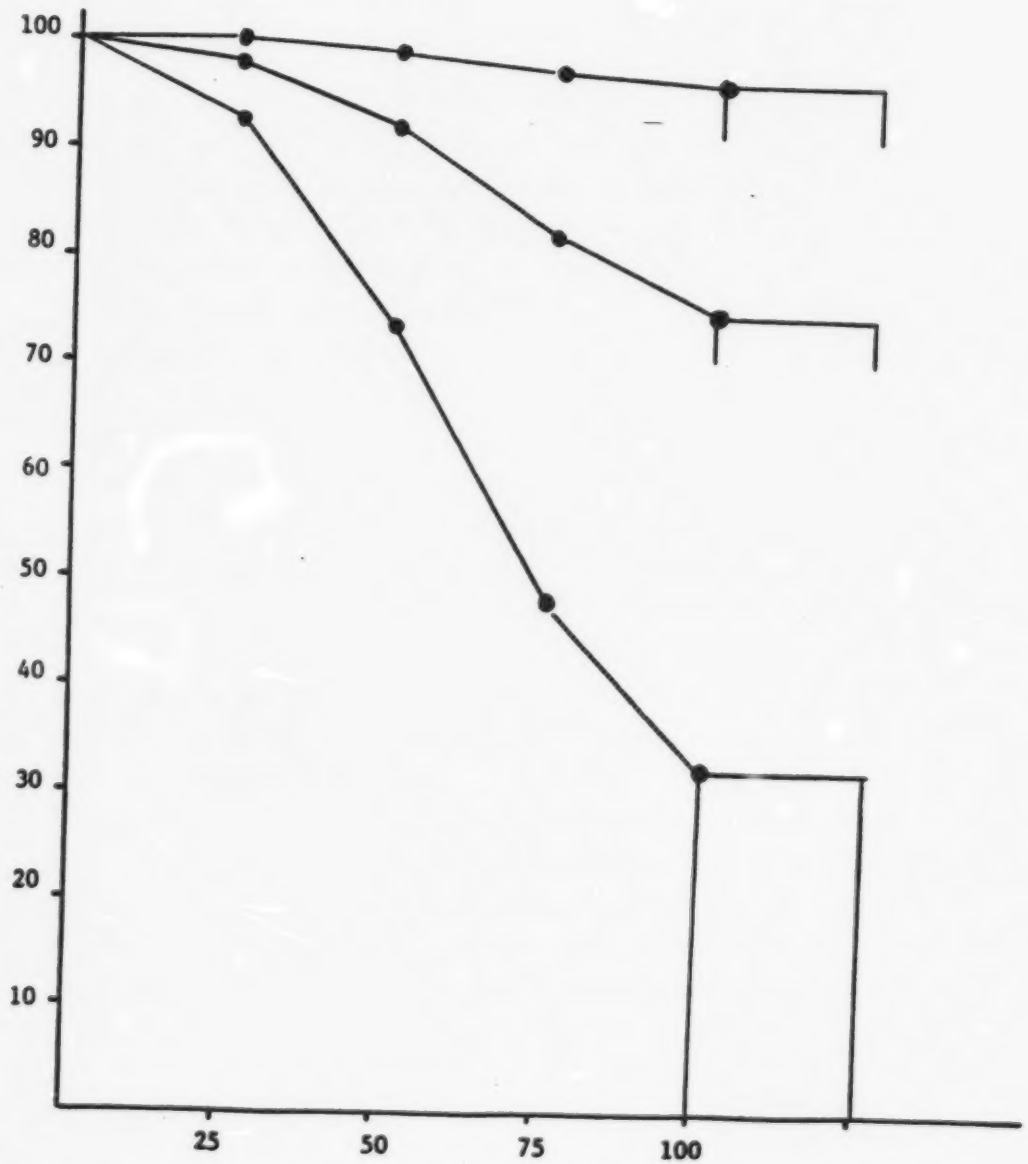

Table 29 - Cumulative Liberation Yield Diagram - Ore - Wolframite

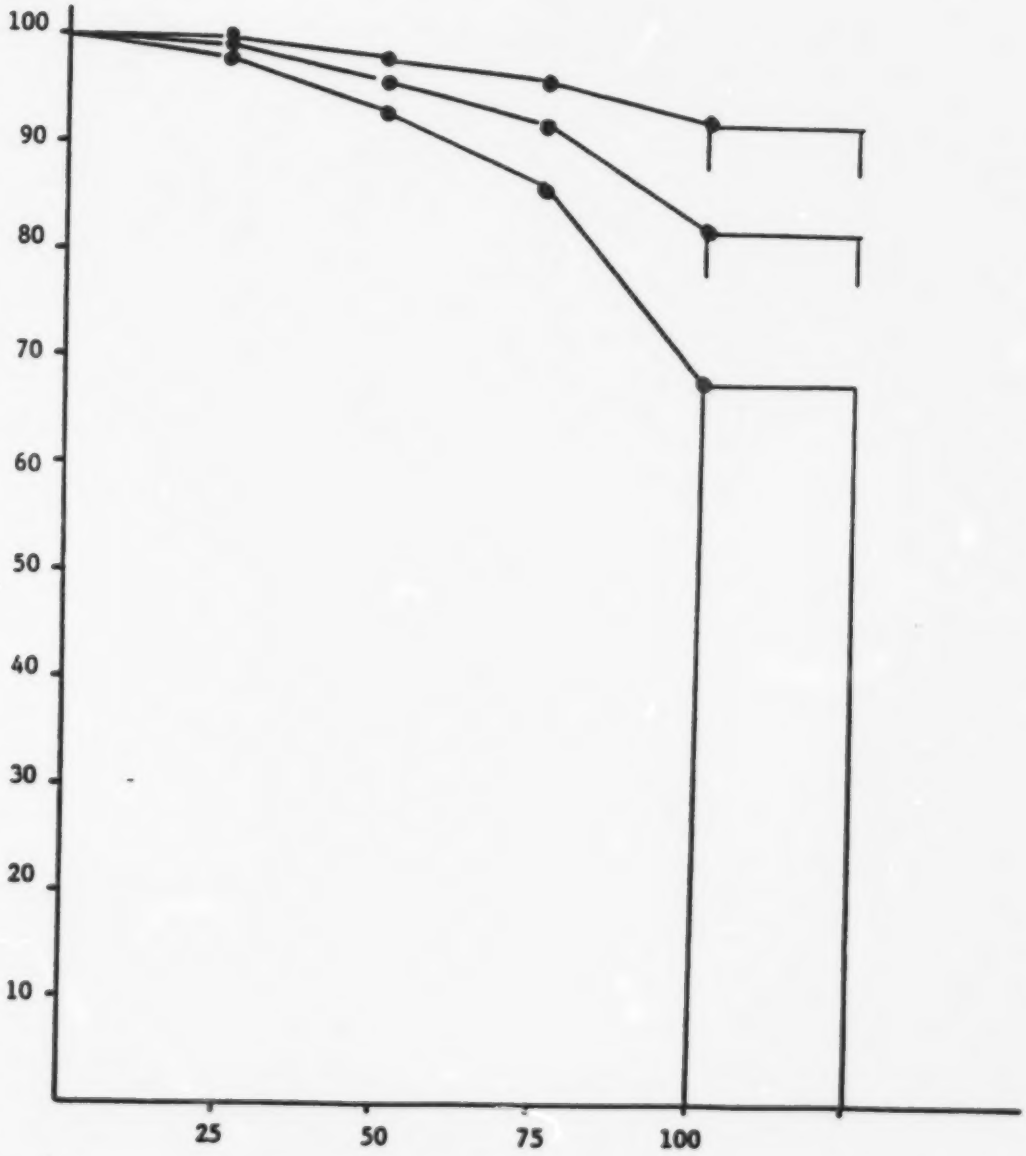

Table 30 - Cumulative Liberation Yield Diagram - Ore - Fluorite

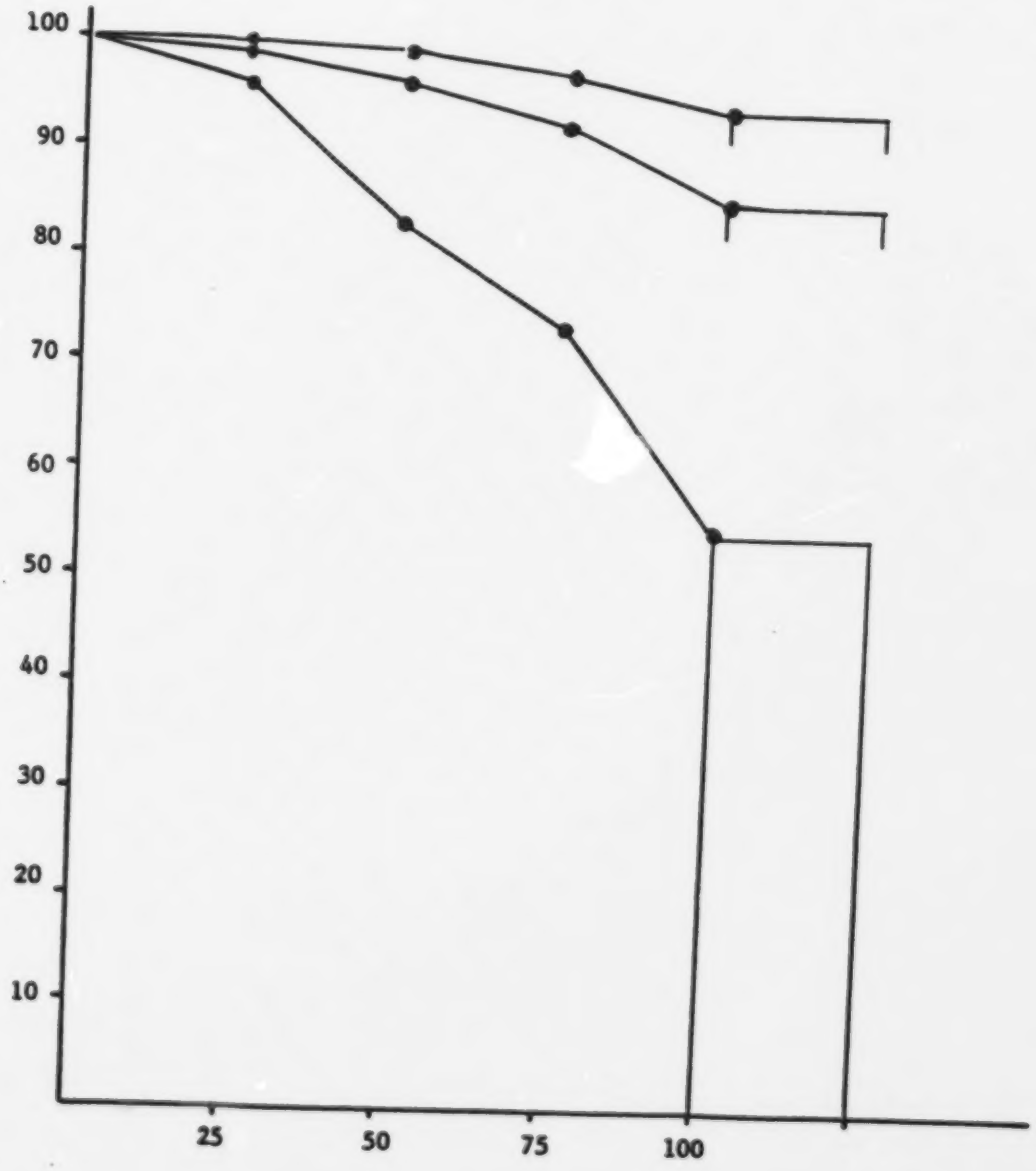

Table 31 - Cumulative Liberation Yield Diagram - Ore - Arsenopyrite

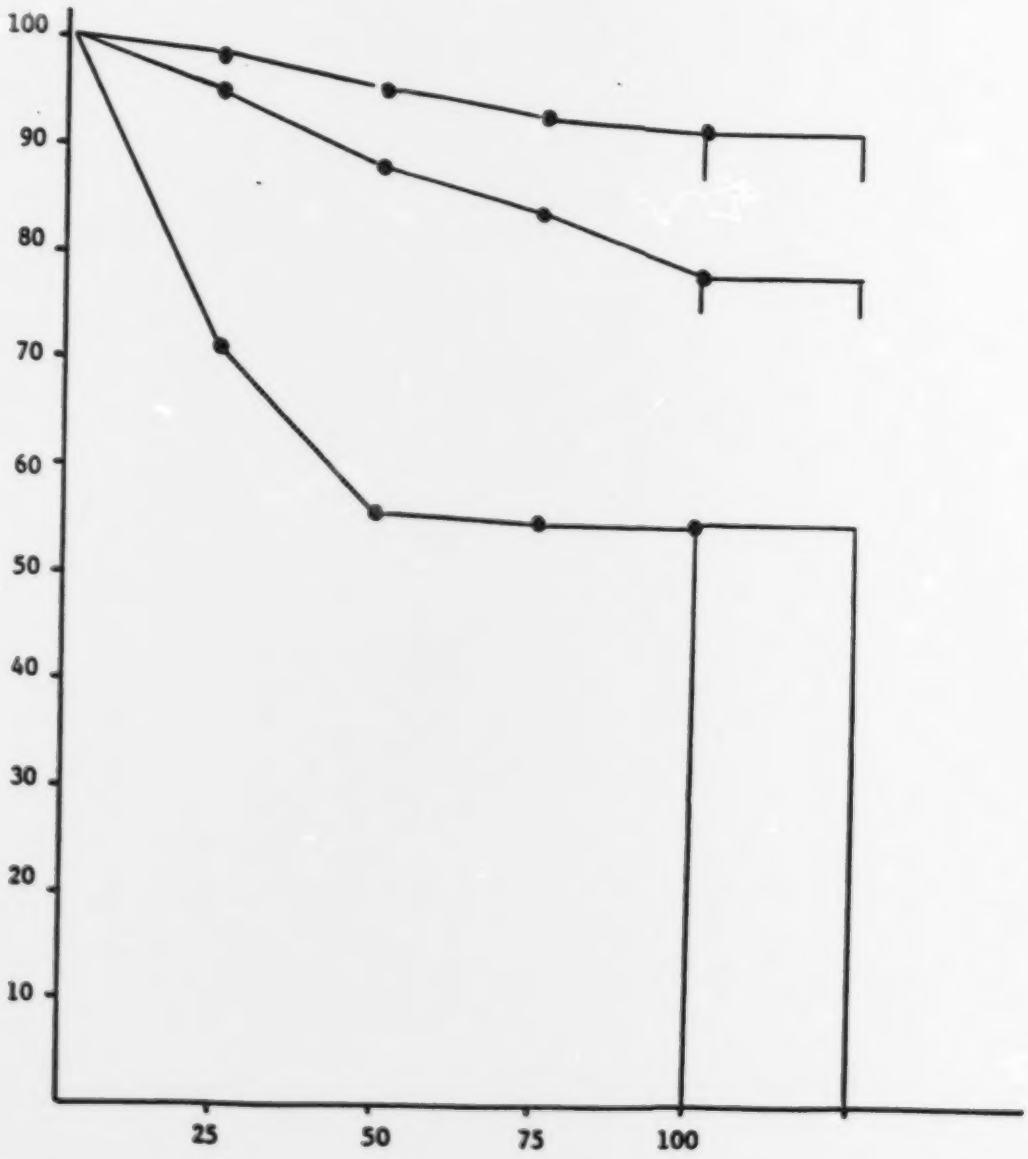

Table 32 - Cumulative Liberation Yield Diagram - Ore - Molybdenite

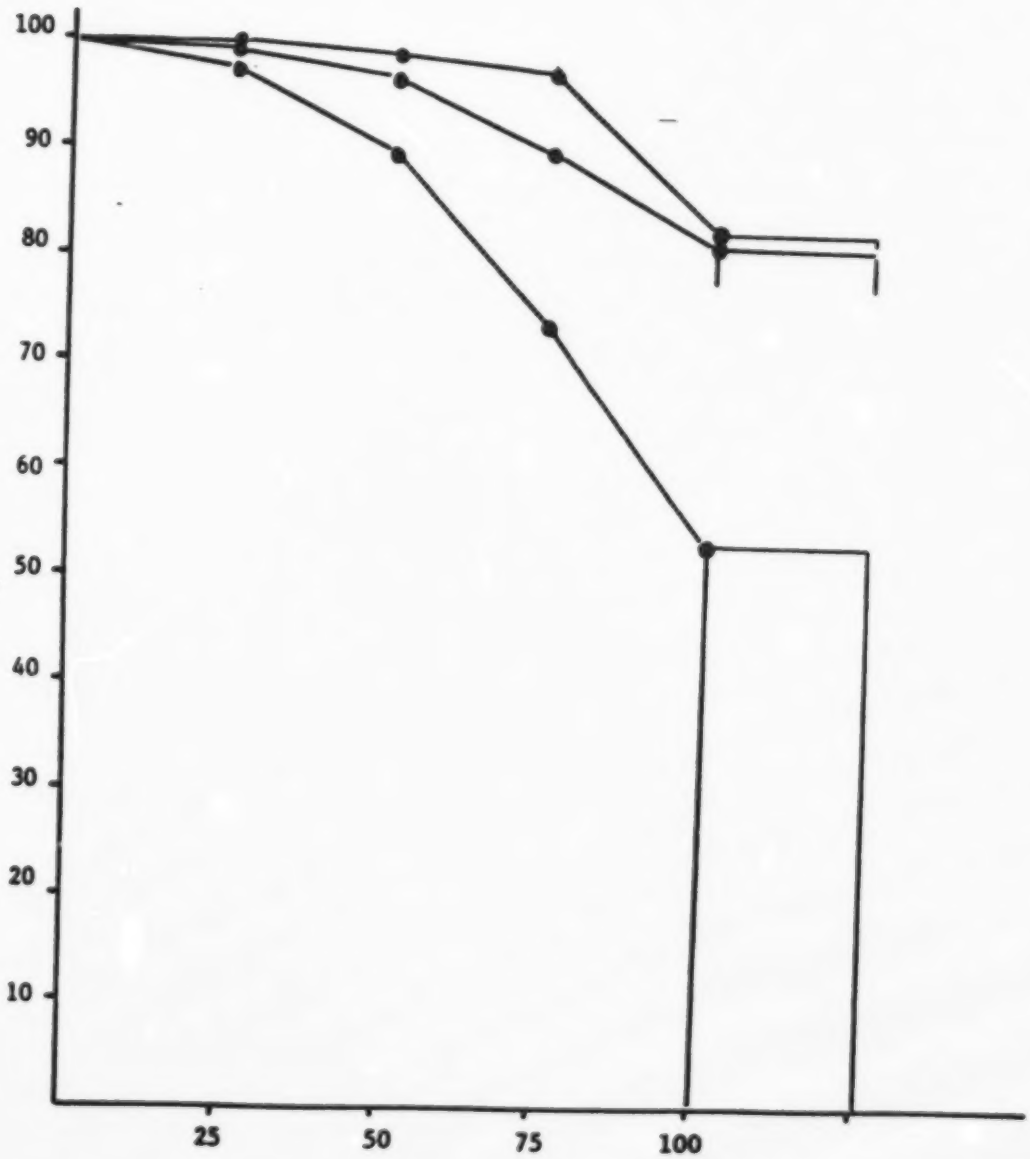

Table 33 - Cumulative Liberation Yield Diagram - Ore - Sphalerite

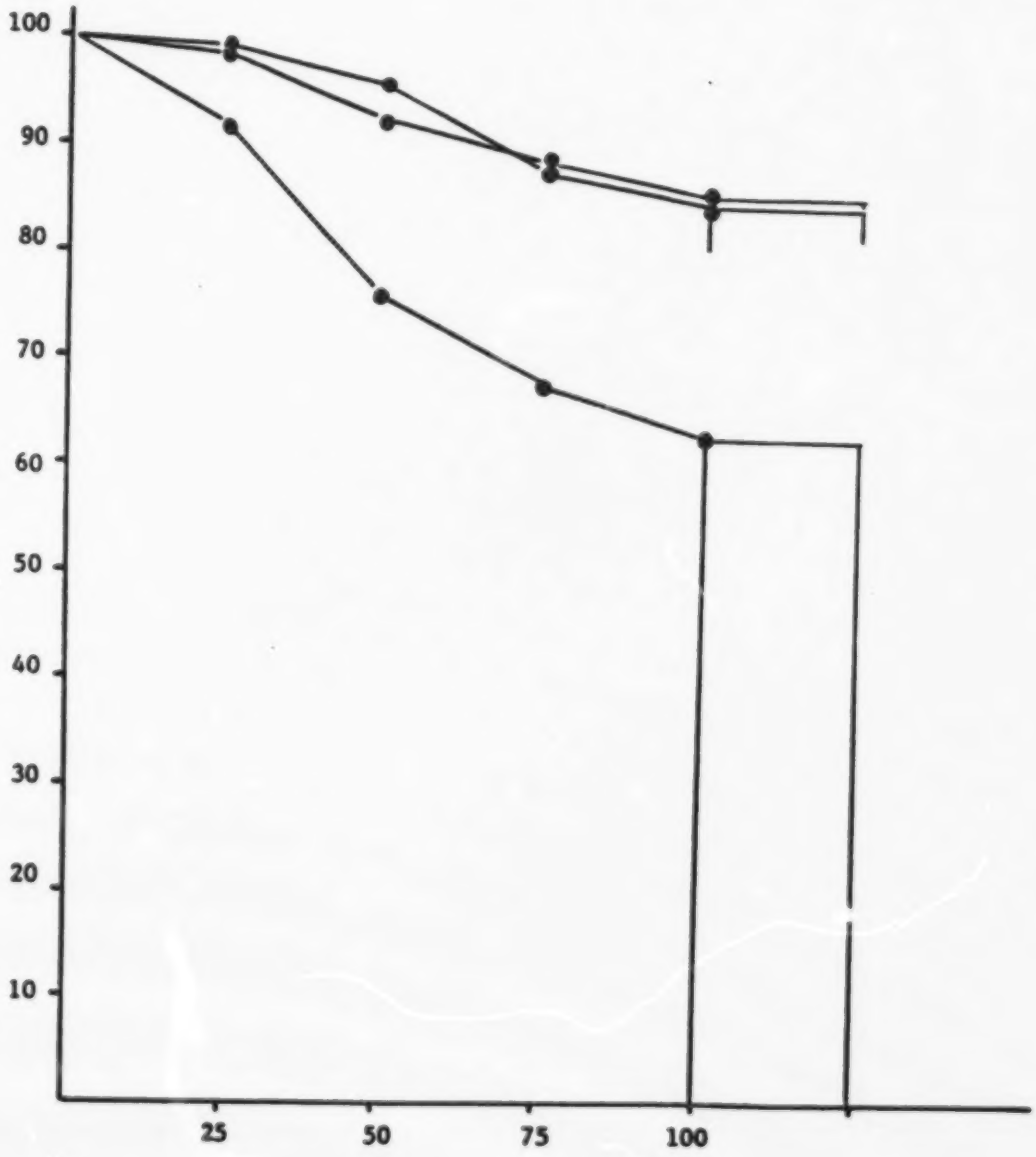

Table 34 - Cumulative Liberation Yield Diagram - Ore - Galena

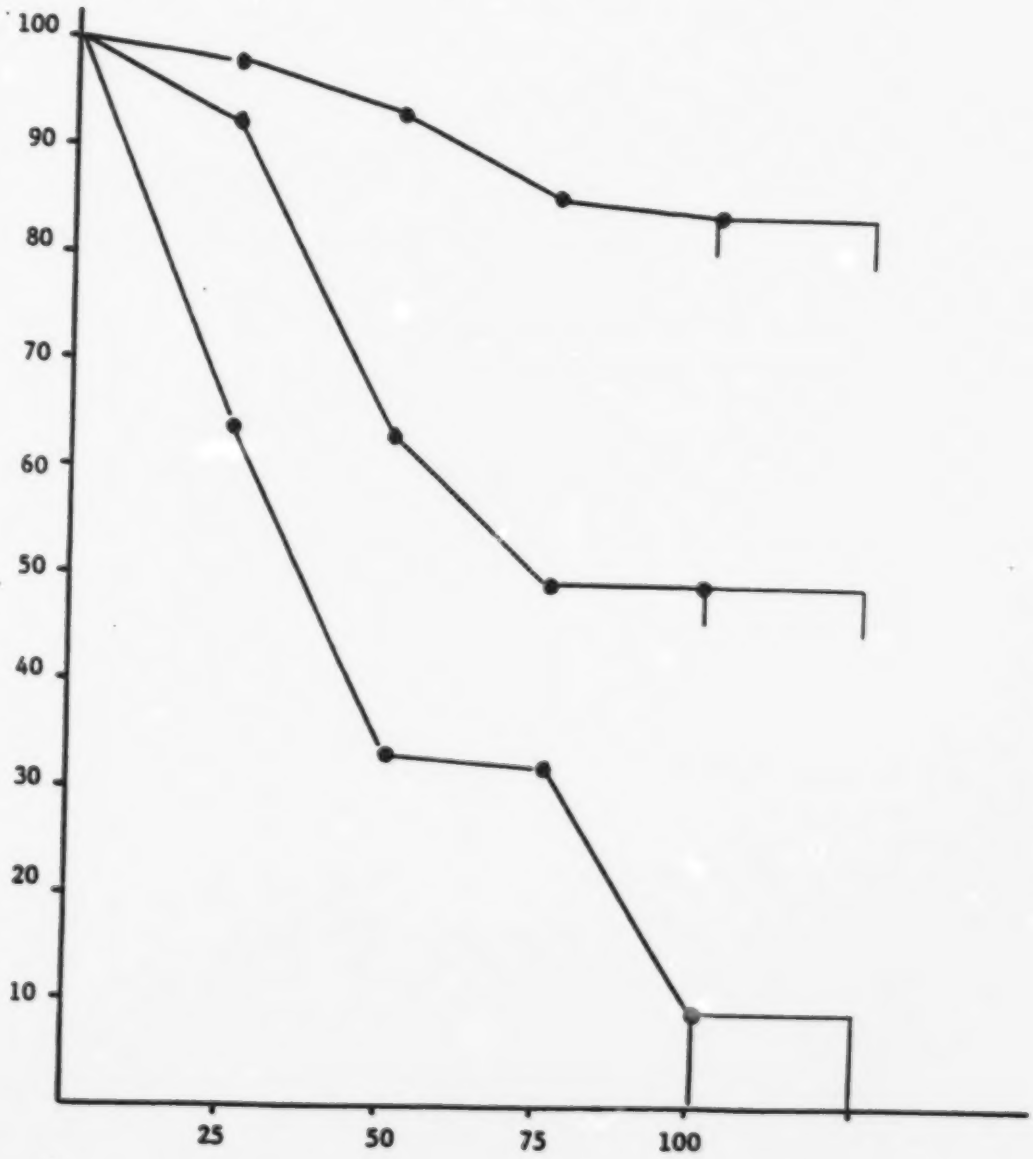

Table 35 - Cumulative Liberation Yield Diagram - Ore - Chalcopyrite

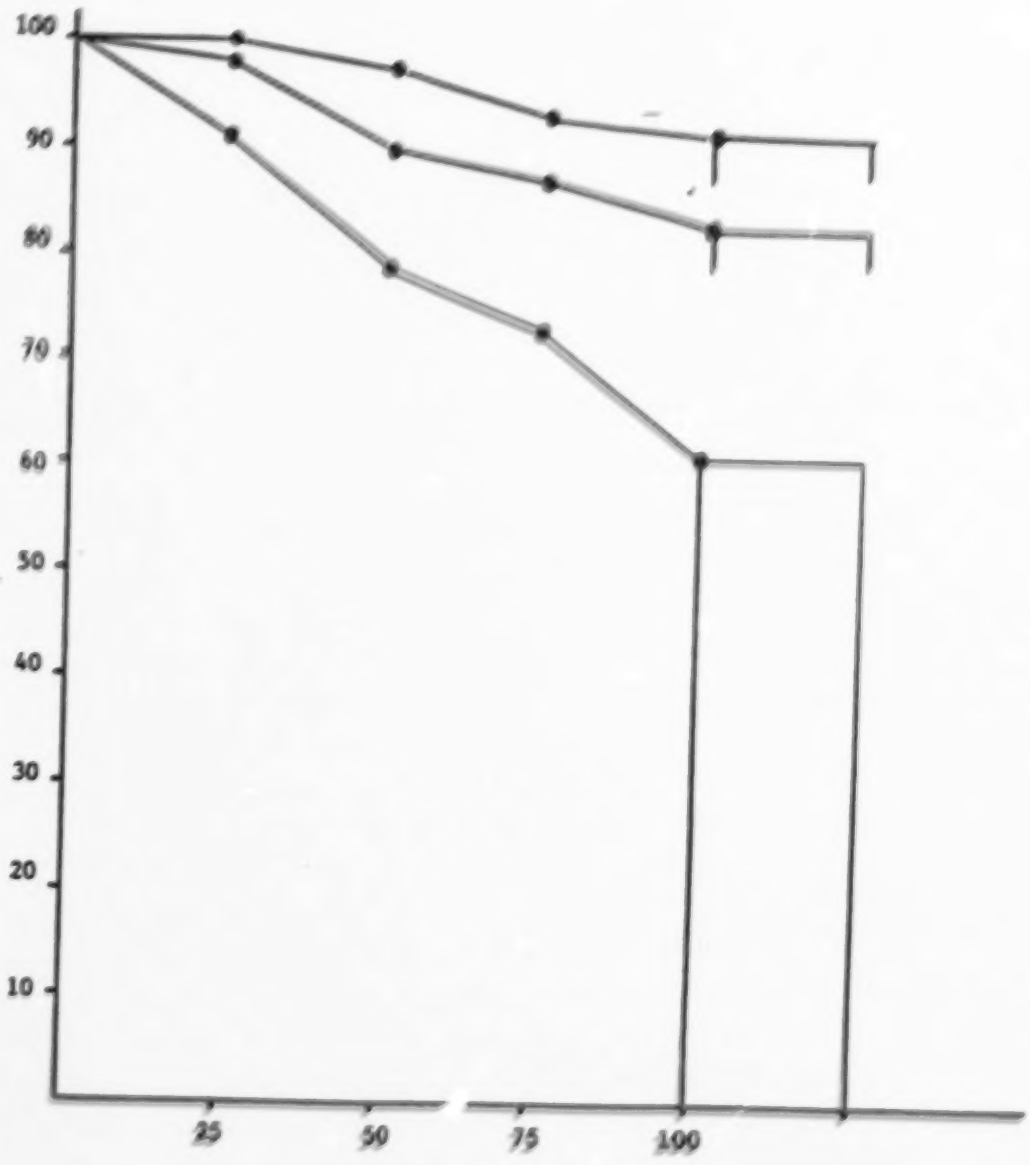

Table 36 - Cumulative Liberation Yield Diagram - Ore - Pyrite

4.0 DISCUSSION OF MINERAL BENEFICIATION

Mineralogical studies of the ore mineral assemblage were performed on feed, flotation concentrate, and gravity concentrate products from the Mount Pleasant tin mine, Charlotte County, New Brunswick. The mineralogical examination was conducted on five screen fractions of the ore feed (+20 mesh, +40 mesh, +100 mesh, +200 mesh and +400 mesh), and directly on the concentrate products.

The mineral assemblage, listed in Table 3, comprised a series of depositional events, where ore minerals of copper, lead, zinc, indium, tungsten, tin, molybdenum, bismuth and possibly yttrium-rare earths (see Table 6) were deposited upon an alteration assemblage. The latter, comprising primarily silica, topaz, fluorite, kaolinite and chlorite represent replacement minerals in a protore of feldspathic porphyry breccia, quartz veins and subjacent microgranitic stock.

Beneficiation of the ore minerals was typically limited by the fine particle size and liberation size of each mineral species. However, as noted by Petruk (1973), the mineralization was hosted by highly fractured to crushed grains of quartz and topaz or the strongly altered breccia matrix comprised of quartz with lesser chlorite, clays, fluorite and serpentine. It was expected that separation from the silicate-dominant gangue could be readily achieved.

Particle sizes of the ore minerals vary from less than one micron (eg. bismuth in arsenopyrite) to over 1200 microns (eg. wolframite, sphalerite). Within the coarse ore screen fractions, masses of sulphides - oxides - fluorite were observed. The distribution of the coarse masses was erratic. The ore minerals, more commonly, occurred as crystals and crystal aggregates ranging up to 200 microns in diameter.

However, the particle size range exhibited considerably less variance for several mineral species of interest including bismuth, bismuthinite, chalcopyrite, and rare earth-yttrium minerals. For most particles, these minerals were unliberated if particle sizes exceeded 75 microns.

Satisfactory beneficiation of the ore minerals from the greisenized breccia required intensive grinding. To properly assess the grind requirements, mineral liberation curves were plotted for minerals of interest (see Tables 37 through 40). The curves indicate not only completely liberated mineral grains but also in Tables 39 and 40, the recovery of those particles containing greater than 75% liberation (i.e. mineral of interest). The high volume percent (greater than 75%) binary and/or polymetallic particle types typically report to the concentrate. In the gravity circuit, however, the relationship between volume percent and weight percent also controls the potential recovery or loss of the binary particles, particularly where specific gravity differences are high (eg. galena - silica).

The range of specific gravities may provide the potential for several types of gravity concentrates. The minerals of interest and specific gravity factors are listed below:

Mineral	Density	
Fluorite	3.18	Grouping 1
Sphalerite	4.0	
Chalcopyrite	4.2	
Molybdenite	4.6	
Tetrahedrite	4.6-5.6	Grouping 2
Bornite	5.0	
Pyrite	5.0	
Arsenopyrite	6.0	
Wolframite	7.1-7.5	Grouping 3
Galena	7.5	

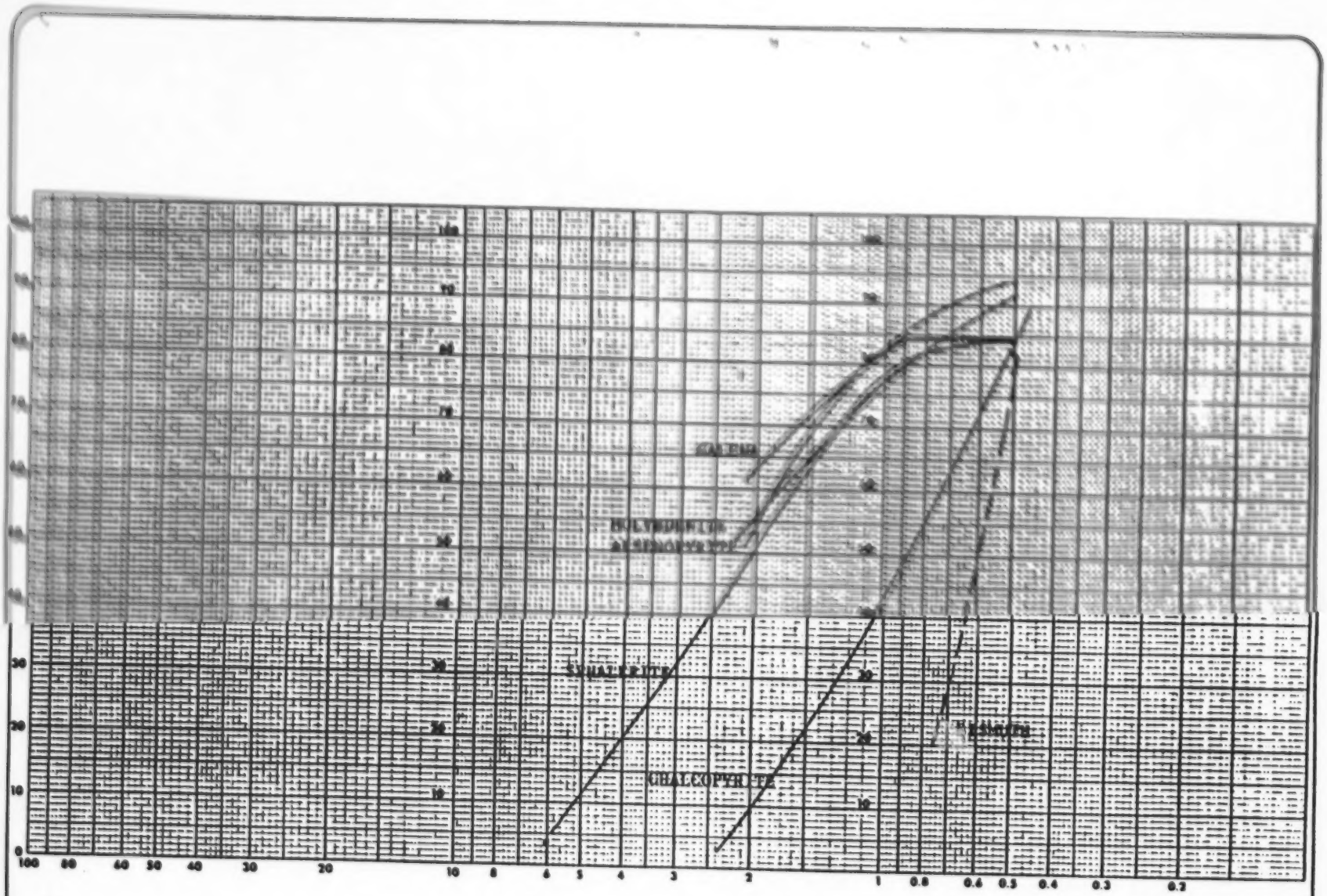

Table 37 - Liberation Curves - Complete Liberation - Sulphides

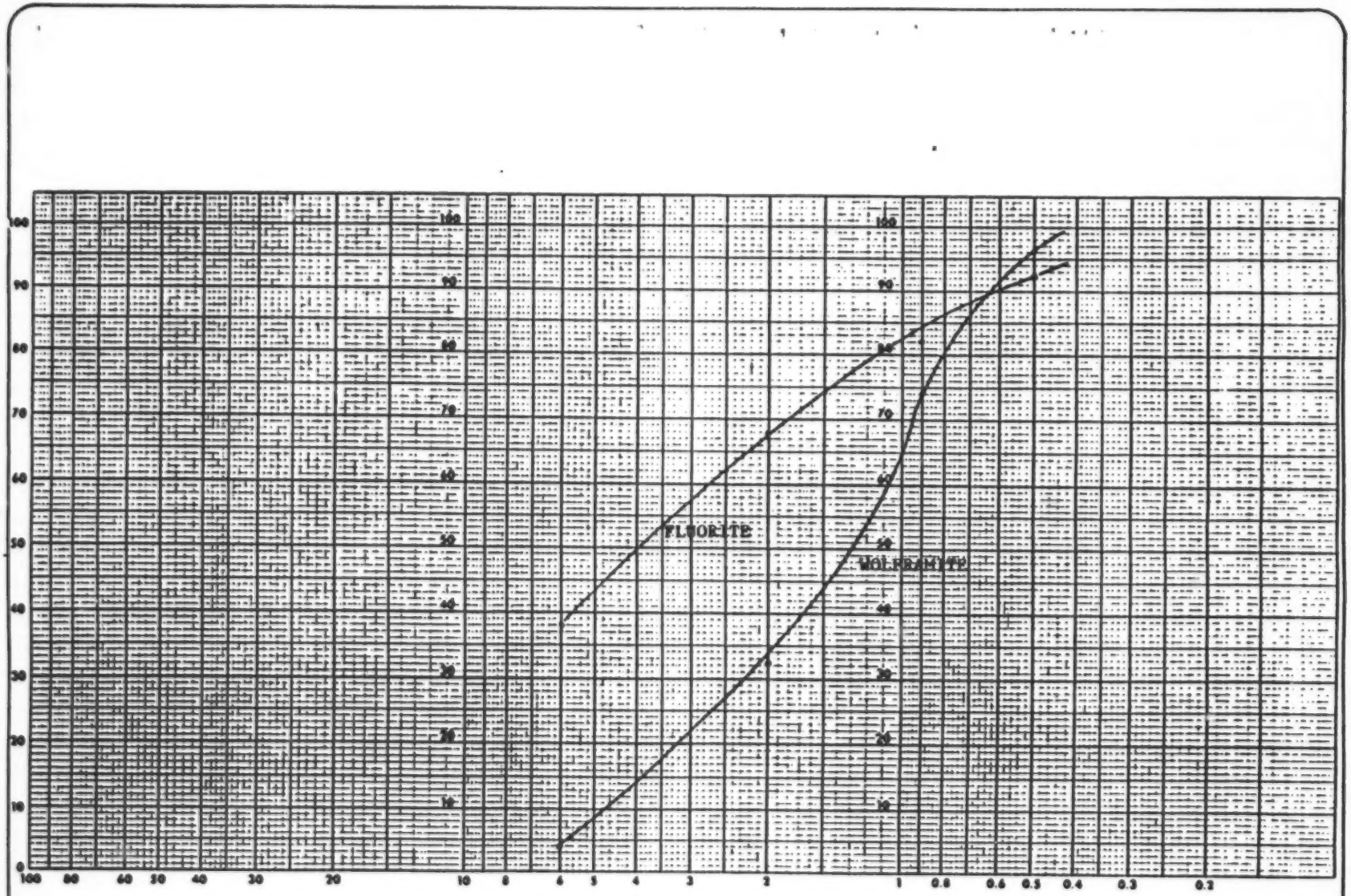

Table 38 - Liberation Curves - Complete Liberation - Wofram ite, Fluorite

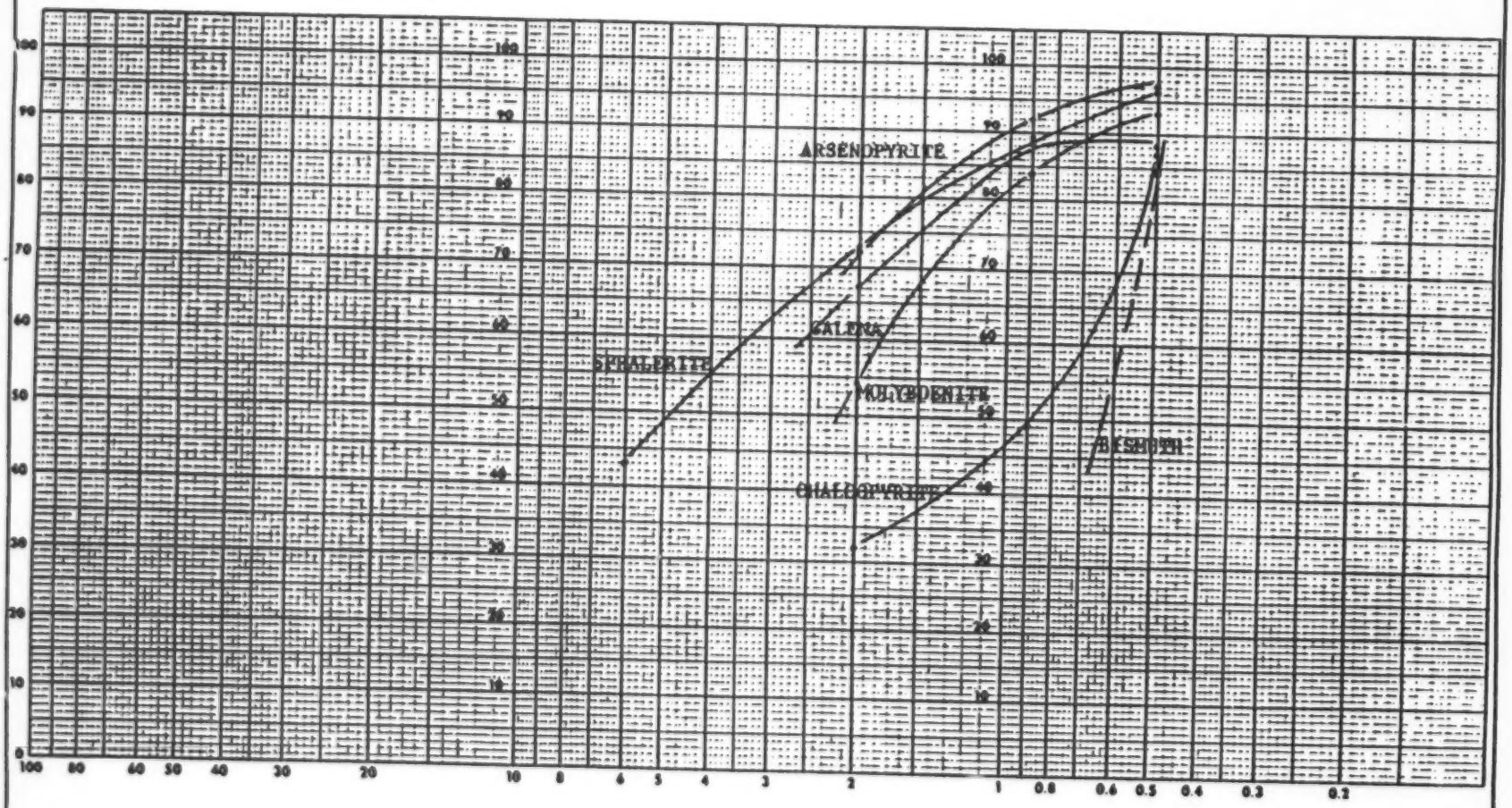

Table 39 - Liberation Curves - +75% Liberation - Sulphides

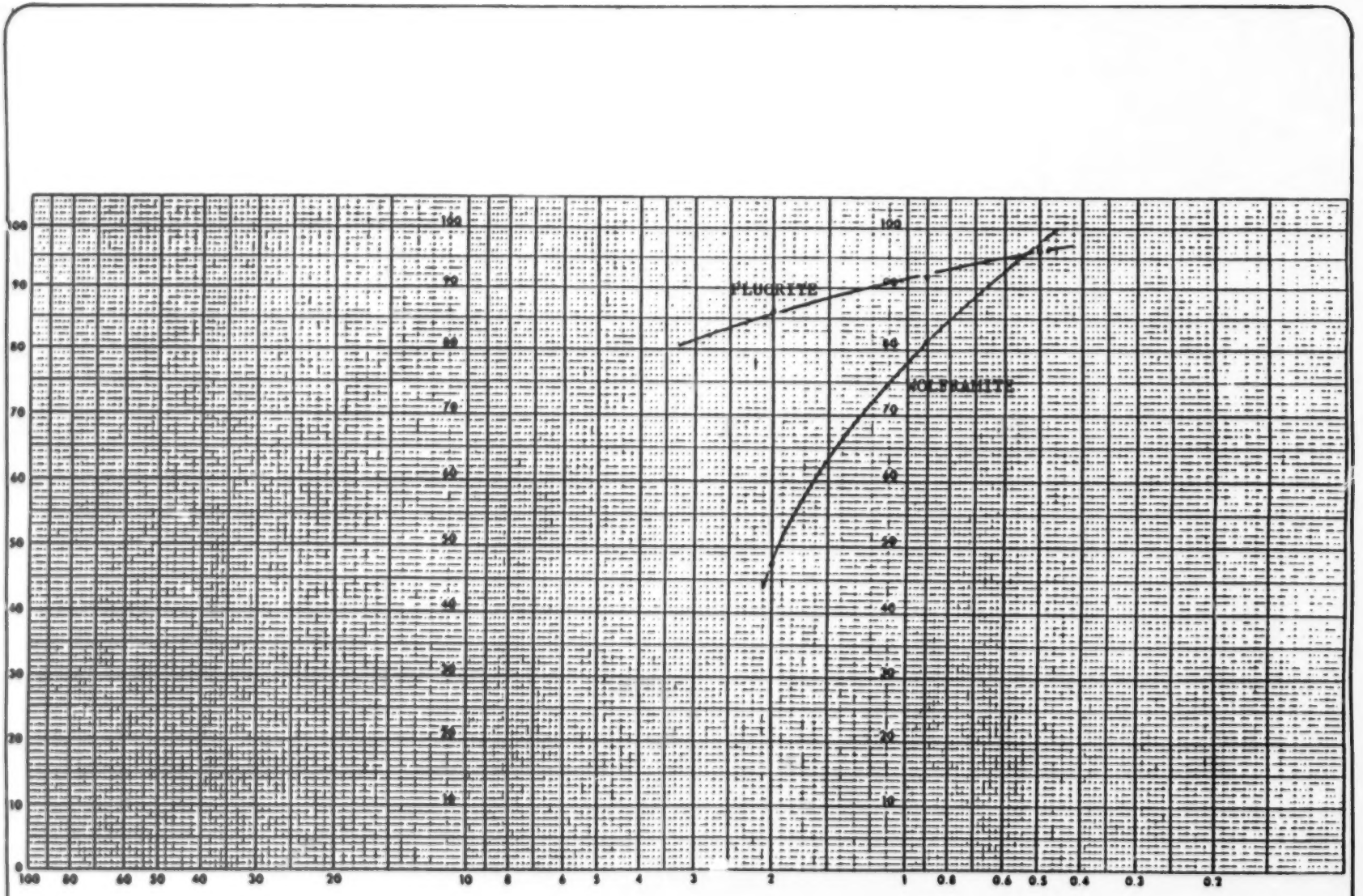

Table 40 - Liberation Curves - +75% Liberation - Wolframite, Fluorite

Optimization of gravity processing routes may allow for three product groupings, as shown, based on S.G. ranges. The latter galena - wolframite product could be easily separated by an oxide or sulphide flotation stage.

The liberation curves indicate that grinds of 100% passing 200 mesh (74 microns) with P_{50} of approximately 50 microns may be required to effectively liberate greater than 85% of each wanted mineral species. The major ore minerals comprising wolframite, fluorite, sphalerite, galena, arsenopyrite/loellingite, and molybdenite exceed 85% liberation at particle sizes from 50-75 microns. Particle liberation decreases rapidly at dimensions above 100 microns. Liberation of minor ore minerals including pyrite, chalcopyrite, bismuth and bismuthinite, typically exhibit steep liberation curves with effective liberation only at particle sizes below 50 microns diameter (Tables 37 and 39). Effective liberation of the major sulphide species, with particles containing greater than 75 volume % of wanted mineral, typically ranged from 89 volume % to 96 volume % below 75 microns diameter.

4.1 Copper-Zinc-Lead

The copper mineralization occurred primarily as chalcopyrite with lesser tetrahedrite-tennantite, bornite, covellite, and stannite-kesterite-stannoidite.

In general, the copper minerals exhibit poor to moderate liberation below 75 microns particle size and are typically associated with sphalerite. The copper minerals may exhibit variable liberation from crystallographically controlled inclusion-type and interstitial cement-type associations with sphalerite. Tetrahedrite-tennantite, the youngest primary copper sulphide mineral, was associated commonly with arsenopyrite and loellingite, bismuthinite and bismuth.

The liberated copper minerals can be selectively recovered to a copper flotation product although the portion of copper reporting to a zinc concentrate may be prohibitive. In addition, the copper concentrate will contain several minor elements including tin from stannite-kesterite, antimony and arsenic in tetrahedrite-tennantite and possibly indium from roquesite (Petruk, 1973)which could adversely affect marketability.

Zinc occurs primarily as sphalerite with minor stannite-kesterite. The sphalerite displays excellent liberation potential for flotation or gravity recovery. However, the content of submicron to 45 micron inclusions in the minus 200 mesh sphalerite will dilute the zinc grades.

Lead occurred primarily as galena with minor to trace amounts of galenobismutite and cosalite. Galena exhibited relatively high degrees of liberation (84-89 volume %) of particle diameters of 50-75 microns and typically comprised massive crystals with few, if any, inclusions.

In addition, a portion of the galena, occurring with sphalerite would report to a sphalerite (zinc) flotation product. Much of the liberated galena would easily report to a lead flotation concentrate.

Recovery of the copper-lead-zinc into a bulk sulphide gravity concentrate also shows considerable promise. The gravity concentrate may also preferentially concentrate very fine liberated galena.

4.2 Molybdenum, Bismuth

Molybdenite exhibits moderate liberation at coarse particle sizes and increases with particle comminution. The molybdenite commonly occurred in association with silicate gangue, bismuth and wolframite. The liberated molybdenite, particularly in the coarse size fractions, may report to either a bulk sulphide gravity concentrate or a flotation concentrate. The latter is expected to provide additional, if not enchanced recovery, particularly at the fine particle sizes required for optimum liberation. Losses during the gravity separation may be due to the high surface area flakes.

Bismuth and bismuthinite, the primary carriers of the metal, are characteristically fine grained with adequate liberation only at particle dimensions of less than 50 microns. Effective liberation of binary particles comprising both bismuthinite and native bismuth is expected to exceed 80 volume % of available bismuth in the minus 50-75 micron particle size range. However, the remainder of the bismuth mineralization occurs within arsenopyrite and loellingite or silica. With the former association, both gravity or flotation processes will tend to concentrate the bismuth into the bulk sulphide concentrate or a specific arsenopyrite-loellingite-bismuth flotation product.

The bismuth occurring with silica would probably require a direct leach processing route. In terms of economic processing, the bismuth-silica binaries would probably be lost to a gravity or flotation tailings product. The leaching of bismuth could be applied to the gravity or flotation concentrate although regrinding may be required for economical extractions.

4.3 Tungsten, Tin

The tungsten occurs primarily as wolframite although Petruk (1973) reported traces of tungsten in rutile and molybdenite. Liberation of the coarse grained masses of wolframite occurred above 200 microns although grinding to pass 74 microns will be required to liberate in excess of 50% of the wolframite. In addition, effective liberation of the wolframite reaches greater than 90% at particle sizes of 50-75 microns. Recovery of wolframite can be achieved by gravity separation into a combined tungsten-base metal concentrate or into an oxide flotation product, similar to the product supplied by NBNRE. Cleaning of the flotation and/or gravity products by variable intensity magnetic separation may produce a high quality wolframite concentrate. Contaminants in the tungsten are expected to include molybdenum, bismuth and minor silicates which form binary associations with the wolframite.

Tin mineralization occurred primarily as cassiterite, with minor stannite-kesterite. The liberation of cassiterite was not studied in detail. However, the mineralogical observations suggest that much of the tin mineralization occurred as fine grained, acicular needles and masses of cassiterite. The cassiterite was intergrown with sphalerite, fluorite, and chlorite.

Although limited separation of the cassiterite by grinding may be achieved, in part due to the differences in hardness between the sphalerite, fluorite and cassiterite, recovery by gravity would be constrained by the fine particle sizes and degree of liberation. Flotation recovery of tin may provide an alternative although much of the tin will likely accompany a bulk sulphide and/or fluorite concentrate within binary particles.

4.4 Fluorite

The fluorite commonly occurred as coarsely liberated grains between particle sizes of 200 and 600 microns (Table 38). Effective recovery of fluorite particles comprising greater than 75%, by volume, of fluorite increases to 85 volume % at 200 microns with a progressive increase to 94 volume % below particle sizes of 75 microns. The fluorite typically contained myriad inclusions of sulphides, oxides, phosphates, carbonates, and fluocarbonates.

Recovery of fluorite is typically by flotation with one to several reagents including sodium silicate, oleic acid and quebracho. The coarse liberation suggests that early flotation of fluorite should be examined and could precede a flotation and/or gravity treatment for sulphide-oxide recovery following a regrinding stage on the fluorite tailings stream.

4.5 Rare Earths and Yttrium

The rare earth mineralization comprised phosphates and fluocarbonates. Mineral chemistry indicated that the rare earth minerals were dominated by light lanthanides (Ce,La).

The phosphates, chiefly comprising monazite, primarily formed grains of less than 50 microns in diameter and occurred in binary associations with fluorite. Liberated particles of 20-35 microns were observed in the NBNRE flotation concentrate. Similar mineral associations were observed for the fluocarbonates. Bastnaesite and its associated cerium-lanthanum fluocarbonates were poorly liberated with particles typically enclosed by or exposed within fluorite.

Recovery of both phosphates and fluocarbonates are expected to pattern the trends of fluorite, during flotation, due to their binary associations. However, liberated particles of monazite, which could be recovered by gravity, if coarse particles were present, may report to the oxide flotation product. The enrichment of cerium by 8 times in the NBNRE oxide flotation concentrate confirms this interpretation. Similarily, yttrium, which may occur as xenotime, indicated an enrichment by 3 times within the NBNRE flotation concentrate. It is suggested that the phosphates are generally of very fine particle size and exhibit poor liberation. Poor results of caustic leach and acid leach tests by NBNRE concur with this interpretation. In addition, the poor acid leach test results are characteristic of monazite and xenotime, which exhibit limited solubility under acid conditions. The leach results also confirm that much of the lanthanide-yttrium carbonate mineralization (bastnaesite group) was not exposed to leach solutions under either acid or caustic conditions.

5.0 CONCLUSIONS AND RECOMMENDATIONS

1. Mineralogical studies were performed on three samples, representing ore feed, gravity concentrate and oxide flotation concentrate, from the Mount Pleasant polymetallic ore deposit, Charlotte County, New Brunswick.

2. The mineralogical examination identified a host of valuable ore minerals of copper, lead, zinc, molybdenum, bismuth, tungsten, tin, fluorine, yttrium and rare earths.

3. The ore minerals of interest occurred in a series of overlapping depositional events with a complex assemblage of oxides, sulphides, arsenides, sulpharsenides, fluorides, sulphosalts, native elements, carbonates, fluocarbonates and phosphates.

4. Mineral liberation studies indicated that intensive grinds of 100% passing 200 mesh (74 microns) are required to provide satisfactory liberation of the ore minerals. Effective liberation of the wolframite, fluorite and the major sulphide species (sphalerite, galena, arsenopyrite, loellingite and molybdenite) and minor sulphides (chalcopyrite, bismuthinite) typically ranged from 85 volume % to 96 volume % at particle sizes of less than 50 - 75 microns.

5. Cumulative liberation yield curves, optimum recovery data, and particle size - liberation curves indicate that optimum complete mineral liberation for the ore minerals was achieved at particle sizes of 75 - 90 microns (sphalerite, galena) and at less than 50 - 75 microns (bismuth, chalcopyrite, molybdenite, arsenopyrite, loellingite, tetrahedrite, fluorite, wolframite).

6. Recovery of the valuable ore minerals may be possible using gravity treatment based on production of three concentrates comprising low density fluorite, moderate density bulk sulphide (Cu-Pb-Zn-Mo-Bi), and high density galena-wolframite. The latter would require subsequent treatment by sulphide or oxide flotation or magnetic separation.

7. The mineral liberation data suggests that flotation of easily liberated fluorite could possibly precede treatment of bulk sulphides and tungsten from the fluorite flotation tailings circuit. The sulphides and/or tungsten could be effectively separated, following a regrind stage to pass 50 - 75 microns, by gravity treatment or by sulphide or oxide (wolframite) flotation.

8. A variety of contaminants and/or diluent minerals are expected within either gravity or flotation products primarily due to the abundance of unliberated binary and polymetallic particles at dimensions below 50 - 75 microns. Hydrometallurgical techniques may be required to recover the minor elements. This group of elements includes the bismuth, yttrium and rare earths. Poor liberation of the rare earth-yttrium minerals, attributed to very fine particle dimensions, and low solubility under acid or caustic conditions limits the potential recovery.

9. It is recommended that the following points or tasks be addresed in further developmental work.

   (a) detailed mineral liberation studies of a tight series of screened fractions of ore, concentrate and tailings products to fully assess the mineral - metal balance

(b) screen fraction weight and elemental assay data from various size ranges, including +65 mesh, +100 mesh, +150 mesh, +200 mesh, +270 mesh, +320 mesh, +400 mesh, +25 micron, +15 micron, +10 micron and +5 micron, with mineralogical liberation calculations for each fraction

(c) mineral liberation to include detailed analysis of binary and polymetallic particles reporting to specific fractions or products due to variable mineral partitioning

(d) mineral liberation data on actual milling circuit products to determine factors controlling optimization of mineral recovery such as circuit performance.

(e) a detailed program of metallurgical testwork utilizing gravity techniques including spirals or cones, shaking tables with sand and slime decks, and possibly Holman or Bartles-Mozley frames. The feed to a gravity circuit may also require hydrosizer or cyclone classification

(f) a program of flotation testwork utilizing direct concentration of one or several products and flotation in various combinations with gravity treatment

(g) an overall assessment of all previous mineralogical, geological and metallurgical data to evaluate the potential value of any particular processing route.

APPENDIX I

Photomicrographs and EDXA Spectral Plots

250 microns

Photomicrograph 1 - 100x R.L. Gravity Concentrate
Overview displaying numerous liberated grains of arsenopyrite, pyrite, wolframite, fluorite, galena, silicates and sphalerite-chalcopyrite. High degree of liberation with few binary particles of arsenopyrite-wolframite, arsenopyrite-bismuth and wolframite-silicates

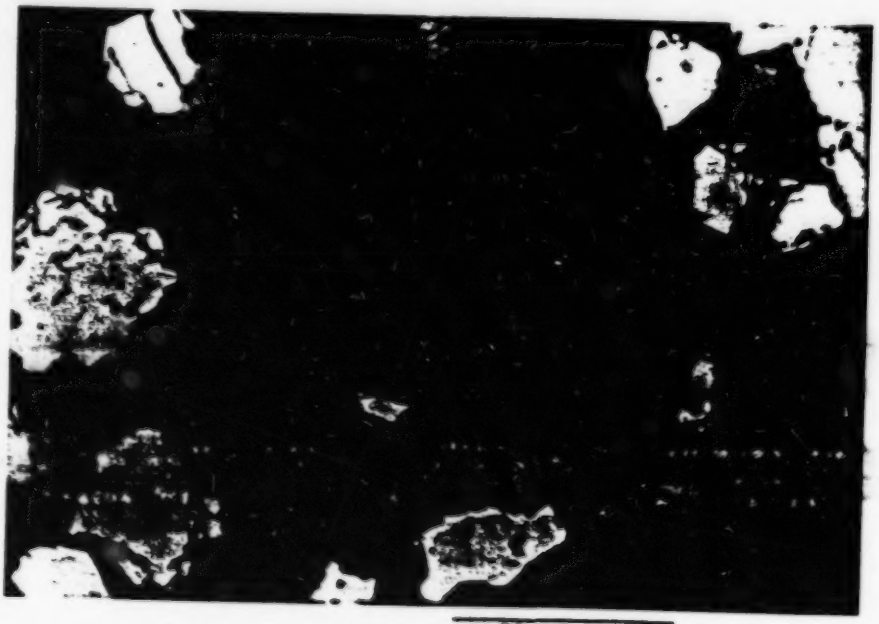

50 microns

Photomicrograph 2 - 500x R.L. Gravity Concentrate
Coarse binary particle of wolframite-molybdenite with grey molybdenite flakes occupying interstitial porosity and fracture/cleavage surfaces in wolframite. Liberated grains include galena, arsenopyrite, fluorite and wolframite

1187A

50 microns

Photomicrograph 3 - 500x R.L. Gravity Concentrate
Coarse binary particle of wolframite enclosing minute subrounded grain of bismuth; also several fully liberated wolframite particles

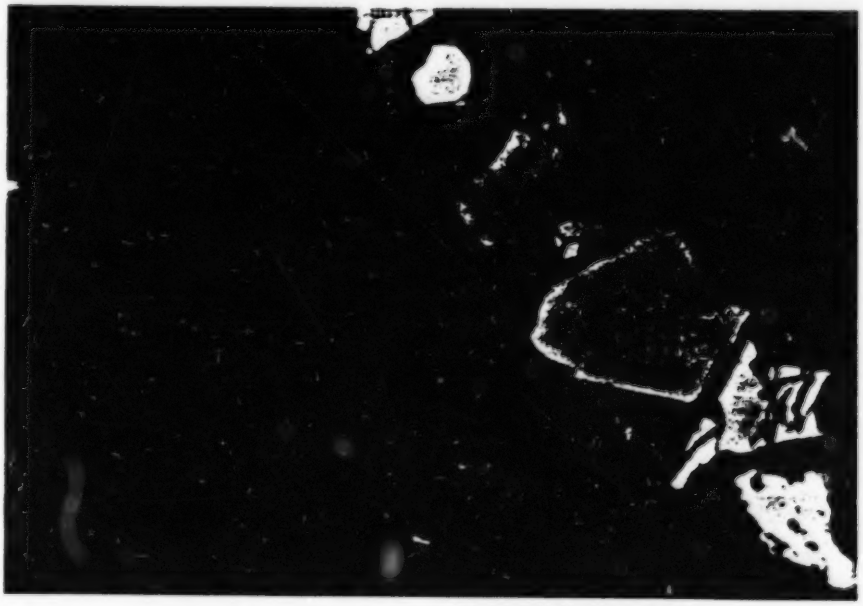

50 microns

Photomicrograph 4 - 500x R.L. Gravity Concentrate
Coarse aggregate of deformed molybdenite flakes exhibiting complete liberation. Note wide variation in flake size to a maximum length of 55 microns. Also liberated pyrite, arsenopyrite, wolframite and binary galena-silicates particle

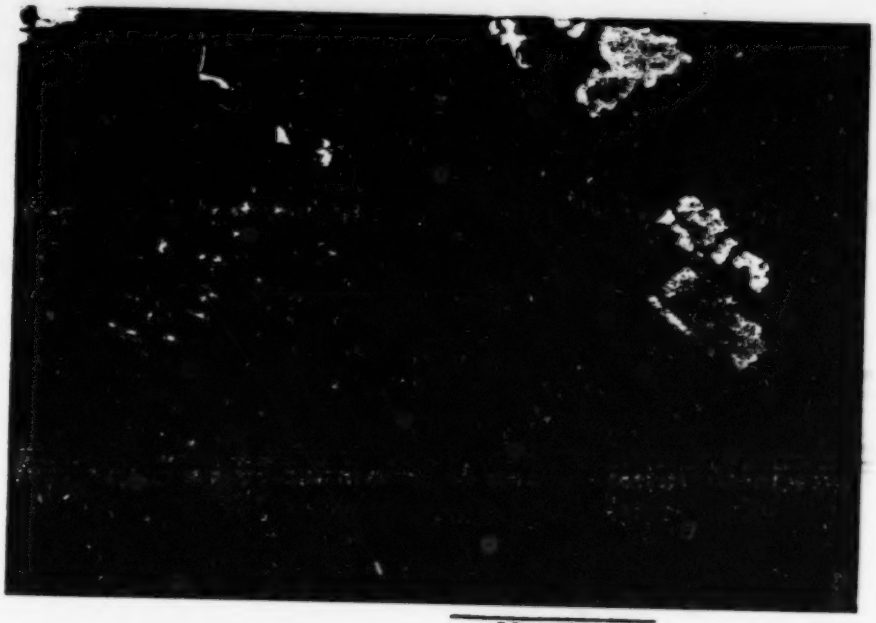

50 microns

Photomicrograph 5 - 500x R.L. Gravity Concentrate
Coarse polymineralic intergrowth of sphalerite with lenticular to elongate to subrounded inclusions of chalcopyrite and extensively disseminated minute particles of stannite-kesterite. The latter also occur as irregular ribbon lamellae. Also, liberated and binary particles of wolframite with silicates

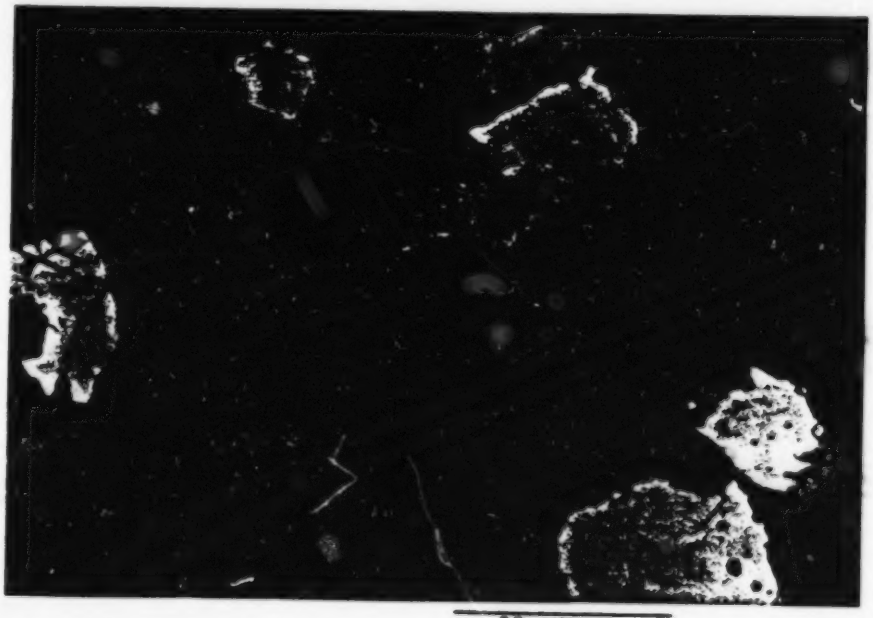

50 microns

Photomicrograph 6 - 500x R.L. Gravity Concentrate
Coarse polymineralic intergrowth of chalcopyrite and pyrrhotite with sphalerite. At right, sphalerite with chalcopyrite-kesterite inclusions along crystallographic planes

1187A

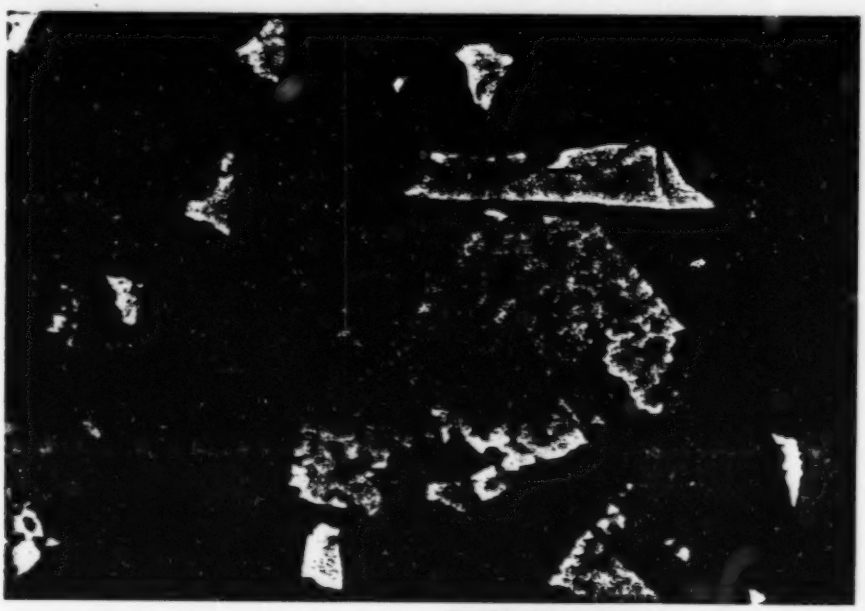

50 microns

Photomicrograph 7 - 500x R.L. Gravity Concentrate
Binary association of galena-pyrite. Galena infills interstitial-intercrystal porosity and crystallographic planes, also coarse galena aggregate crystals cement the pyrite

50 microns

Photomicrograph 8 - 500x R.L. Gravity Concentrate
Binary associations of bismuthinite-pyrite (above) and (below) arsenopyrite cemented by bismuthinite (grey) and native bismuth (yellow-orange)

1187A

50 microns

Photomicrograph 9 - 500x R.L. Gravity Concentrate
Binary associations of native bismuth-chalcopyrite, tennantite-sphalerite (at far right) and arsenopyrite subhedra cemented by native bismuth.

50 microns

Photomicrograph 10 - 500x R.L. Gravity Concentrate
Typical binary association exhibiting simple intergrowth of bismuthinite and native bismuth. Particle reports as liberated for bismuth beneficiation. Also liberated galena, arsenopyrite, wolframite, pyrite and sphalerite

1187A

250 microns

Photomicrograph 11 - 100x - R.L. Flotation Concentrate
Overview of flotation concentrate exhibits abundant liberated wolframite, arsenopyrite and minor base metal sulphides. Also several binary particles of fluorite-wolframite, wolframite-silicates. Note abundance of minus 10 micron fines

125 microns

Photomicrograph 12 - 200x - R.L. Flotation Concentrate
Liberated coarse particles of fluorite (dark, at center), grey-brown wolframite and arsenopyrite. Also, liberated particles in the minus 10 micron fraction

1187A

50 microns

Photomicrograph 13 - 500x R.L. Flotation Concentrate
Complex polymineralic intergrowth of sphalerite (dark grey), chalcopyrite, tennantite (light grey), kesterite (brown) and galena (white). Also numerous liberated particles of wolframite. Note wolframite-silicate binary (center)

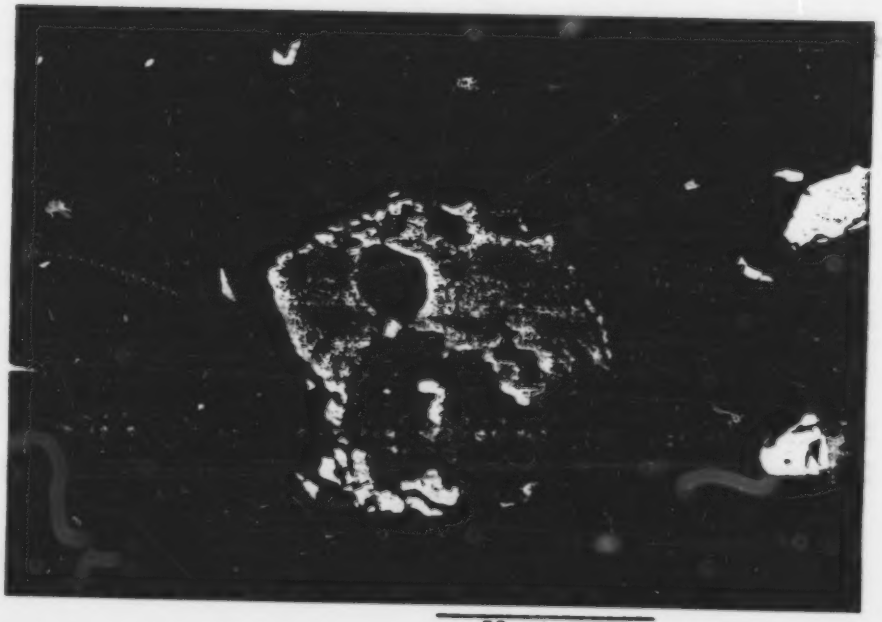

50 microns

Photomicrograph 14 - 500x R.L. Flotation Concentrate
Coarse binary sulphide particle of arsenopyrite replaced by tennantite. Also liberated wolframite; ternary wolframite-cassiterite-silicate (left)

1187A

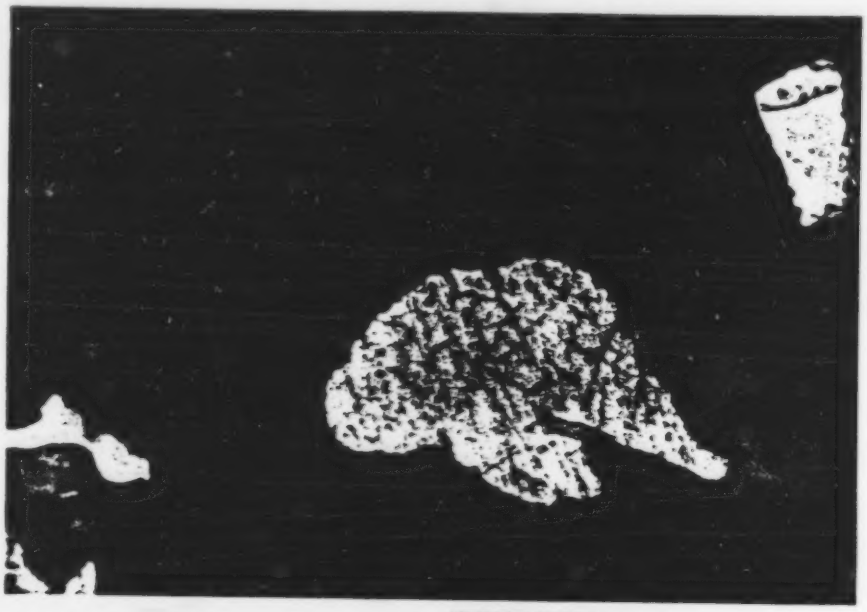

50 microns

Photomicrograph 15 - 500x R.L. Flotation Concentrate
Smooth liberated native bismuth, also wolframite and arsenopyrite

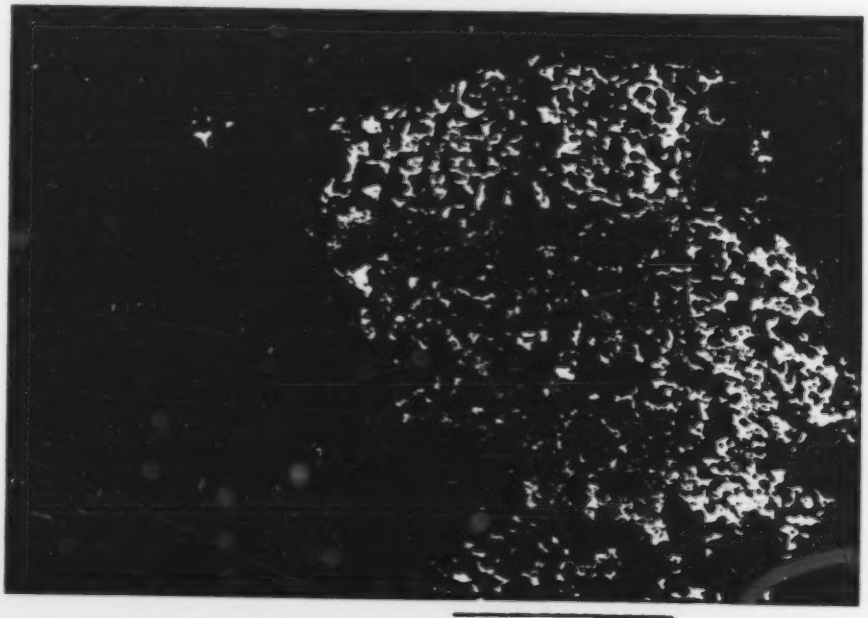

250 microns

Photomicrograph 16 - 100x R.L. MP2,7
Coarse binary type association of fluorite (dark grey) with sphalerite. The latter forms porous aggregates containing interstitial silicates, wolframite, cassiterite, fluorite and galena. Minute droplets of chalcopyrite are disseminated within the sphalerite

1187A

125 microns

Photomicrograph 17 - 200x - R.L. MP2,7

Coarse aggregate particle of sphalerite-chlorite-chalcopyrite (inclusions) - silicates cemented by fine galena and cassiterite along interstitial-intercrystal porosity; also coarse galena enclosing earlier silicates and sphalerite

250 microns

Photomicrograph 18 - 100x R.L. MP1,6

Abundant equant crystals of sphalerite with extensive exsolution textures, also minor interstitial galena, pyrite, chalcopyrite, enclosed by silicates (light grey) and fluorite (dark grey). Liberation at less than 150 - 200 mesh

1187A

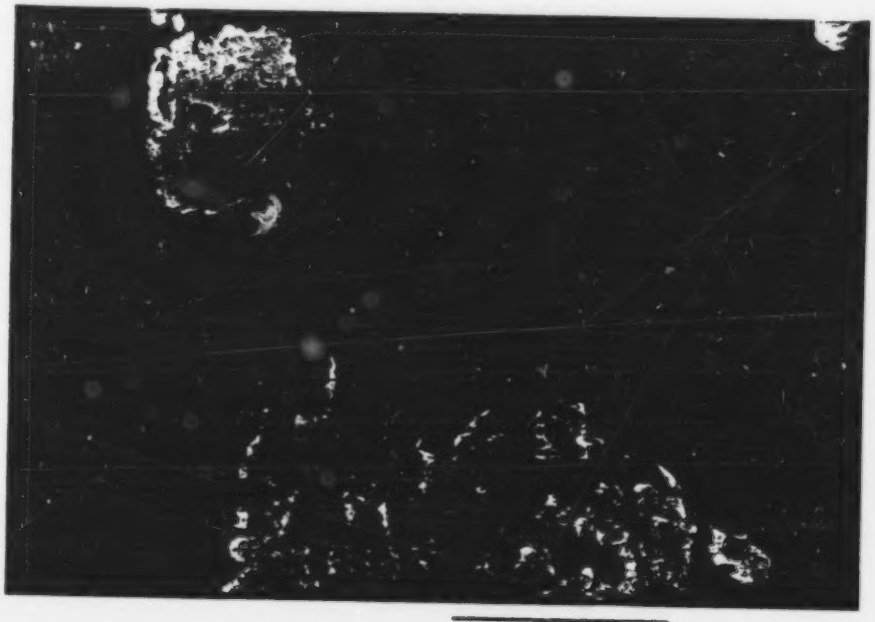

250 microns

Photomicrograph 19 - 100x R.L. MP1,6
Coarse sulphide intergrowth with euhedral to anhedral arsenopyrite cemented by molybdenite followed by sphalerite-chalcopyrite-galena. The coarse grained galena and chalcopyrite fill interstices with fluorite and minor cassiterite

1187A

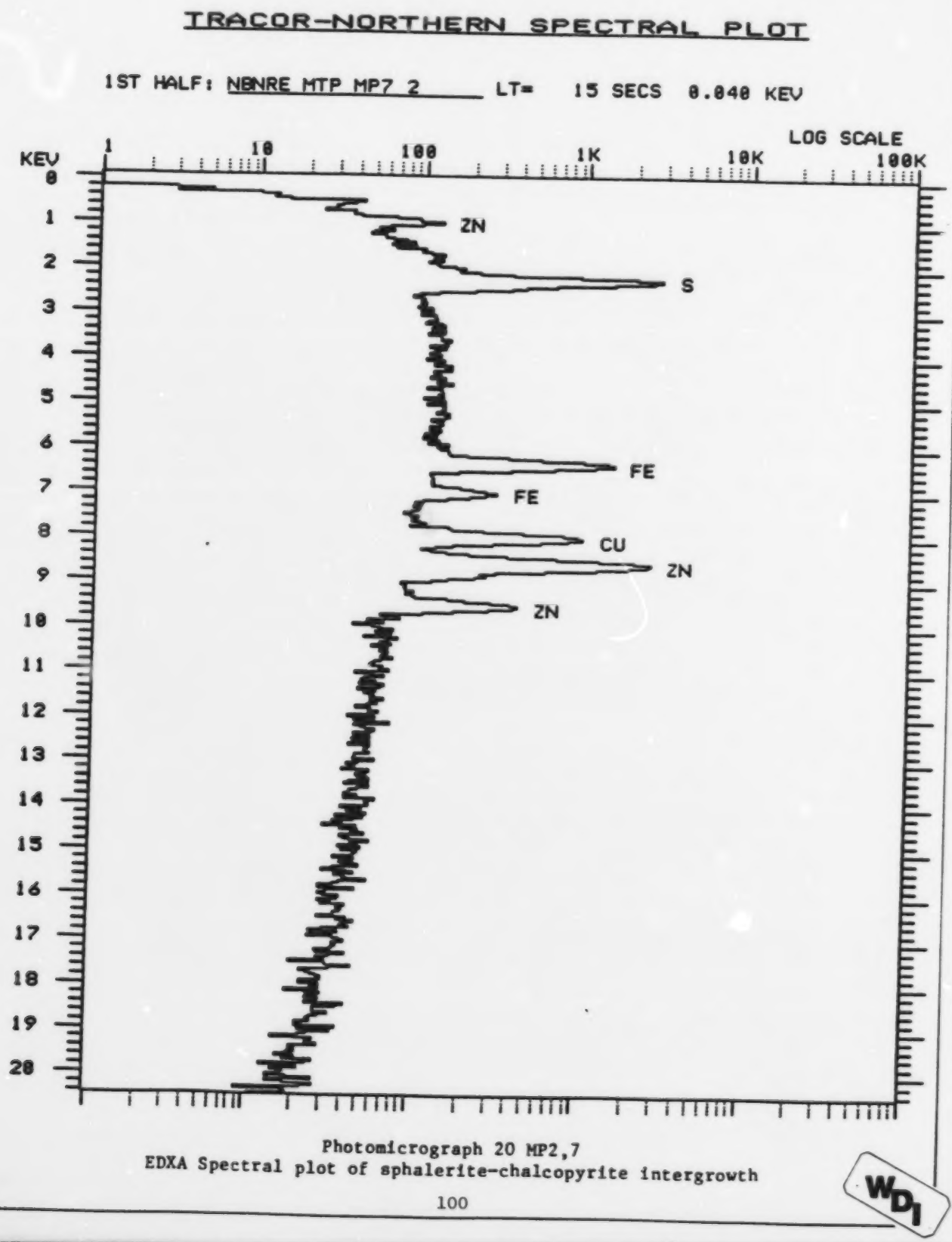

Photomicrograph 20 MP2,7
EDXA Spectral plot of sphalerite-chalcopyrite intergrowth

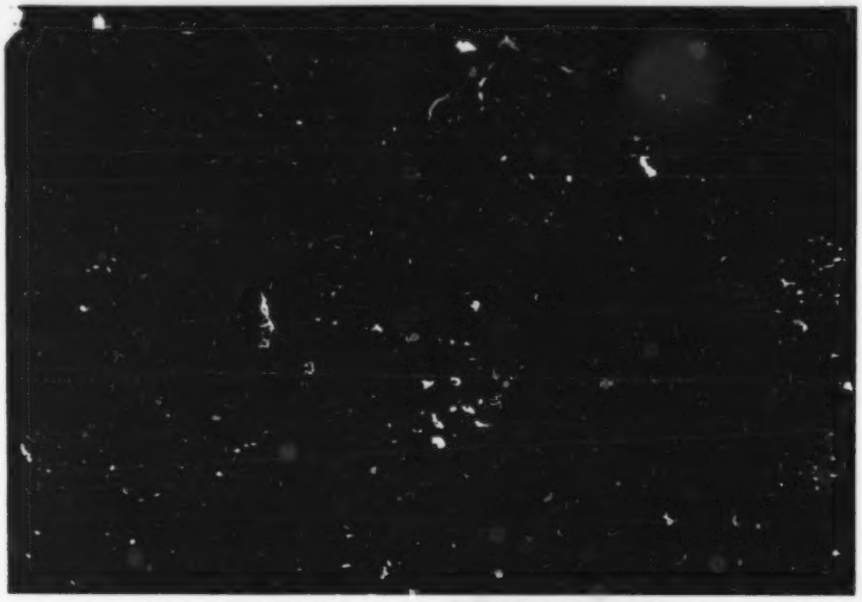

125 microns

Photomicrograph 21 - 200x R.L. MP2,7
Coarse sphalerite exhibits strong crystallographic control over inclusions of pyrrhotite, chalcopyrite, stannite-kesterite. Liberation of inclusions poor with expected dilution of zinc grade

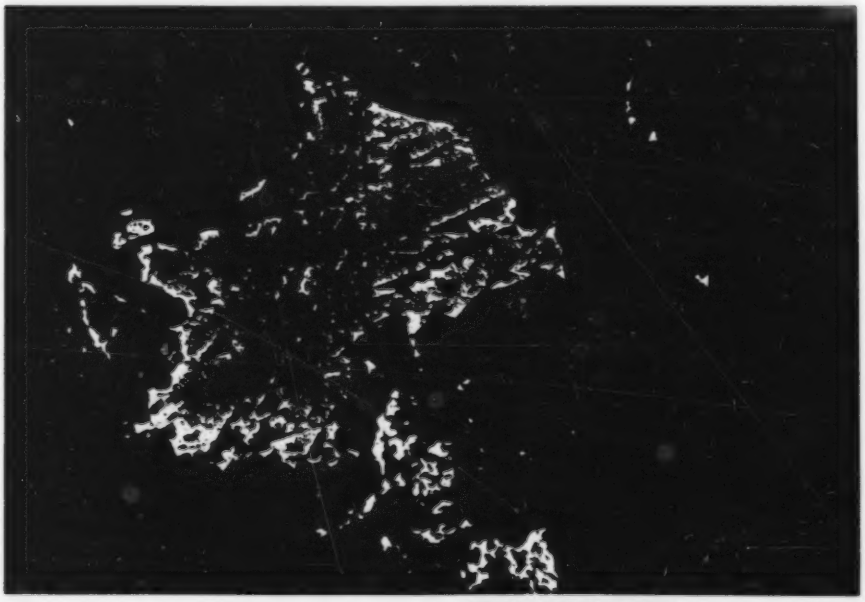

125 microns

Photomicrograph 22 - 200x R.L. MP4,9
Coarse ternary sulphide intergrowth of galena with sphalerite (dark grey) and stannite-kesterite (light grey-brown)

1187A

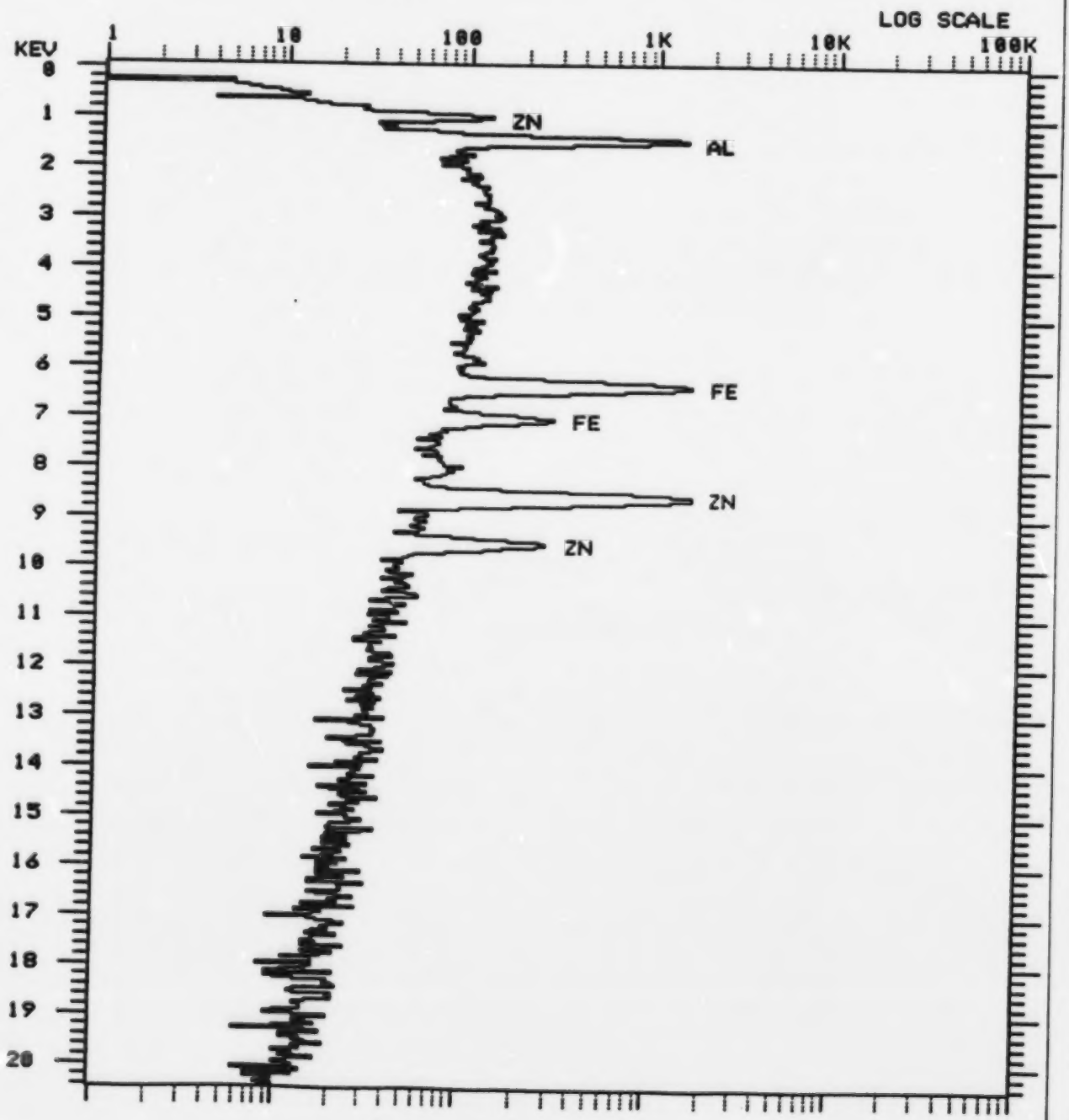

Photomicrograph 23 MP2,7
EDXA Spectral plot of gahnite $ZnAl_2O_4$; zinc rich spinel located as inclusion within interstices of aggregate quartz

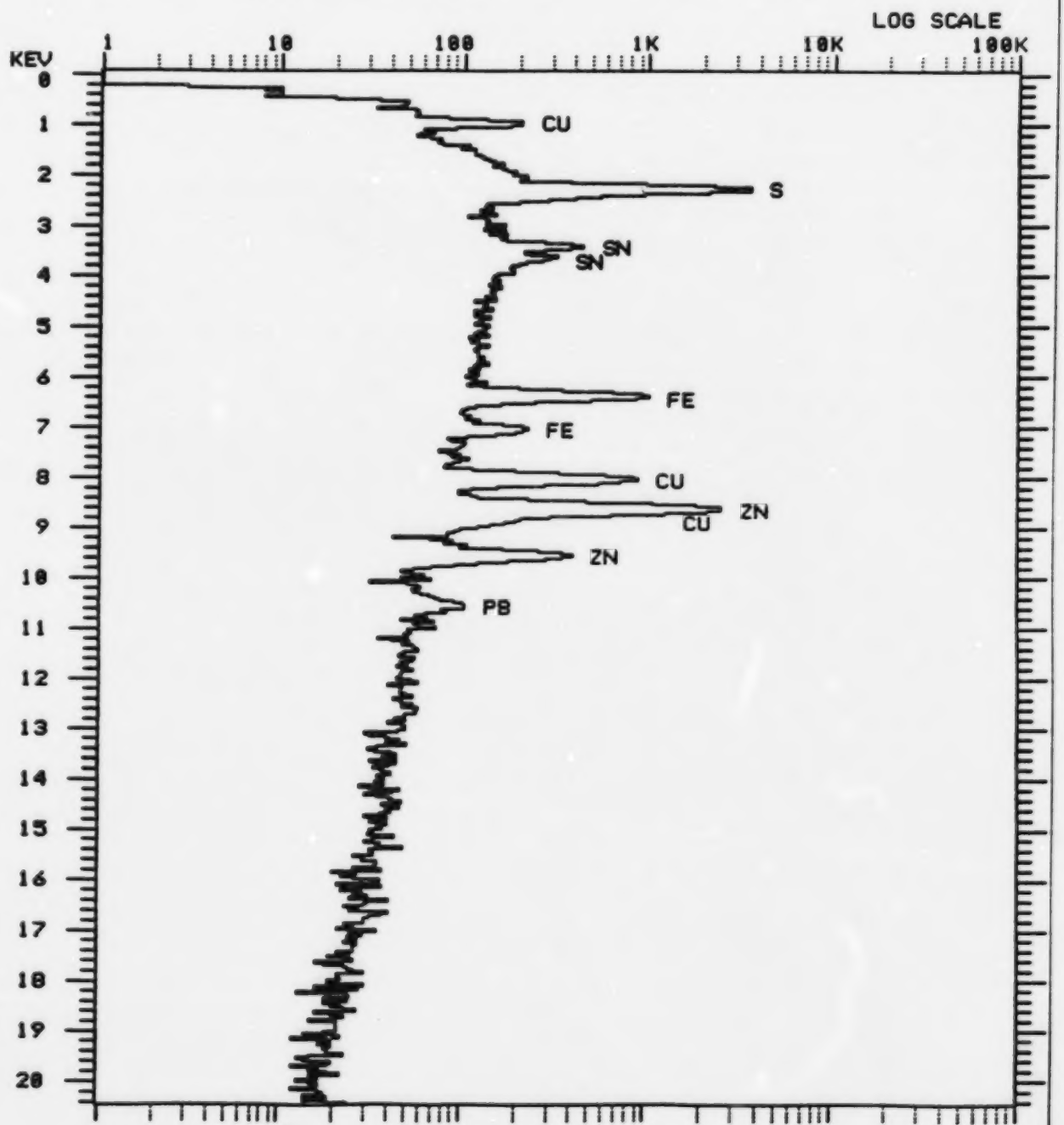

Photomicrograph 24 Gravity Concentrate
EDXA Spectral plot of sphalerite (Zn, Fe) S containing polymineralic inclusion of cassiterite (SnO_2), chalcopyrite ($CuFeS_2$) and galena (PbS)

50 microns

Photomicrograph 25 - 500x R.L. MP5,10
Liberated sulphide particle comprising sphalerite with disseminated subsequent blebs to ribbons of chalcopyrite (yellow), galena-galenobismutite (white), galena (white) and stannite-kesterite (grey-brown)

1187A

WD1

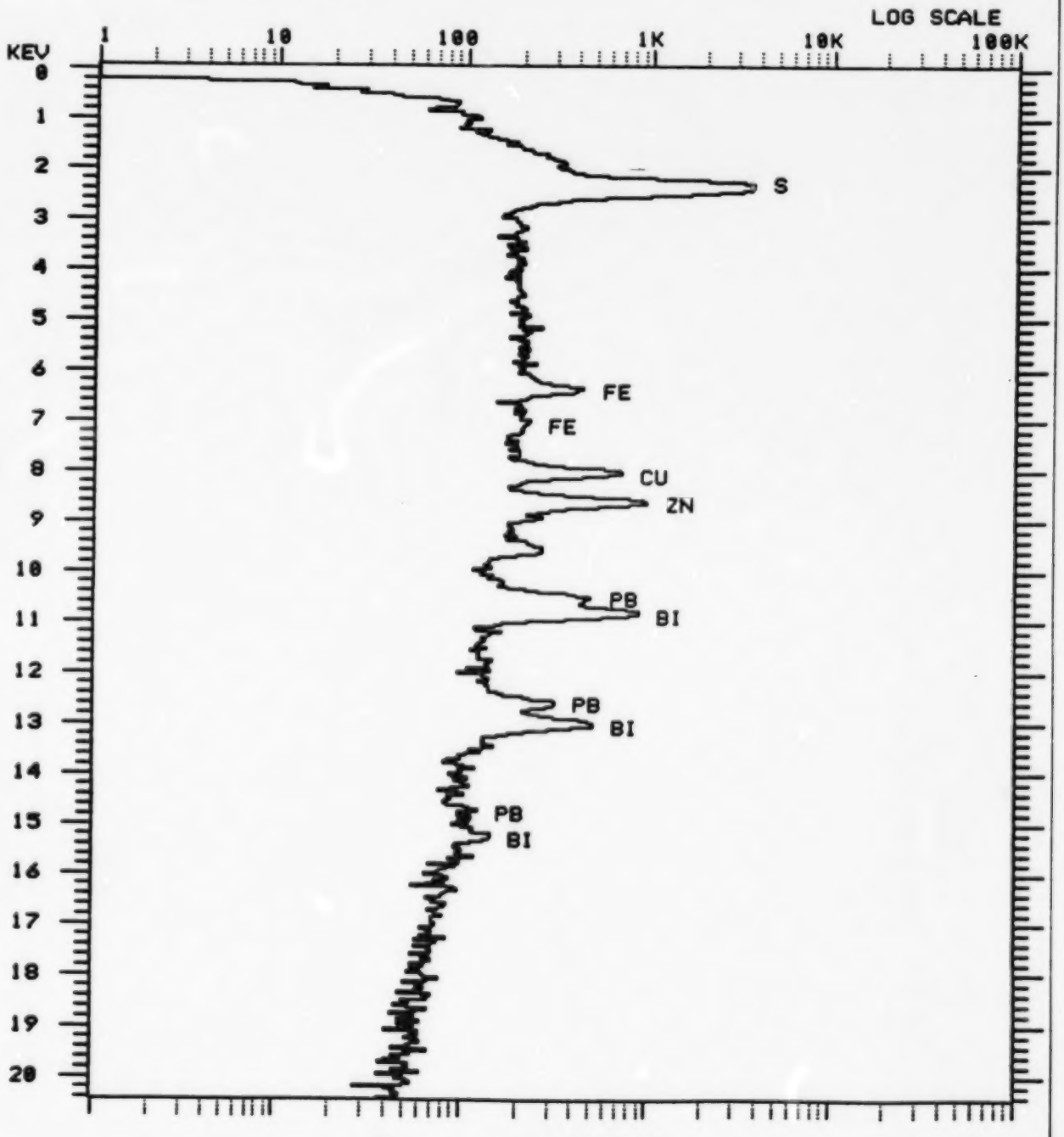

Photomicrograph 26 MP5,10
EDXA Spectral plot of lead-bismuth sulphosalt, galenobismutite, ($PbBi_2S_4$) inclusion within sphalerite-chalcopyrite

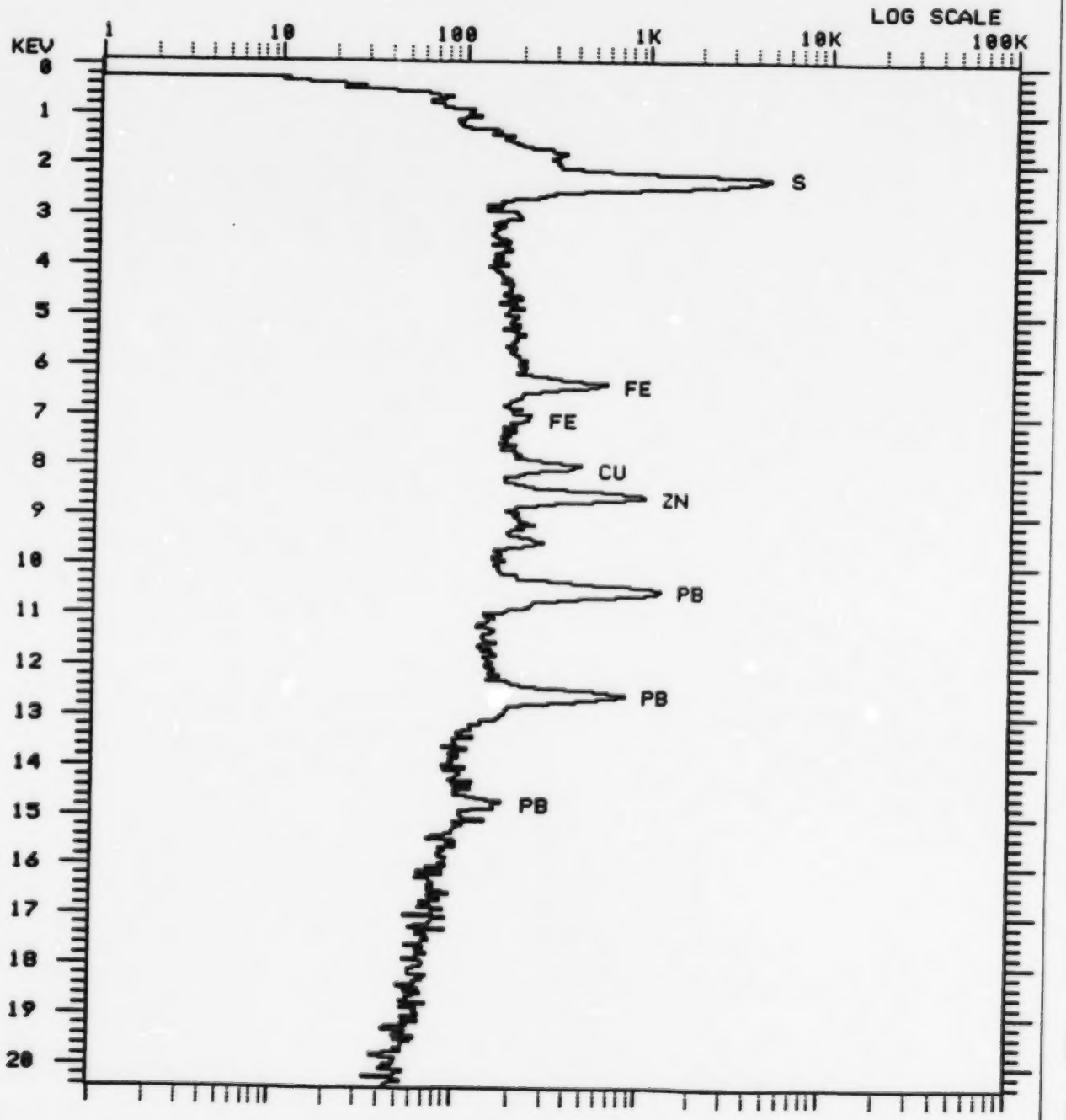

Photomicrograph 27 MP5,10
EDXA Spectral plot of galena, PbS, inclusion within sphalerite-chalcopyrite

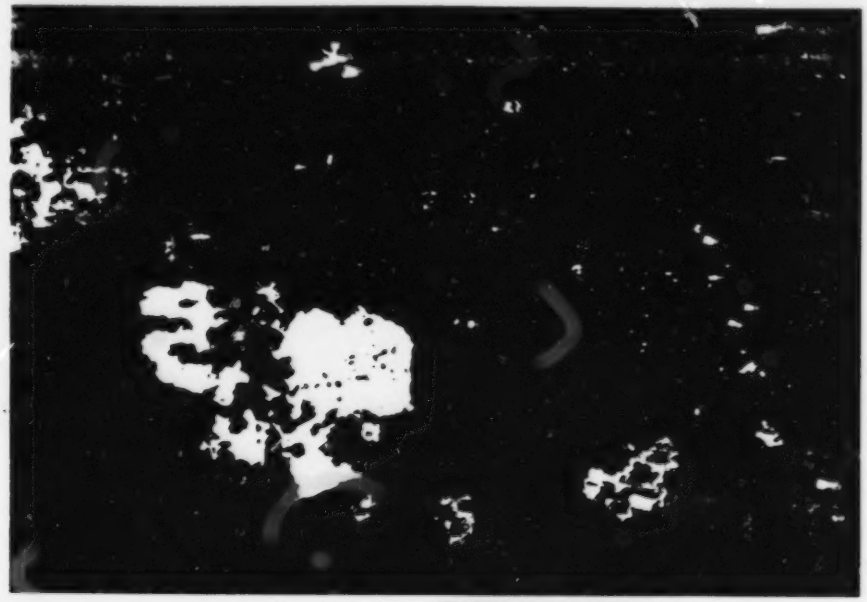

250 microns

Photomicrograph 28 - 100x R.L. MP1,6
Fine unliberated spalerite-chalcopyrite and pyrite disseminated within quartz-topaz-silicate microbreccia. Liberation difficult to impossible at expected grinds

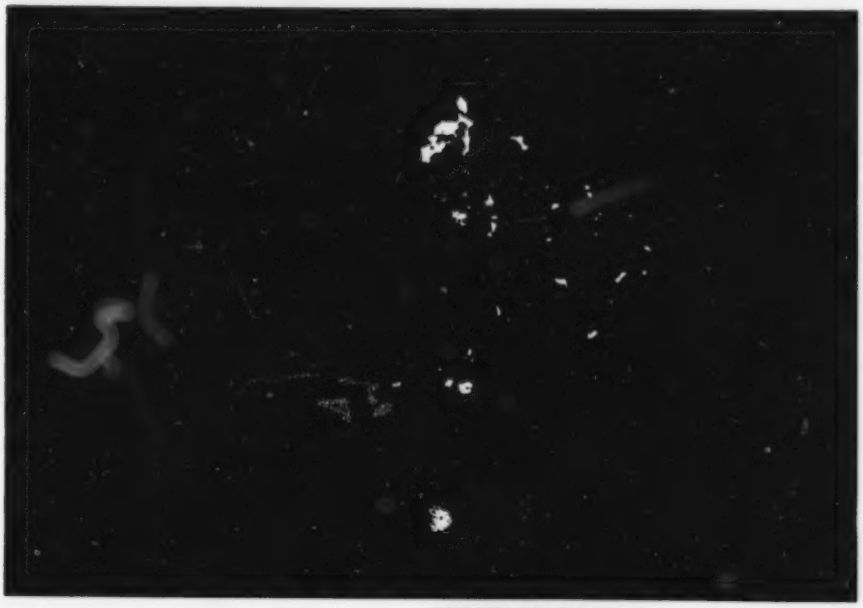

125 microns

Photomicrograph 29 - 200x - R.L. MP3,8
Effective binary association of fluorite-sphalerite with minor interstitial pyrite and pyrrhotite. Sphalerite intergrown with fine acicular crystals of cassiterite. The latter is finely developed within the fluorite

1187A

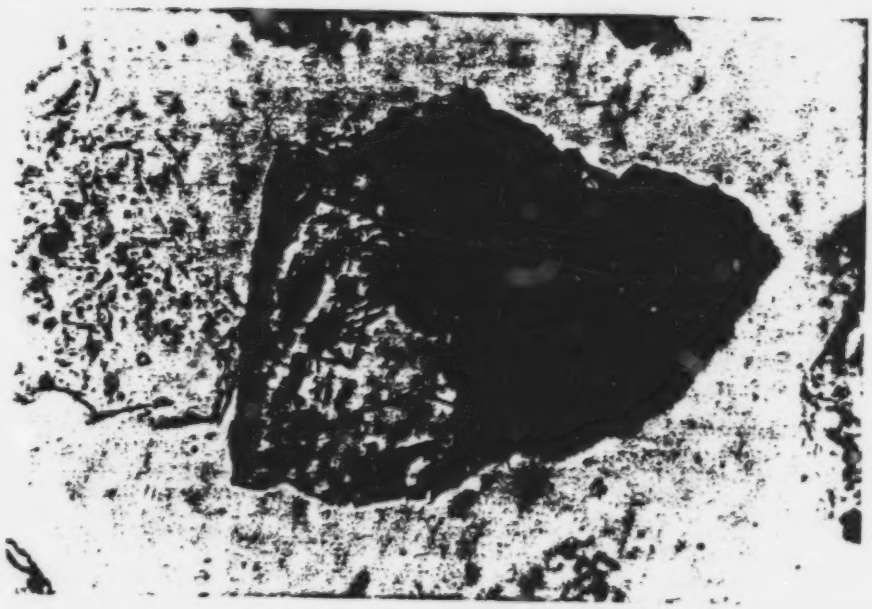

125 microns

Photomicrograph 30 - 200x T.L. MP3,8
As previous, with fine aggregates of euhedral cassiterite needles disseminated within fluorite adjacent to honey-brown sphalerite

1187A

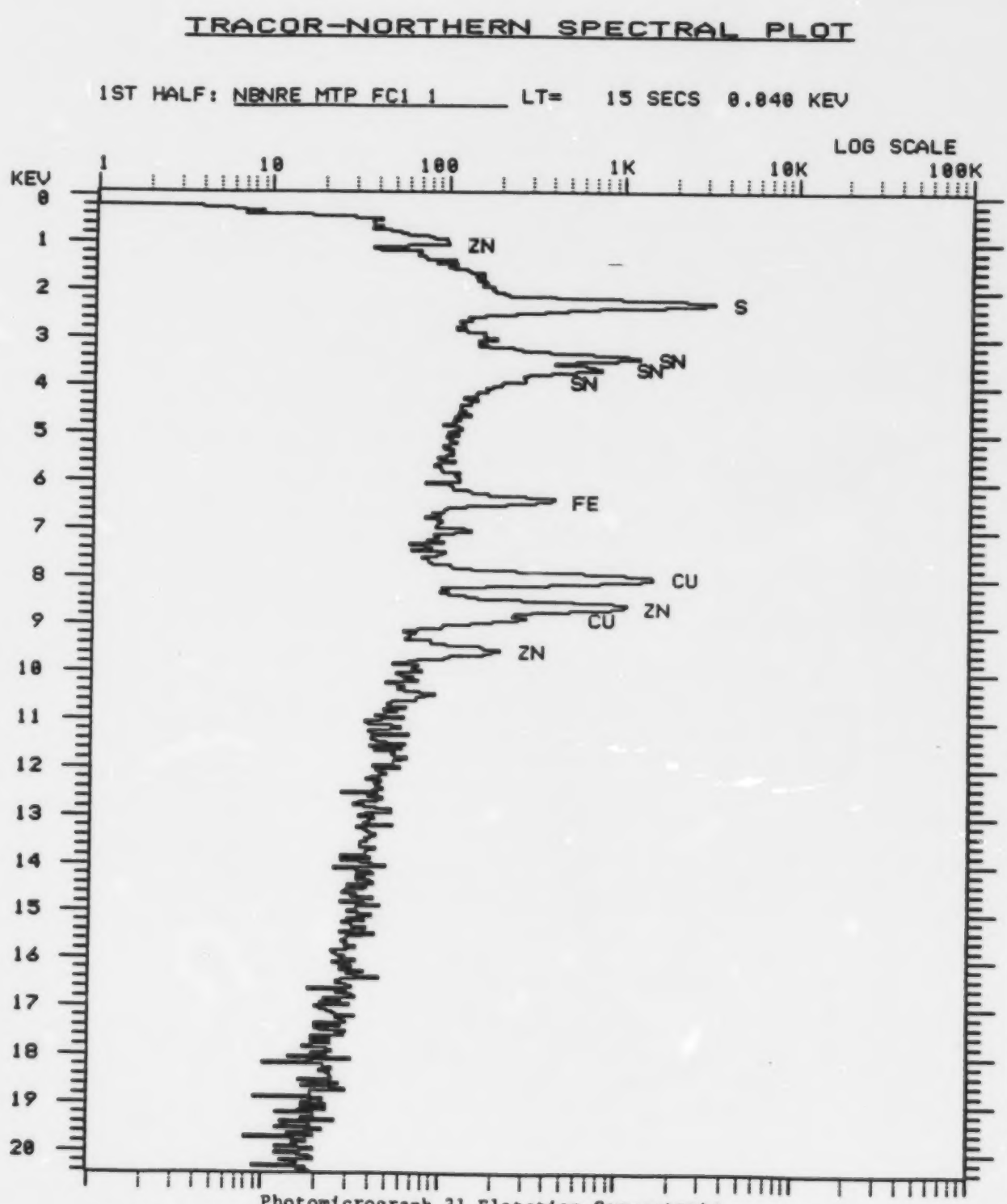

Photomicrograph 31 Flotation Concentrate

EDXA Spectral plot of stannite-kesterite series tentatively identified as kesterite Cu_2ZnSnS_4 with excess iron content (as described by Petruk, 1973)

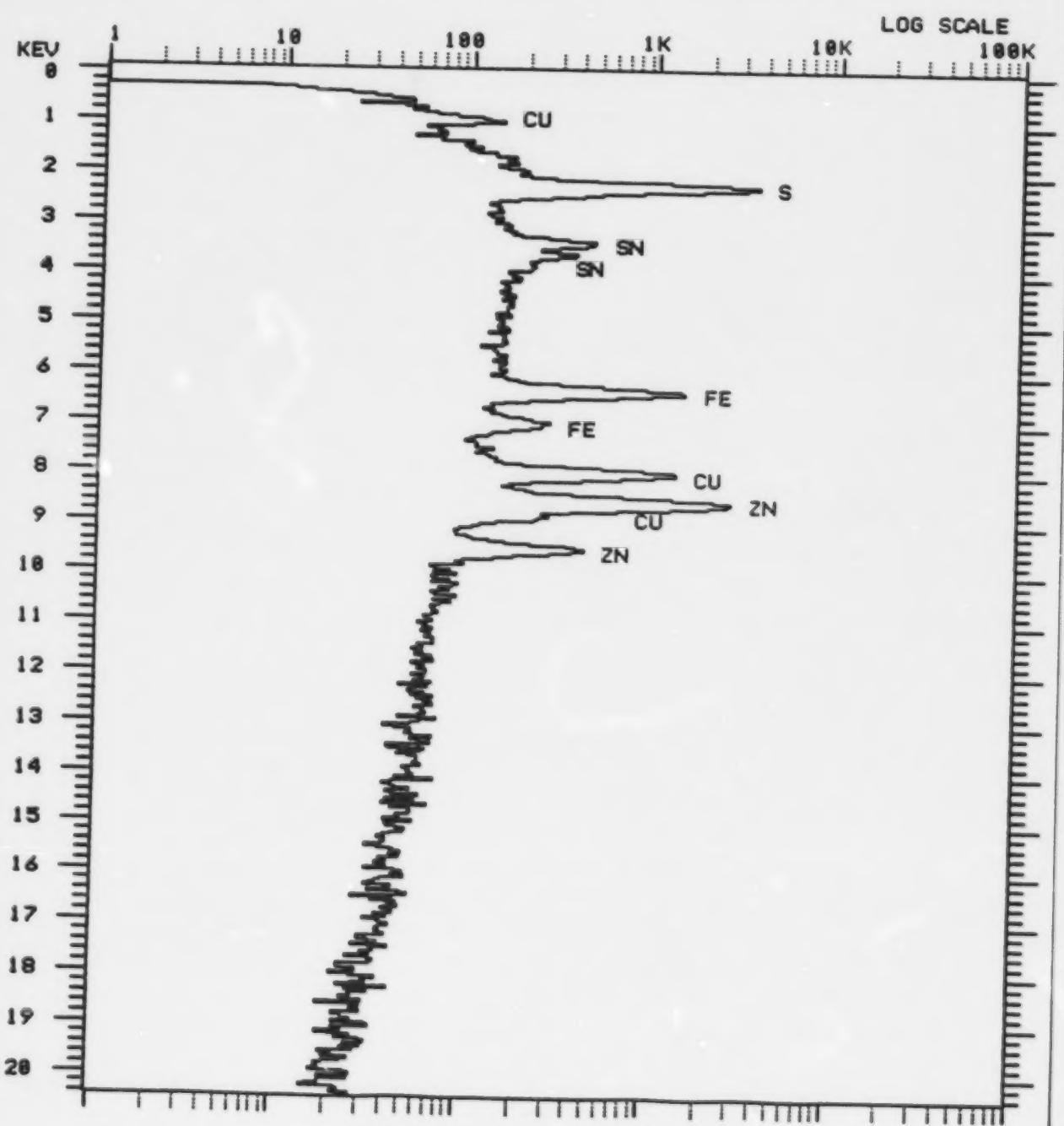

Photomicrograph 32 MP5,10
EDXA Spectral plot of fine cassiterite enclosed by sphalerite-chalcopyrite aggregate

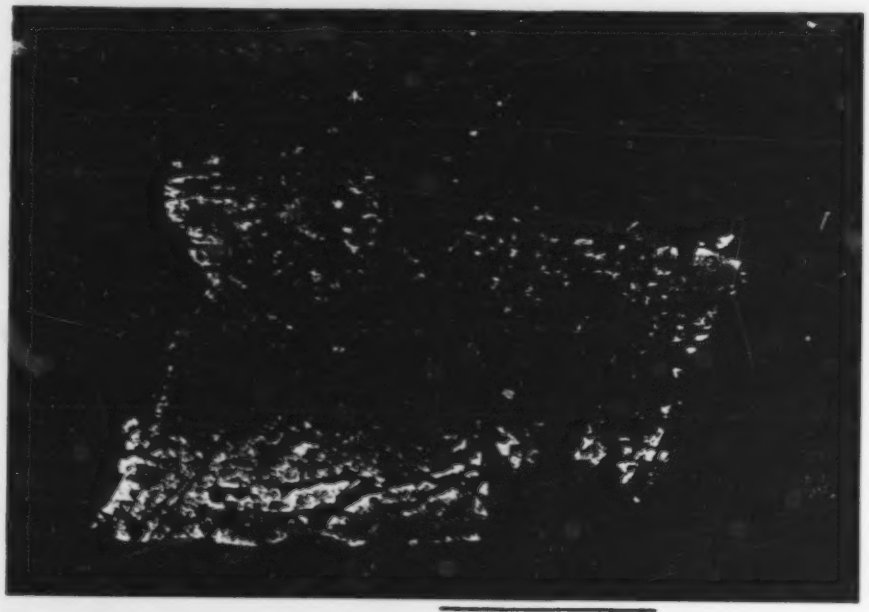

250 microns

Photomicrograph 33 - 100x R.L. MP2,7
Coarse binary association of galena and sphalerite exhibits near complete liberation from silicates and fluorite

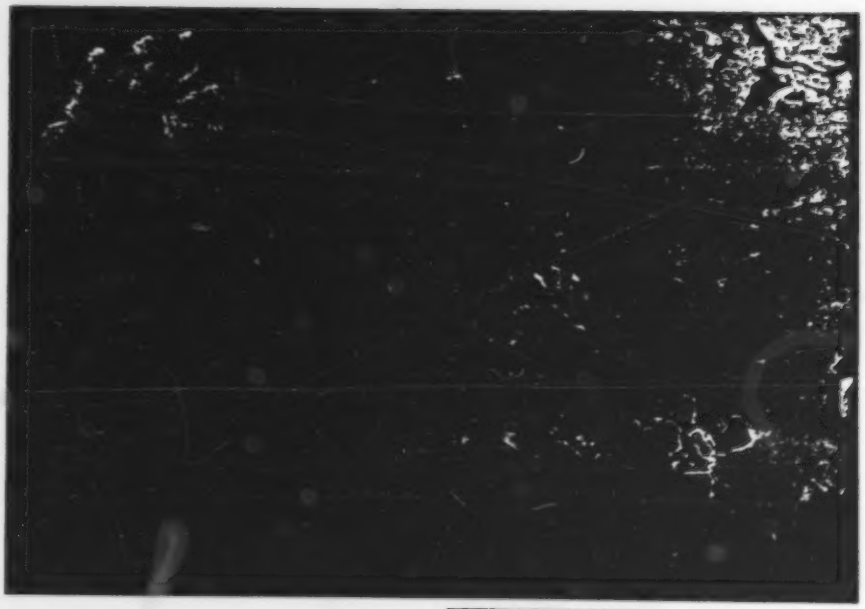

125 microns

Photomicrograph 34 - 200x R.L. MP2,7
Unliberated subhedra to anhedra of tarnished pyrite exhibits cementation by galena. The latter also occurs as separate grains all of which are enclosed by silicate gangue. Effective liberation of galena from pyrite requires fine grinds of less than 325-400 mesh

1187A

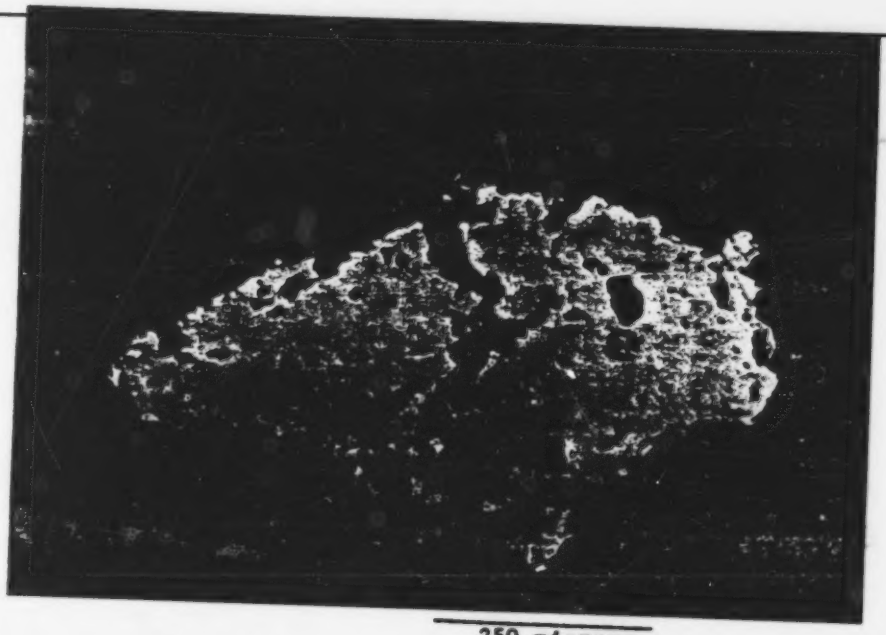

250 microns

Photomicrograph 35 - 100x R.L. MP2,7
Coarsely liberated aggregate particle of chalcopyrite with minor interstitial sphalerite and galena

50 microns

Photomicrograph 36 - 500x R.L. MP2,7
Polymineralic aggregate of chalcopyrite replacing sphalerite (note cleavage control at left) and replaced by irregular ribbon lamellae of bornite followed by dark blue covellite, which rims the entire sulphide particle

1187A

WD1

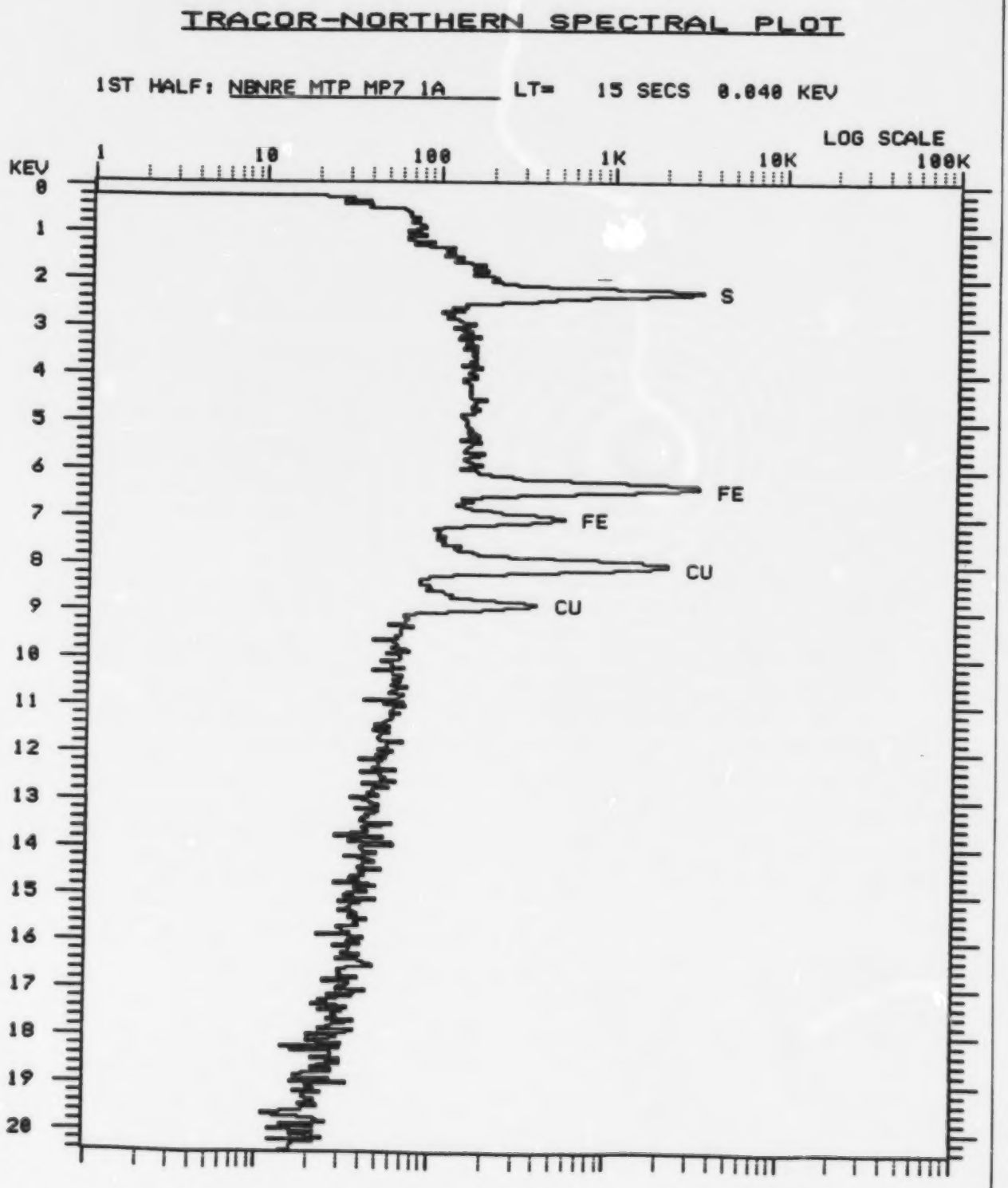

Photomicrograph 37 MP7
EDXA Spectral plot of chalcopyrite, $CuFeS_2$

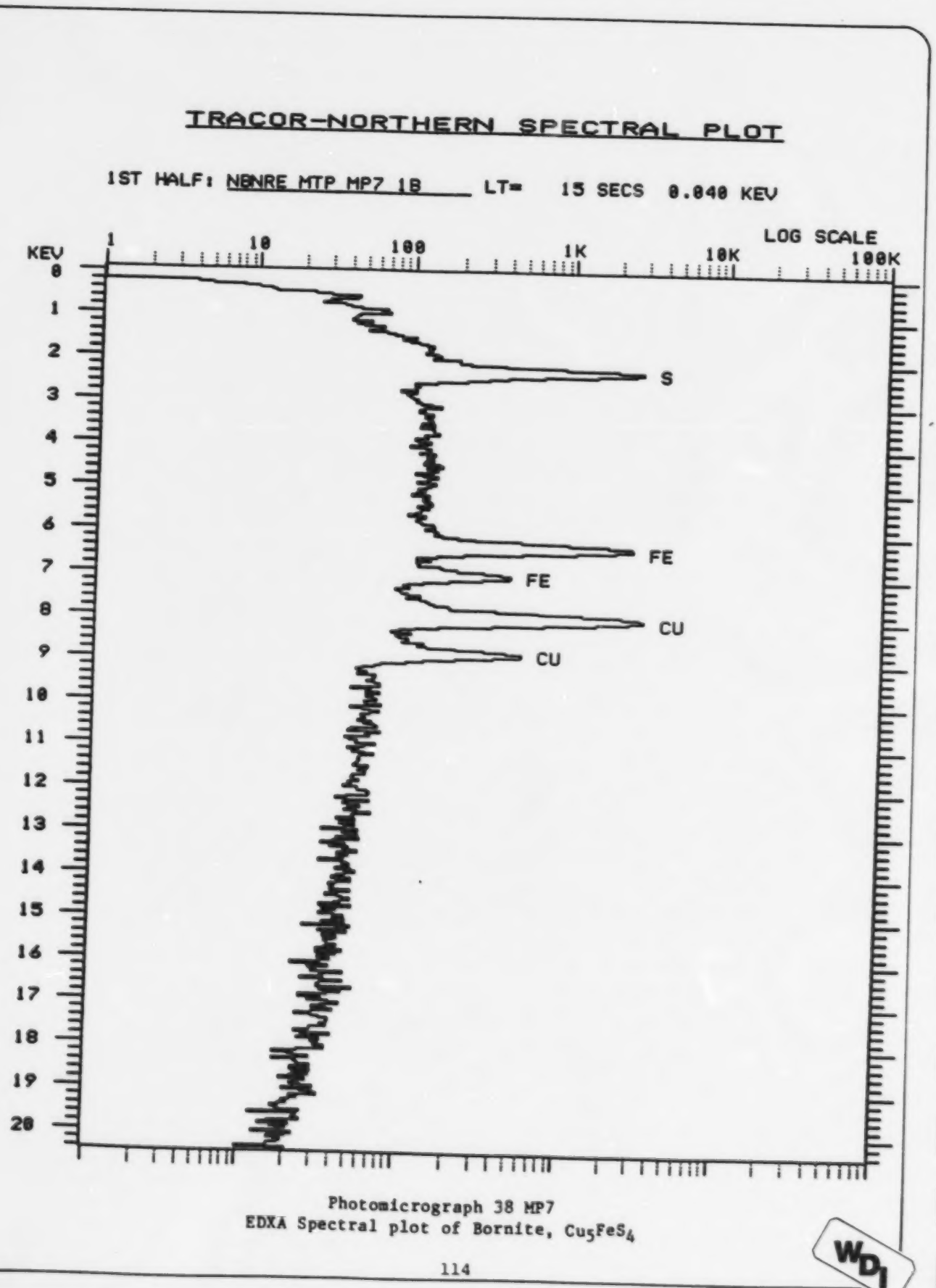

Photomicrograph 38 MP7
EDXA Spectral plot of Bornite, Cu_5FeS_4

125 microns

Photomicrograph 39 - 200x R.L. MP1,5

Aggregate particle exhibiting subhedral to euhedral arsenopyrite (containing minute grains of bismuth), wolframite (enclosing sphalerite-covellite-chalcopyrite) along fractures of quartz. Liberation potential high at 150 - 200 mesh

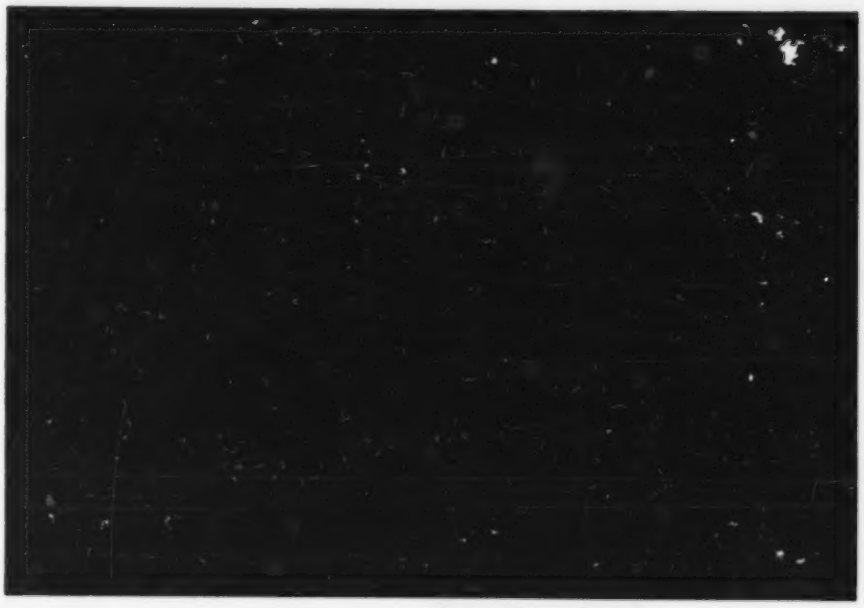

50 microns

Photomicrograph 40 - 500x R.L. MP2,7

Complex sulphide intergrowth with extremely fine crystal dimensions comprising dark grey sphalerite, chalcopyrite, pyrite (white), galena (grey-blue) and tetrahedrite-tennantite (green-grey) with dark fluorite and minor silicates. Bulk sulphide liberation potential high with separation from fluorite at 200 - 270 mesh

1187A

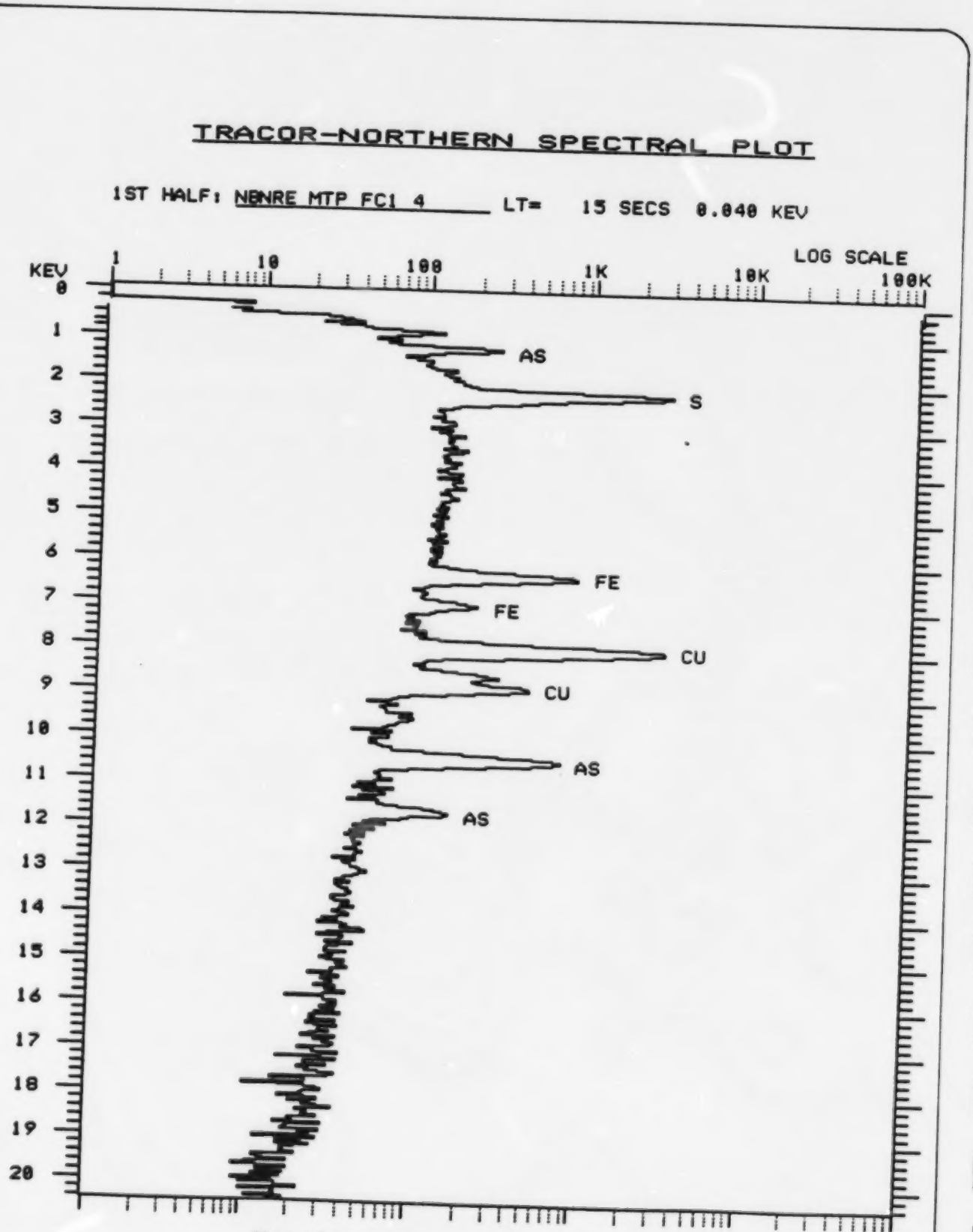

Photomicrograph 41 Flotation Concentrate
EDXA Spectral plot of typical tennantite mineral composition
$(Cu, Fe)_{12}\ As_4\ S_{13}$

WD1

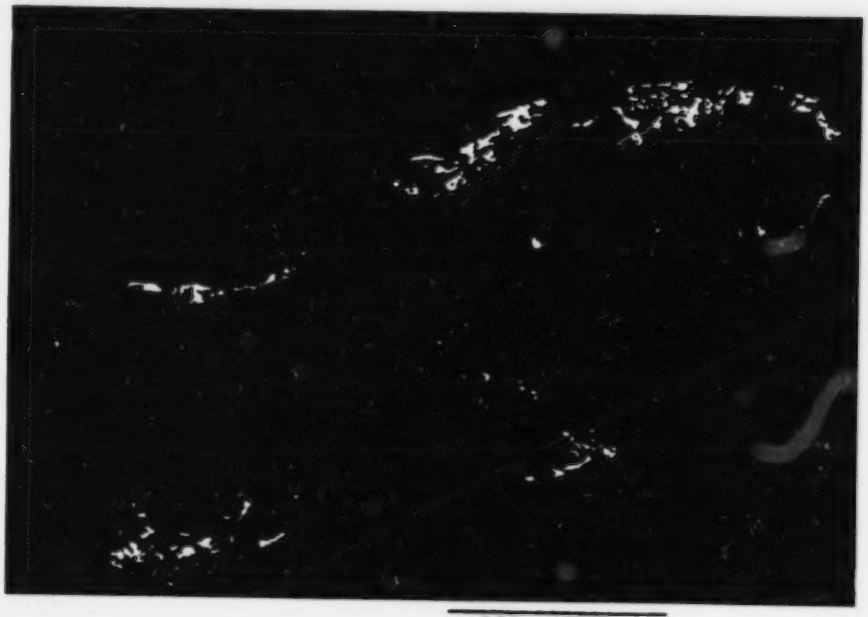

250 microns

Photomicrograph 42 - 100x R.L. MP2,7

Coarse silicate aggregate with patchy to disseminated fluorite (dark grey) and microfracture controlled sulphide mineralization by minute to coarse flakes of molybdenite typically in association with minute crystals of bismuth and prismatic wolframite. Partial liberation, by exposure, very typical molybdenite texture.

50 microns

Photomicrograph 43 - 500x R.L. MP2,7

Fine intergrowth of native bismuth-molybdenite interstitial to wolframite-fluorite-silicates. Liberation at fine grinds with molybdenite-bismuth and molybdenite-wolframite binaries expected

1187A

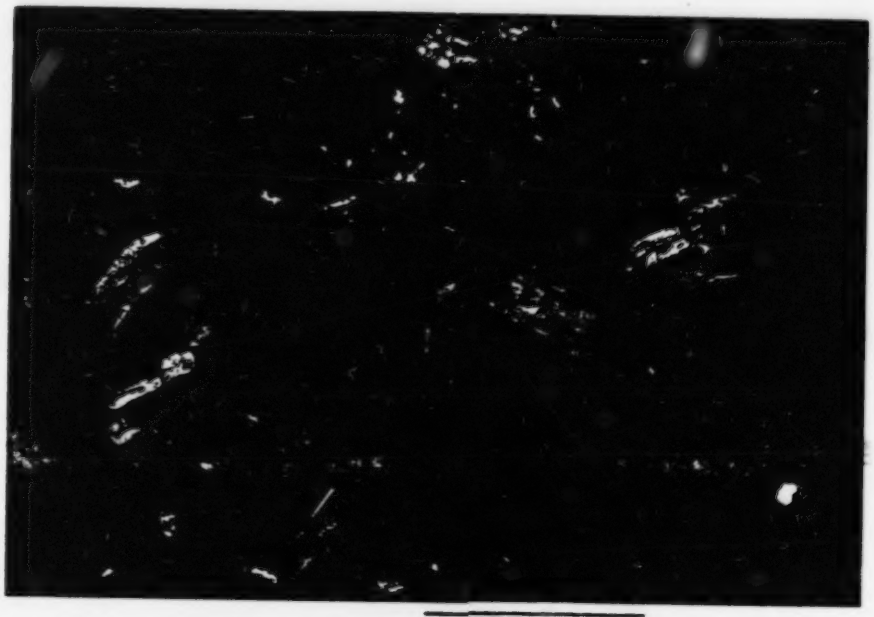

125 microns

Photomicrograph 44 - 200x R.L. MP1,6
Numerous molybdenite flakes disseminated through fluorite-silicate microbreccia interstitial to coarse subhedral to anhedral quartz. Minor native bismuth occurs within microbreccia matrix

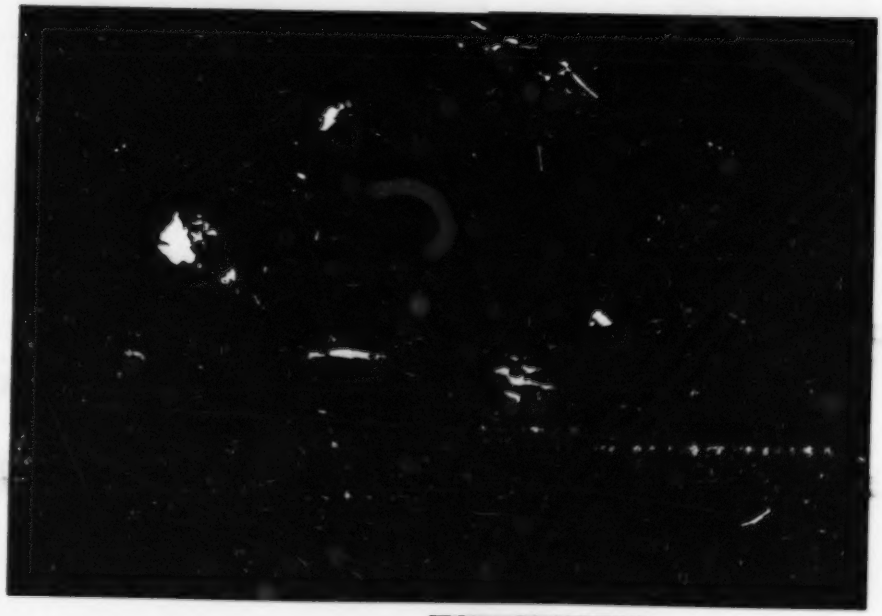

250 microns

Photomicrograph 45 - 100x R.L. MP2,7
Finely disseminated flakes of molybdenite and grains of native bismuth within quartz-topaz-chlorite microbreccia. Fluorite (dark grey-green) also encloses minute sulphides. Liberation potential of sulphides generally poor

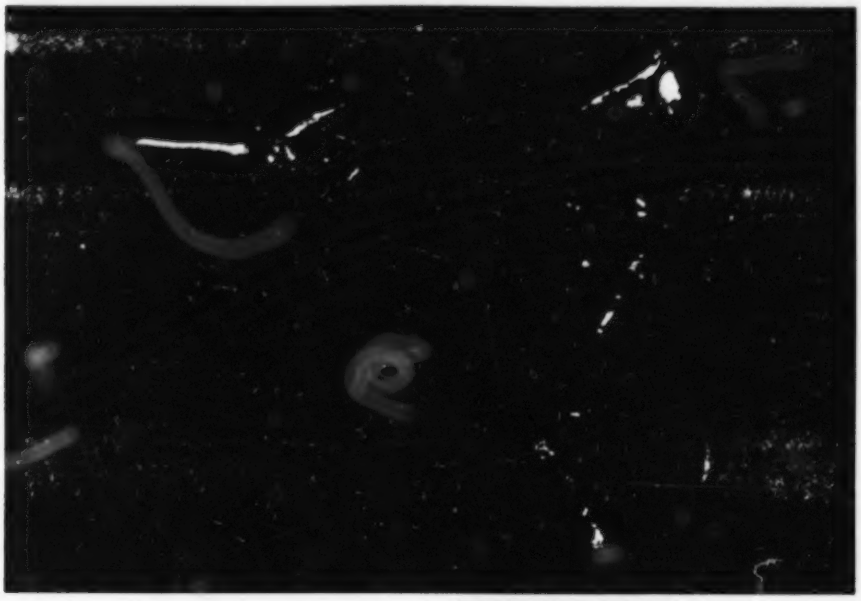

50 microns

Photomicrograph 46 - 500x R.L. MP3,8
Fine warped flakes of molybdenite occur within fluorite hosted by silicates, primarily quartz. Liberation of both molybdenite and fluorite only at very fine grinds

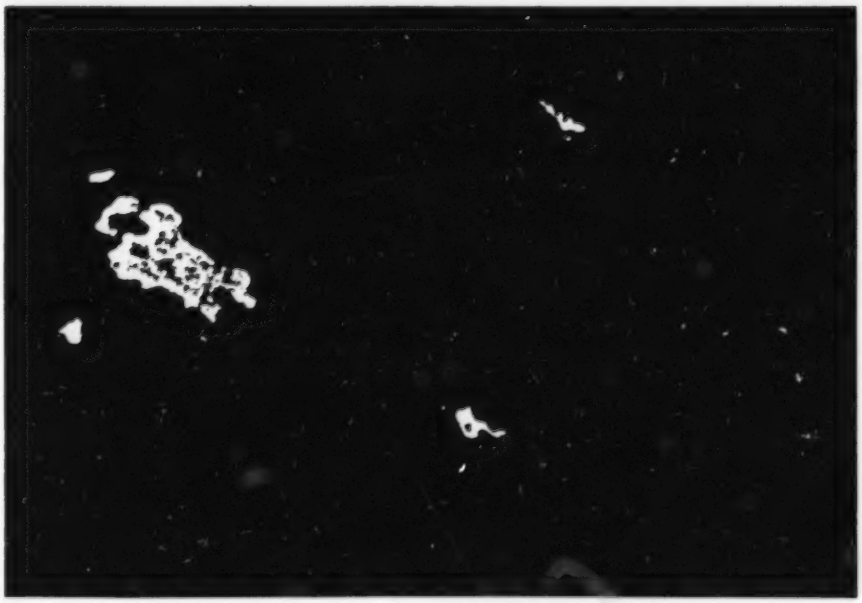

50 microns

Photomicrograph 47 - 500x R.L. MP3,8
Fine flakes of molybdenite, irregular grains of native bismuth, locally in association with molybdenite and coarse prismatic wolframite enclosed within silicates

1187A

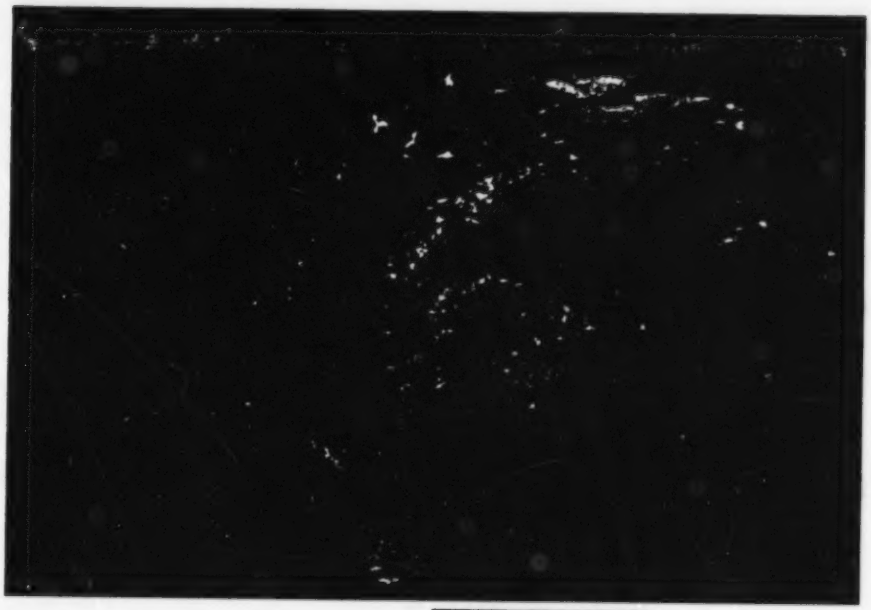

125 microns

Photomicrograph 48 - 200x R.L. MP3,8

Coarse liberated aggregate of molybdenite flakes exhibiting euhedral form and also fine granular aggregate crystals. Minute particles of bismuth occur with the molybdenite.

1187A

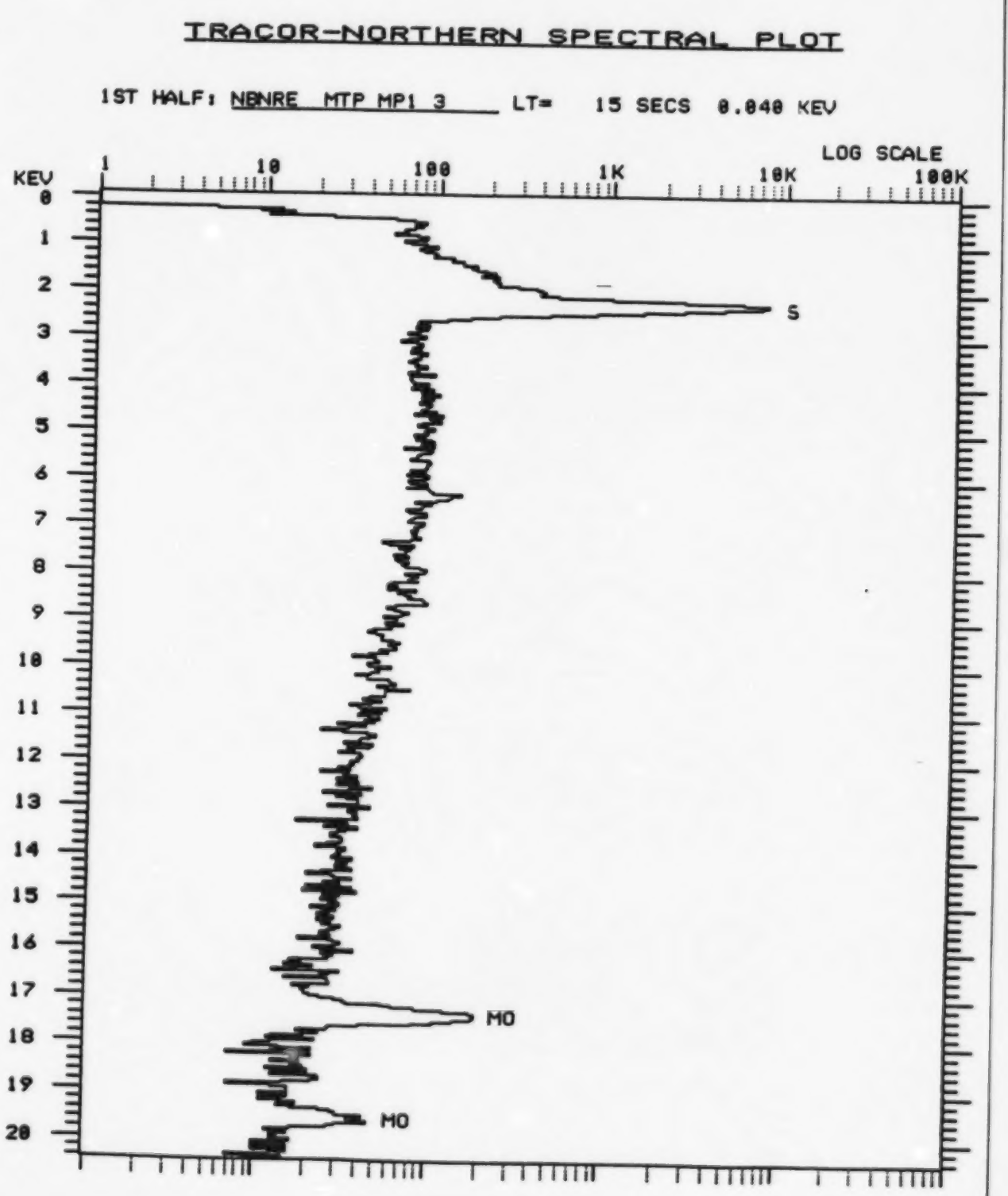

Photomicrograph 49 MP1
EDXA Spectral plot of molybdenite, MoS_2

50 microns

Photomicrograph 50 - 500x R.L. MP2,7

Bismuth mineralization occurs as fine ribbon-type and irregular bleb lamellae within complex polymineralic sulphide aggregate of sphalerite followed by chalcopyrite, galena, tetrahedrite-tennantite and minor wolframite with fluorite-silicate matrix. Mineral liberation poor with bismuth probably reporting to bulk sulphide or lead concentrate

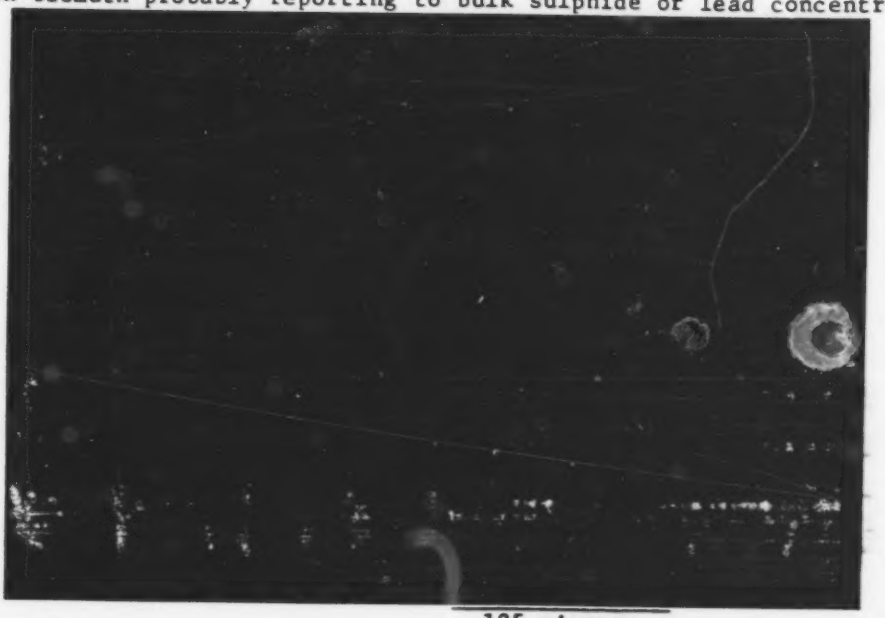

125 microns

Photomicrograph 51 - 200x R.L. MP1,6

Coarse aggregate crystals of loellingite, $FeAs_2$, with abundant intercrystal crystallographically controlled inclusions of native bismuth. Molybdenite cements the loellingite and hosts bismuth within intercrystal dilation porosity

1187A

50 microns

Photomicrograph 52 - 500x R.L. MP1,6

As above, close-up view of dendritic cleavage controlled bismuth and bimineralic bismuthinite-native bismuth; also monomineralic bismuthinite. Loellingite cemented at lower right by wolframite

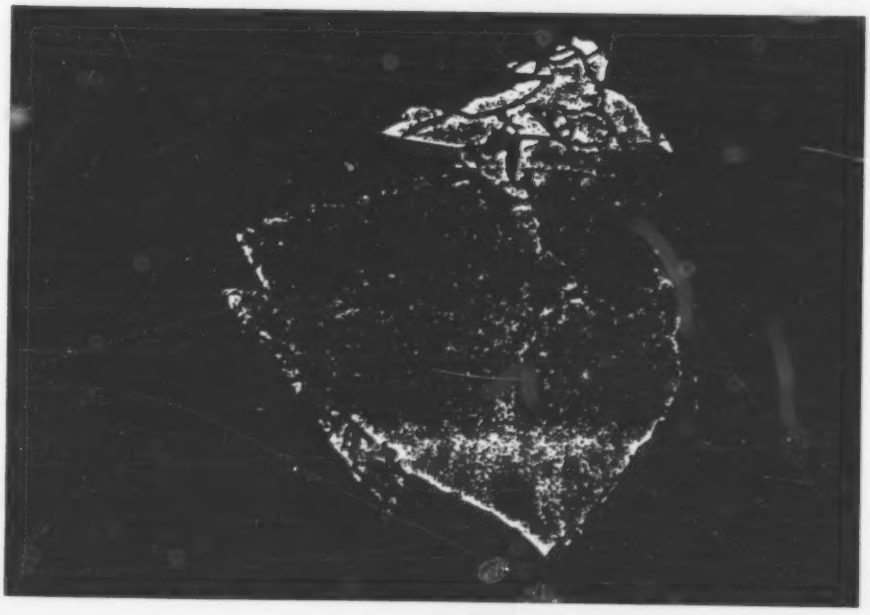

125 microns

Photomicrograph 53 - 200x R.L. MP3,8

Coarse loellingite associated with large elongate grains of bismuth cement and minute inclusions of native bismuth. The loellingite is liberated at coarse particle size with bismuth exposed to potential leach solutions

1187A

125 microns

Photomicrograph 54 - 200x R.L. MP3,8

Coarse aggregate crystals of loellingite exhibiting graphic texture with dendritic inclusions of native bismuth. Liberation of bismuth poor to impossible with potential recovery by leach solution

1187A

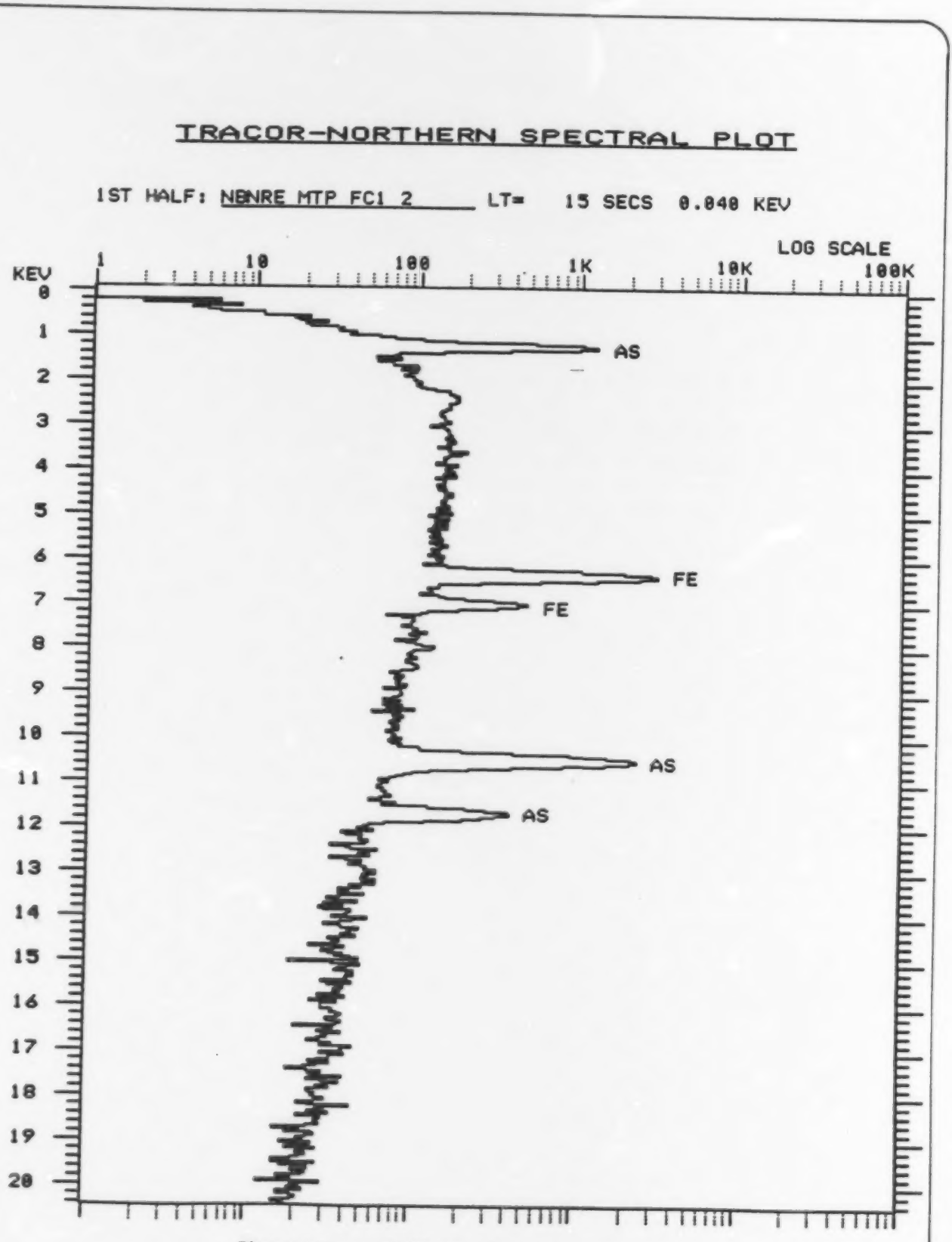

Photomicrograph 55 Flotation Concentrate
EDXA Spectral plot of loellingite, $FeAs_2$

WD1

125 microns

Photomicrograph 56 - 200x R.L. MP3,8
Isolated irregular grains of native bismuth occur interstitial to coarse quartz. Bismuth typically less than 20 microns in diameter

1187A

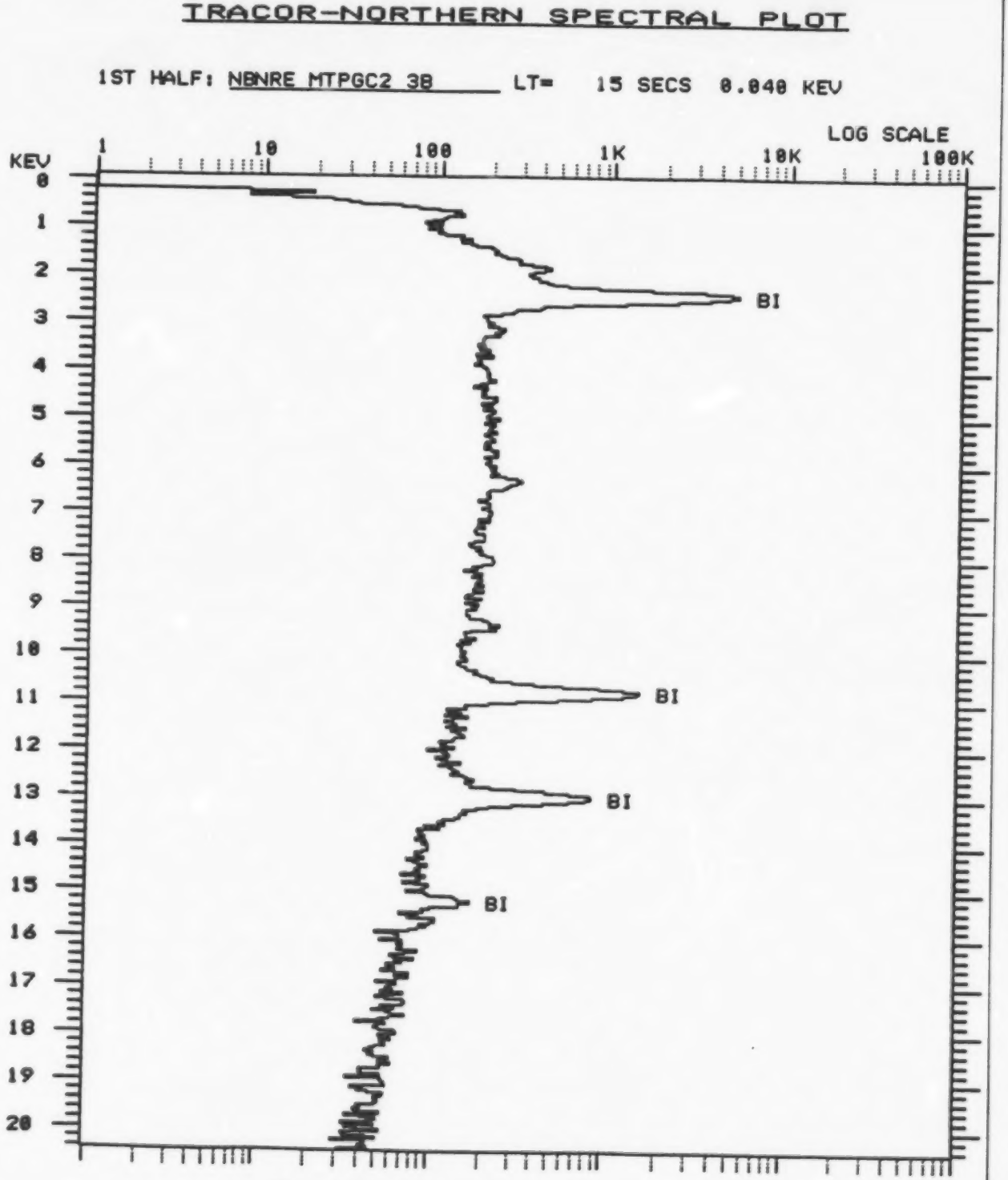

Photomicrograph 57 Gravity Concentrate
EDXA Spectral plot of native bismuth, Bi

WD1

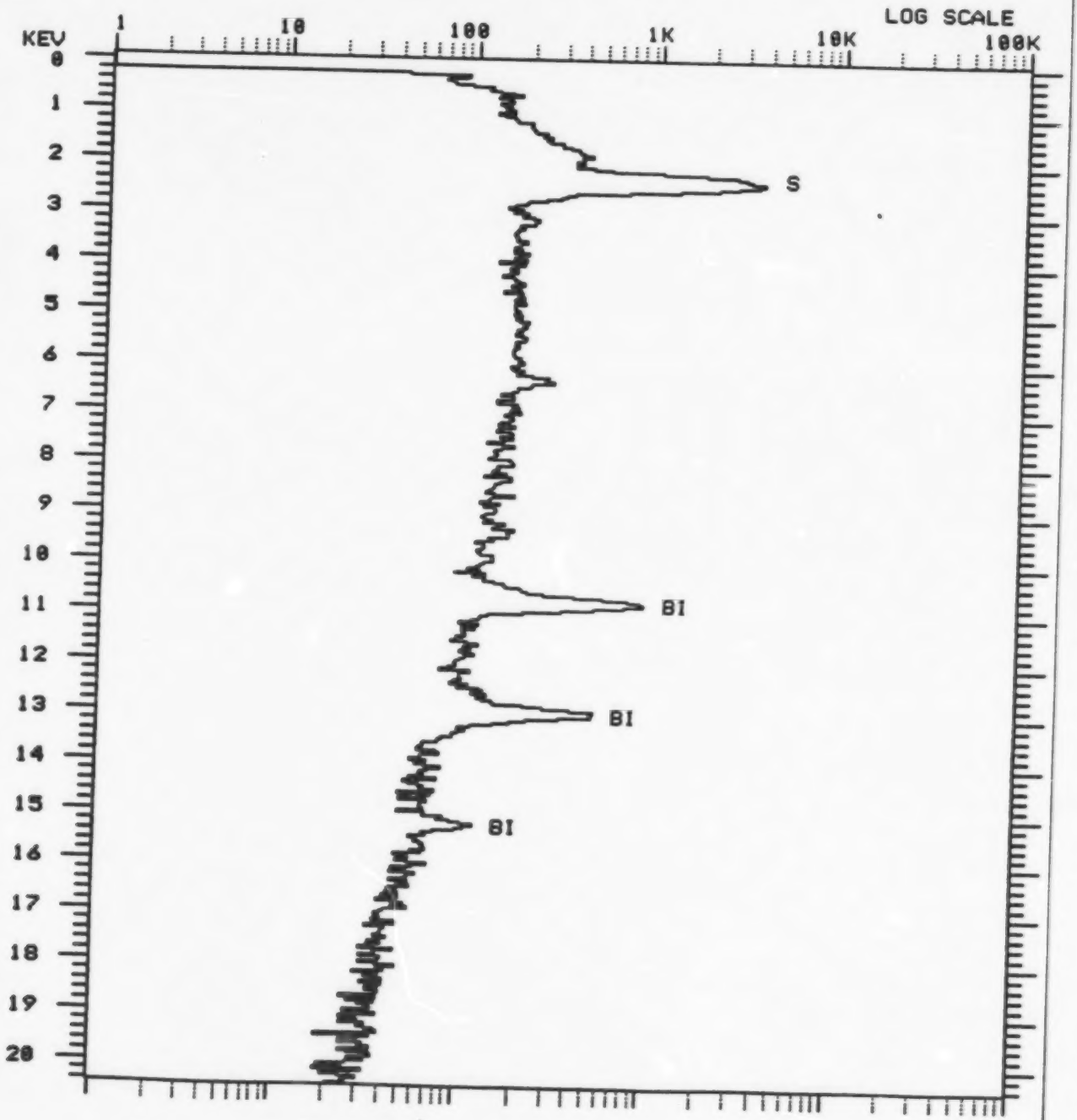

Photomicrograph 58 Gravity Concentrate
EDXA Spectral plot of bismuthinite, Bi_2S_3

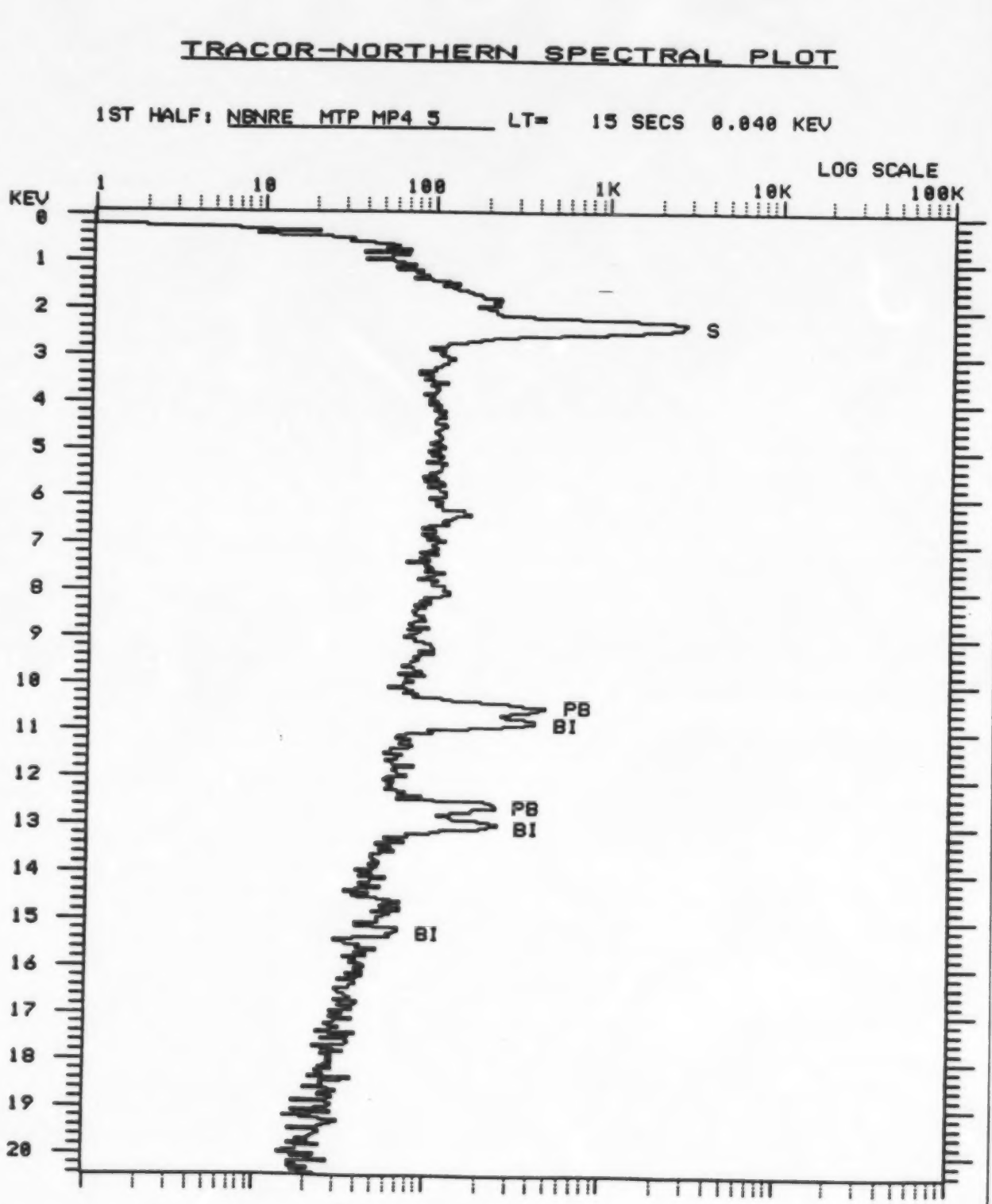

Photomicrograph 59 MP4,9

EDXA Spectral plot of lead-bismuth sulphosalt, tentatively identified as cosalite, $Pb_2 Bi_2 S_5$.

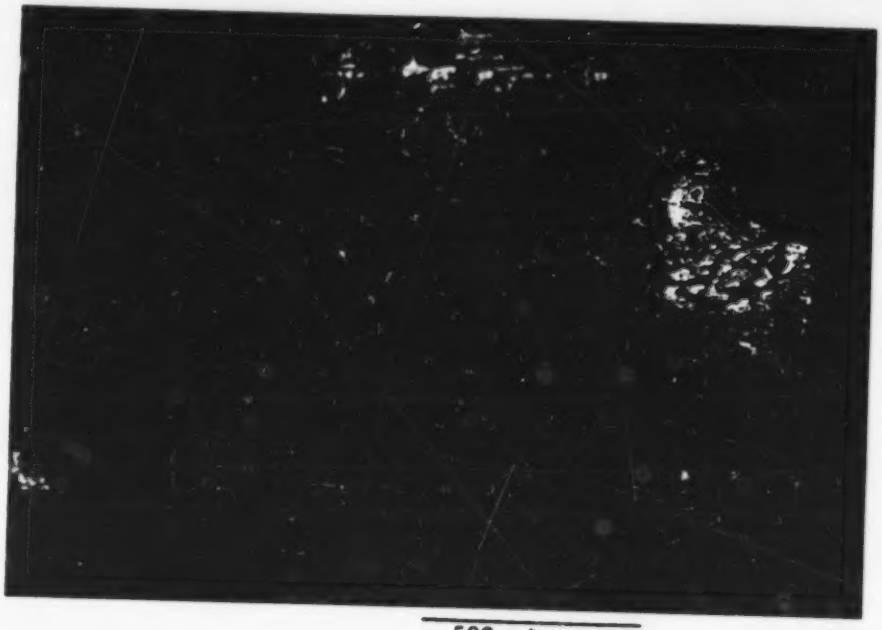

500 microns

Photomicrograph 60 - 50x R.L. MP1,6
Coarse aggregate particle exhibiting large crystals of wolframite intergrown with fluorite and several types of silicate minerals. Minor molybdenite and native bismuth associated with wolframite

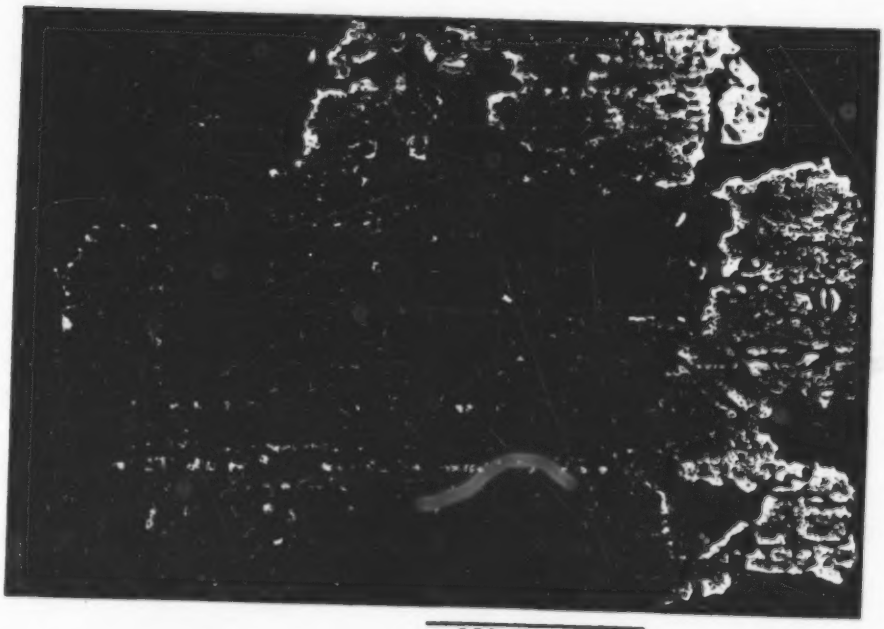

250 microns

Photomicrograph 61 - 100x R.L. MP2,7
Prismatic wolframite enclosed within silicate minerals and spatially associated with coarse arsenopyrite-loellingite-bismuth cemented by minor sphalerite-chalcopyrite

1187A

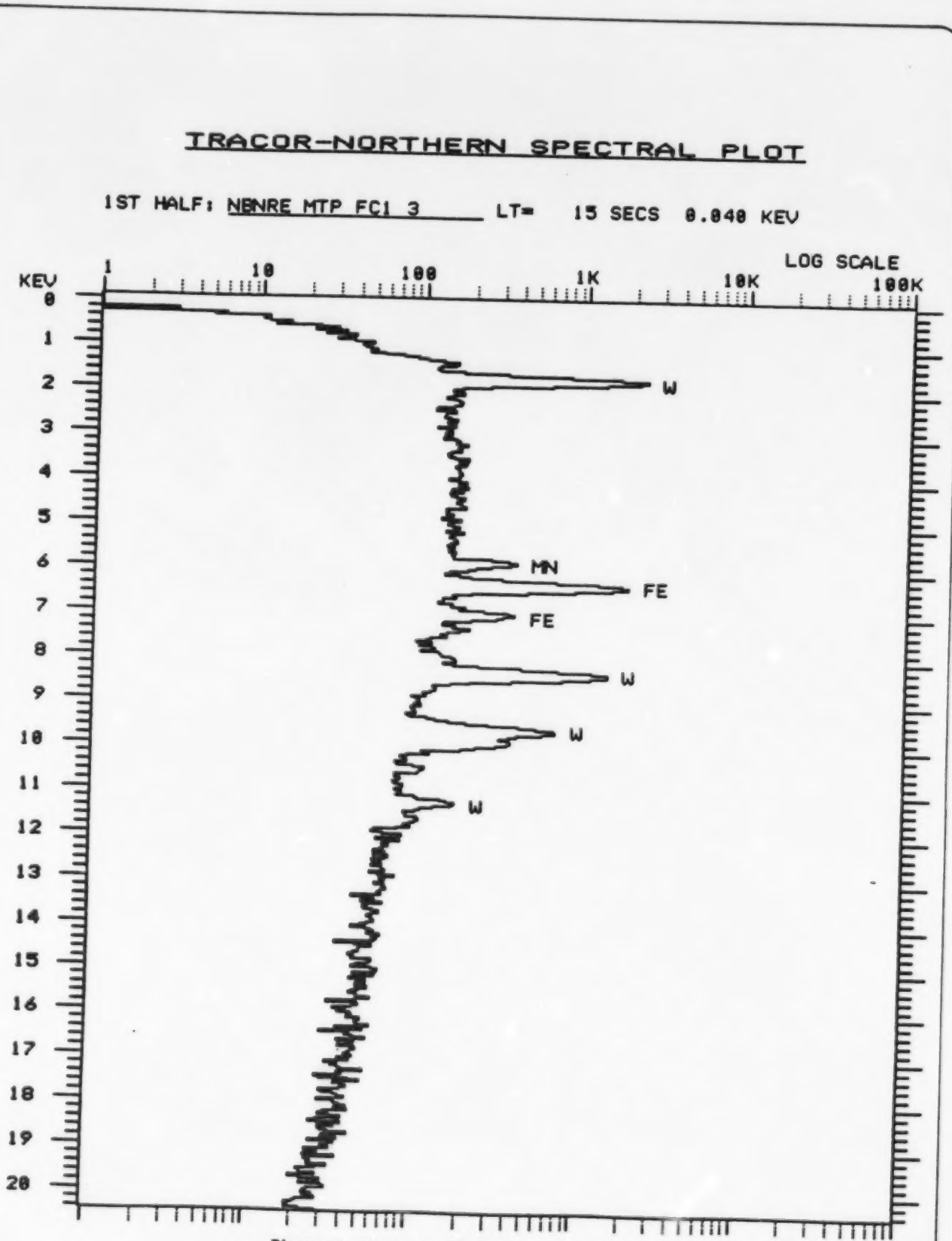

Photomicrograph 62 Flotation Concentrate
EDXA Spectral plot of wolframite, variety ferberite (Fe,Mn) WO_4

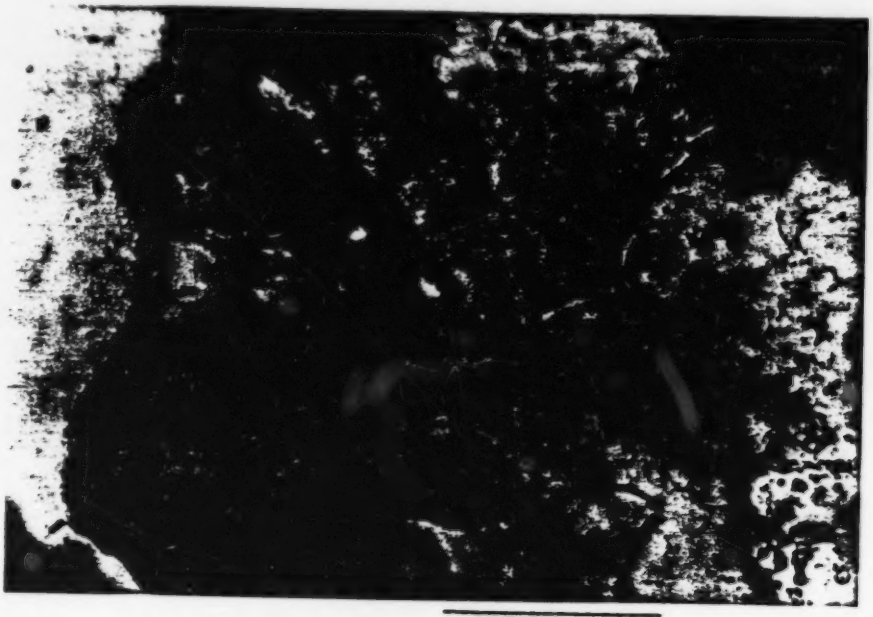

125 microns

Photomicrograph 63 - 200x T.L. MP2,7

Fine grained fluorite, primarily mauve coloration, and cloudy iron carbonates interstitial to quartz and topaz

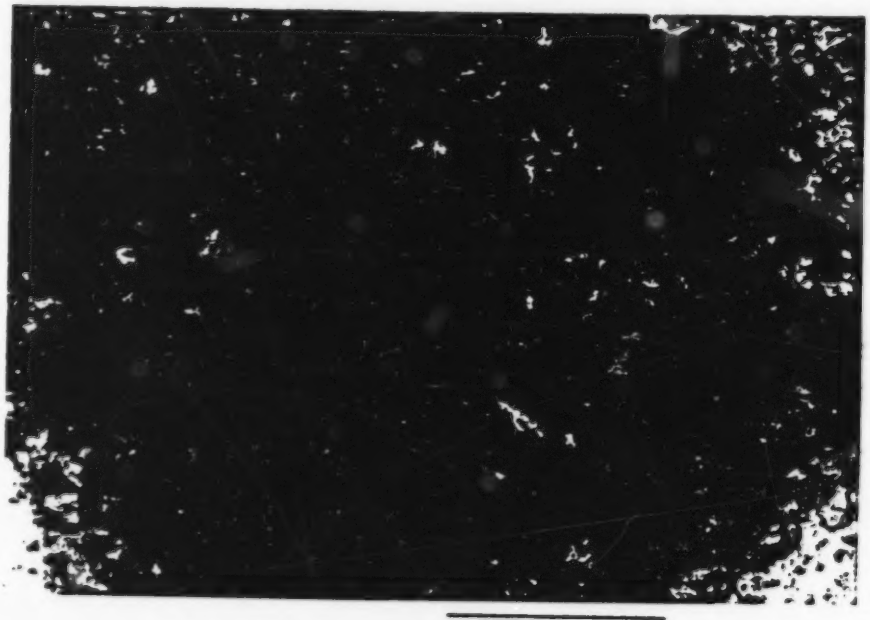

250 microns

Photomicrograph 64 - 100x T.L. MP1,6

Fine grained, clear to weakly mauve coloration, fluorite with carbonates in silica-topaz-chlorite greisen breccia

1187A

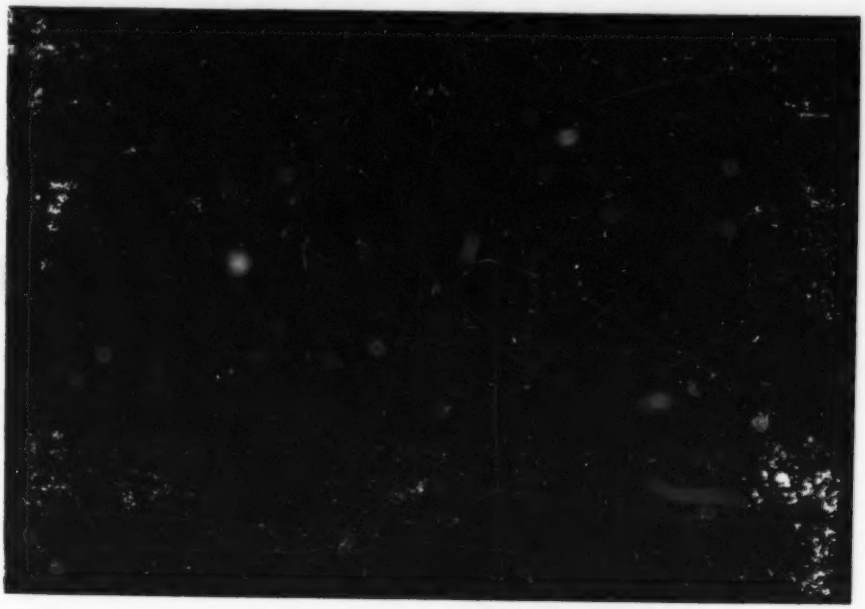

250 microns

Photomicrograph 65 - 100x T.L. MP1,6
Fine grained mauve fluorite intergrown with kaolinite, chlorite and lesser carbonates interstitial to quartz aggregate grains. The quartz contains myriad inclusions of zircon, clays and apatite.

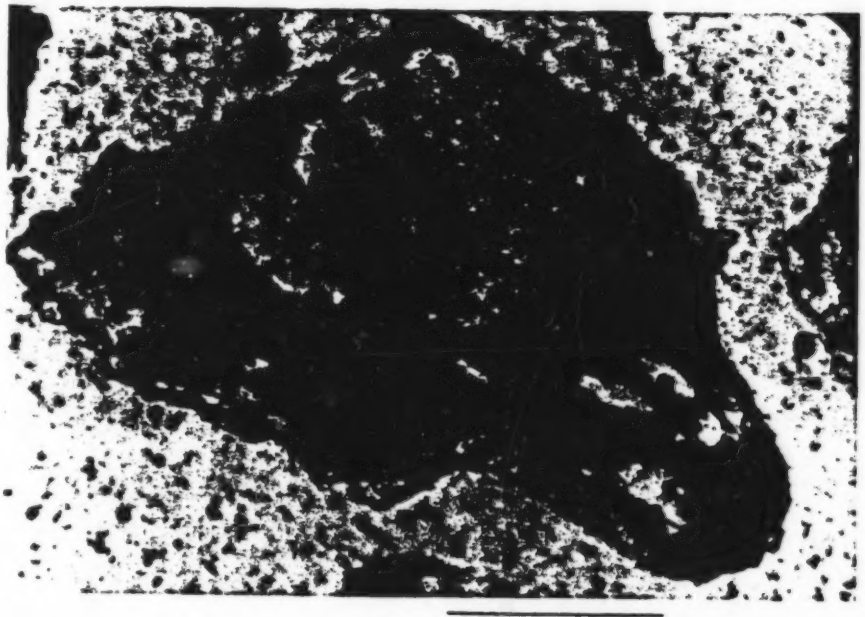

250 microns

Photomicrograph 66 - 100x T.L. MP2,7
Ternary association comprising clear and mauve varieties of fluorite with brown chlorite, minor cassiterite and carbonates

1187A

125 microns

Photomicrograph 67 - 200x T.L. MP3,8
Fully liberated crystal fragment of mauve fluorite with well developed cleavage pattern and few inclusions

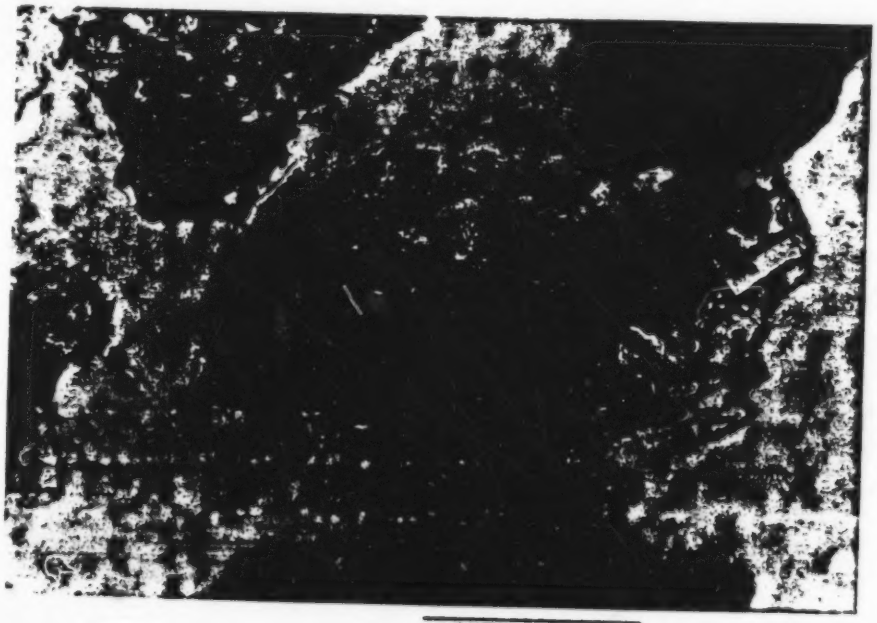

125 microns

Photomicrograph 68 - 200x T.L. MP3,8
Aggregate particle comprising clear and mauve varieties of fluorite with lesser yellow clays and minute subsequent yellowish to brownish yellow inclusions comprising cassiterite, rutile and monazite-xenotime. Minor ferroan carbonates also occur along cleavages of fluorite
1187A

WD1

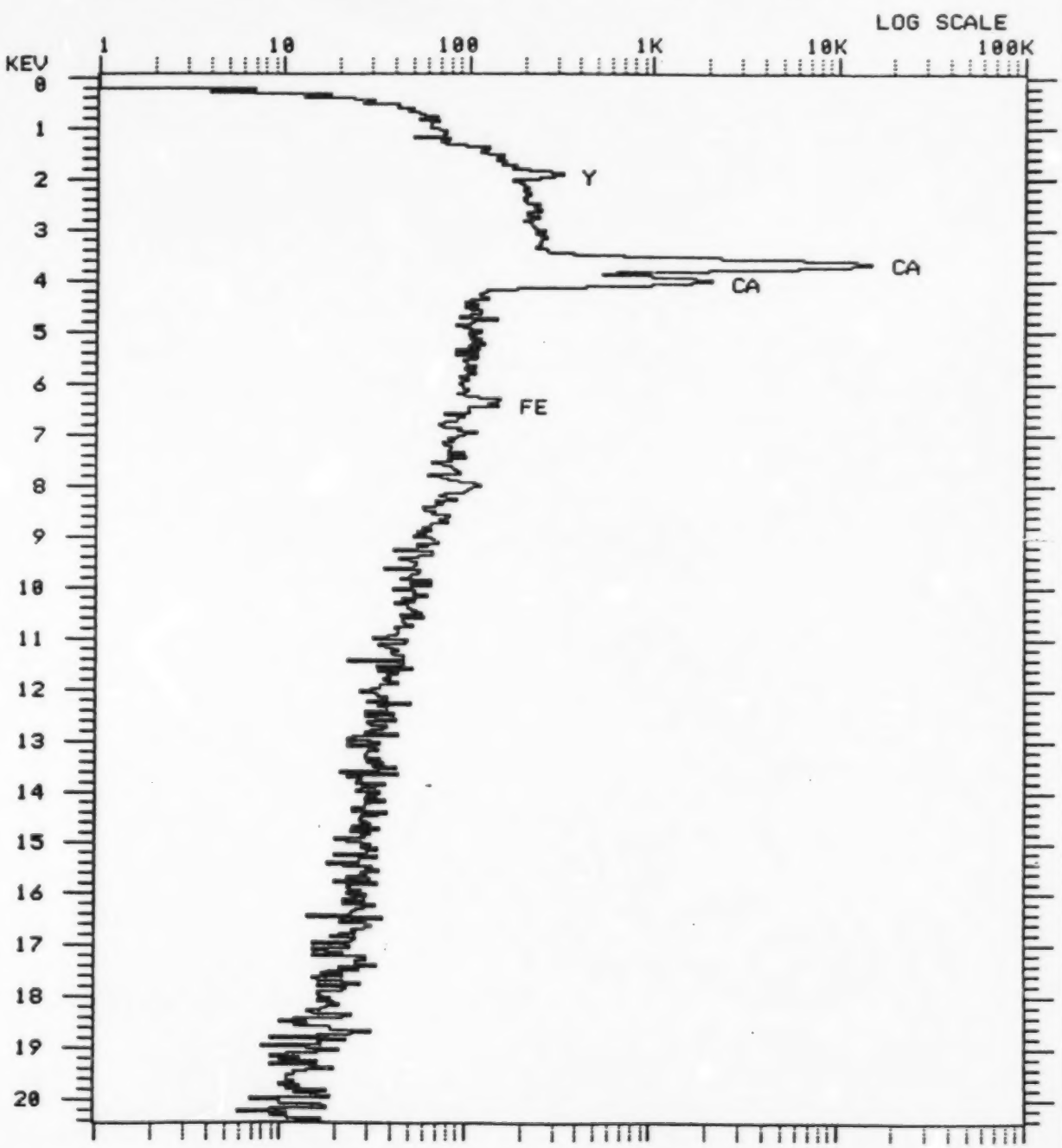

Photomicrograph 69 MP2,7
EDXA Spectral plot of fluorite exhibiting minor to trace quantities of yttrium, possibly in solid solution as yttrofluorite (Ca,Y) (F, O_2)

WD1

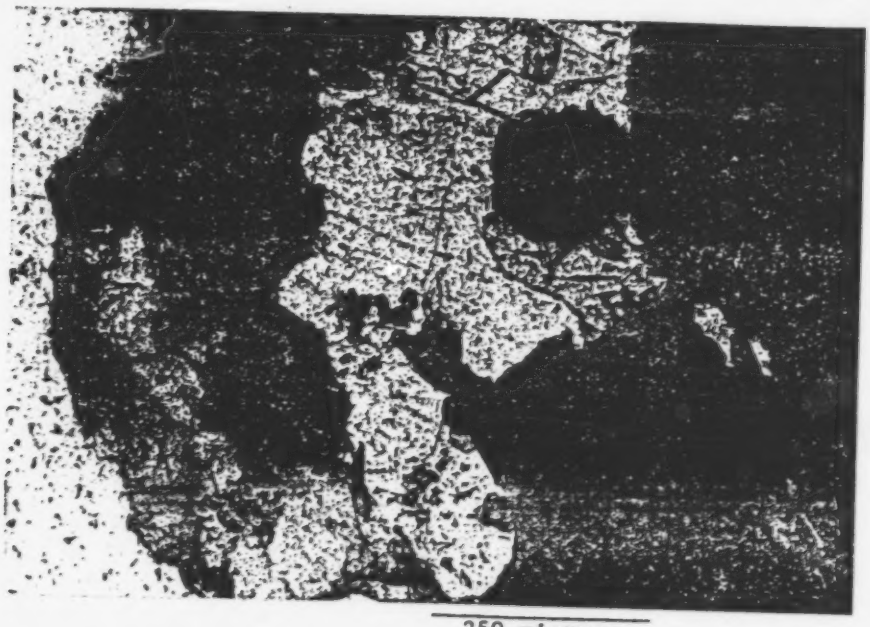

250 microns

Photomicrograph 70 - 100x T.L. MP1,6
Binary intergrowth particle of clear and mauve fluorite with radial arrays of fibrous green chlorite. Cassiterite occurred as subsequent inclusions, within both fluorite and chlorite, as individual and aggregate crystals

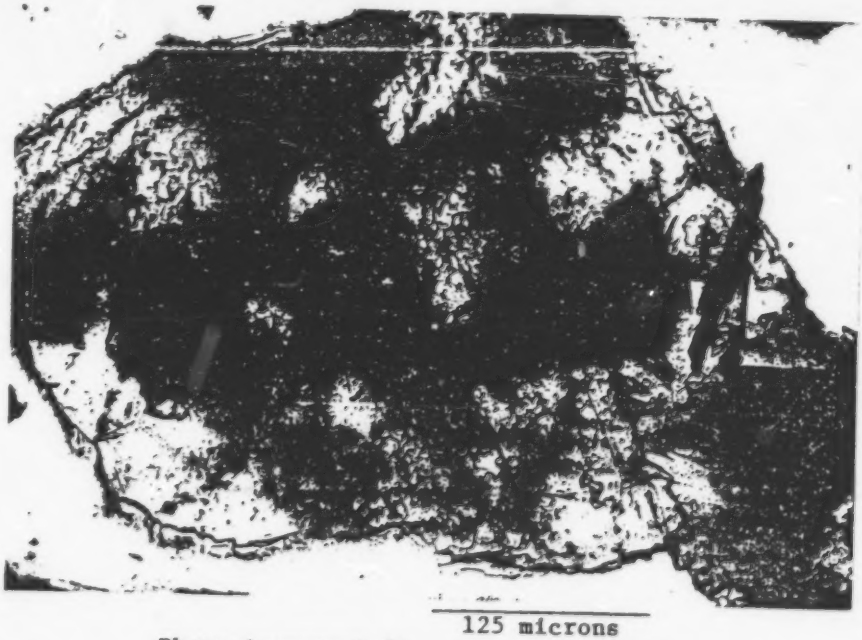

125 microns

Photomicrograph 71 - 200x T.L. MP2,7
Coarse fragment primarily comprised of clear to locally mauve, fluorite with acicular green chlorite, pale brown subequant cassiterite, subsequent rhombs of ferroan-manganese carbonates and cerium-lanthanum fluocarbonates ranging in composition from bastnaesite to synchysite
1187A

WD1

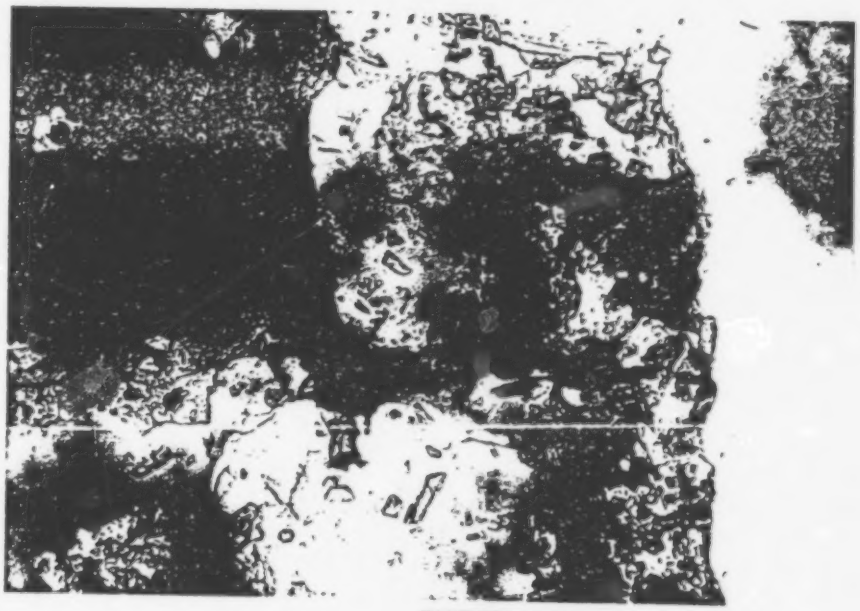

125 microns

Photomicrograph 72 - 200x T.L. MP1,6
Fluorite, clear variety, associated with opaque sphalerite, cloudy brown ferroan carbonates and fine inclusions including acicular rutile, subsequent monazite and cerium fluocarbonates of the bastnaesite-synchysite series

1187A

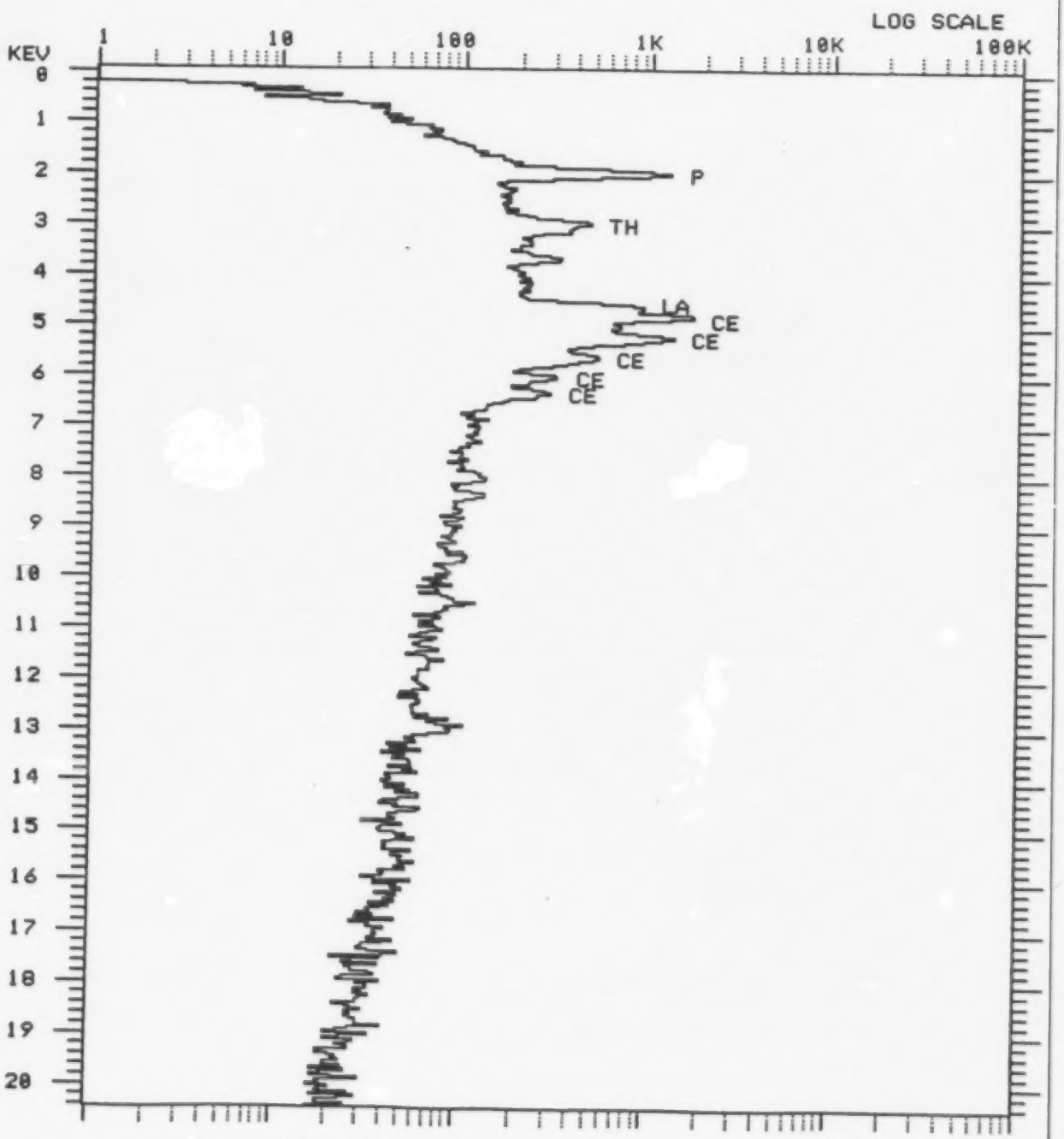

Photomicrograph 73 Flotation Concentrate
EDXA Spectral plot of monazite, cerium-lanthanum phosphate containing calcium-thorium substitution for REE, with formula (Ce,La,Th,Ca) PO_4

WD1

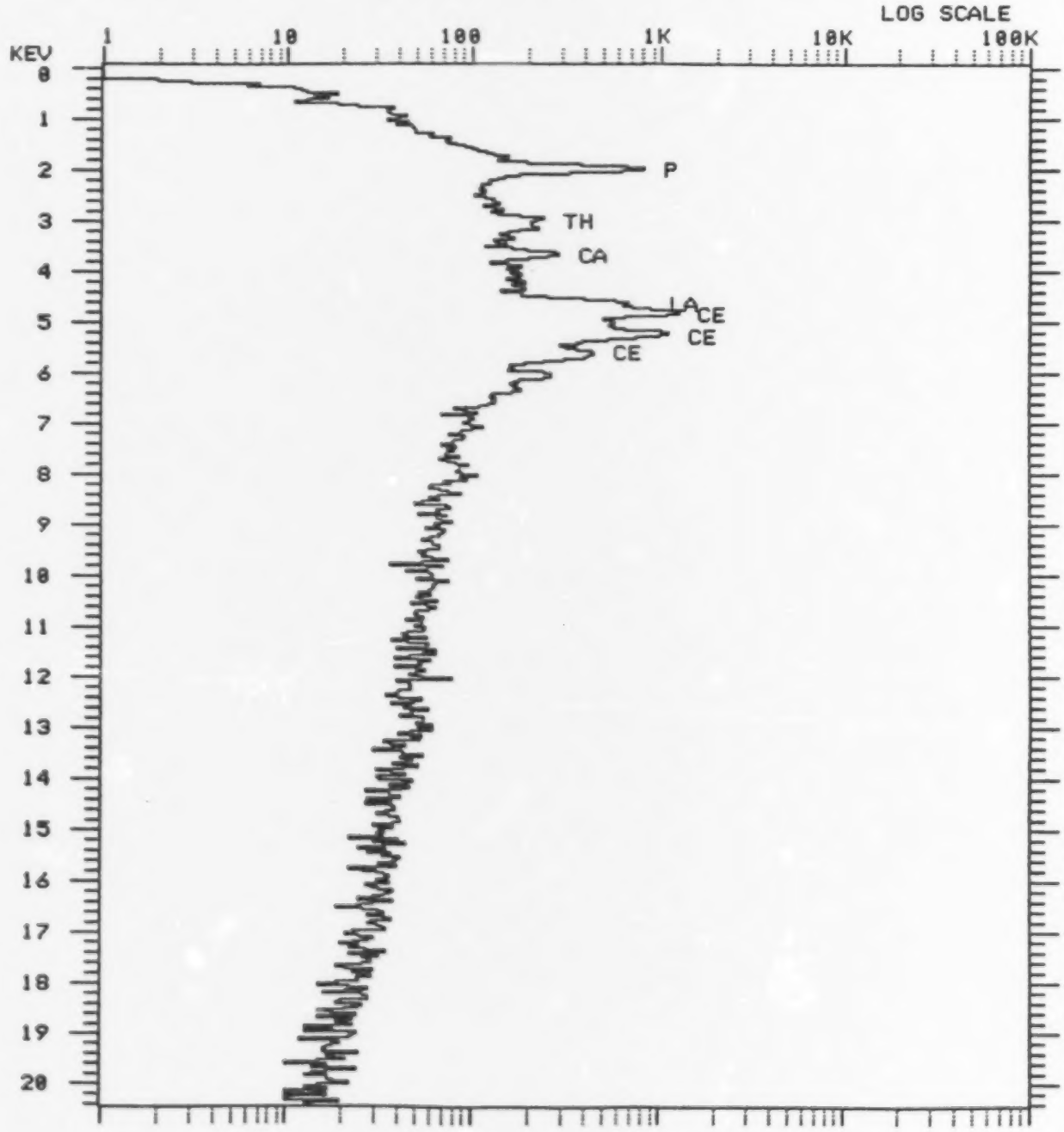

Photomicrograph 74 MP2,7
EDXA Spectral plot of monazite (Ce,La,Ca,Th) PO_4 noting variations in REE:Ca:Th ratios

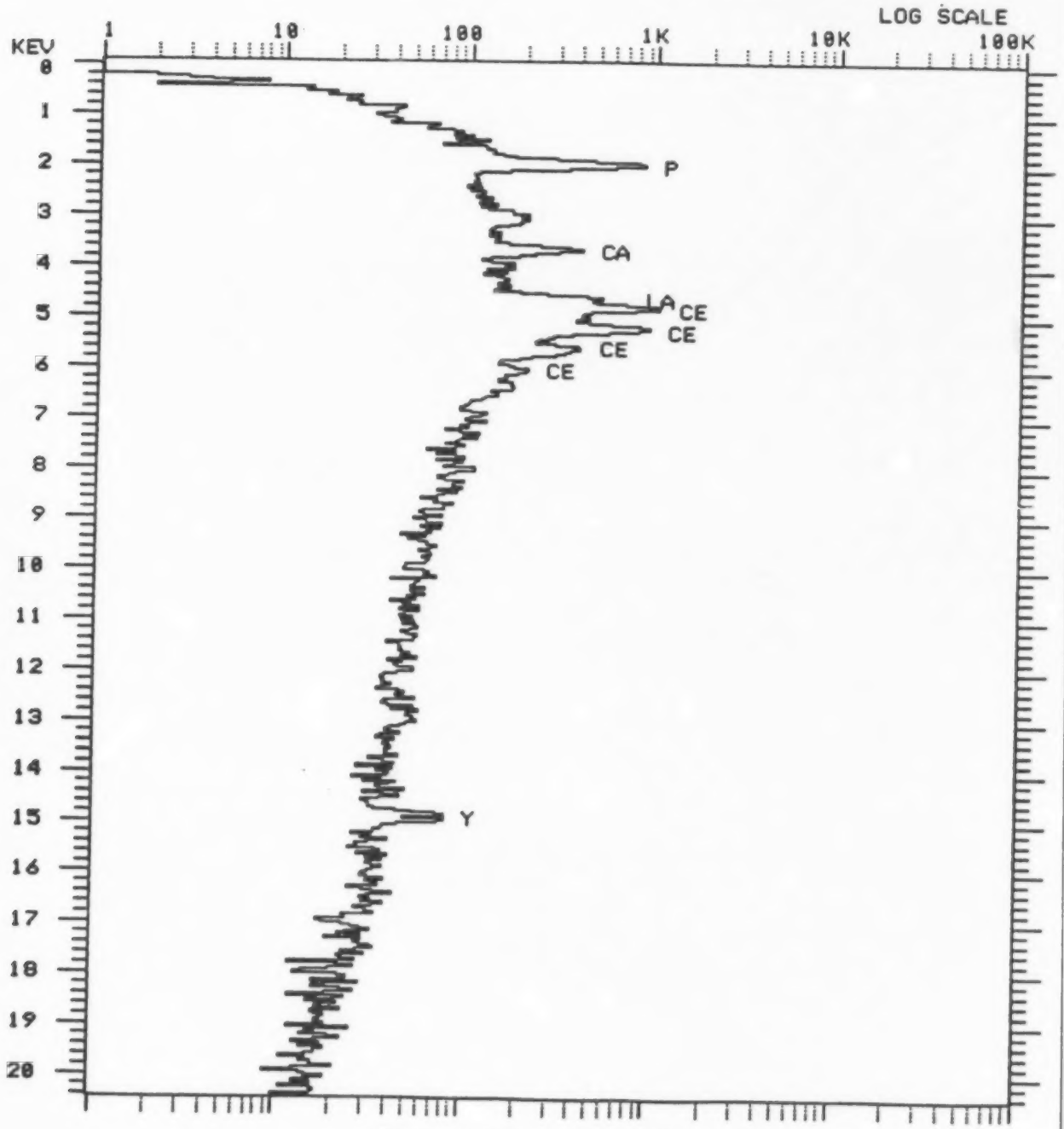

Photomicrograph 75 MP2,7
EDXA Spectra plot of monazite (Ce,La,Ca,Th) PO_4 and xenotime, Y PO_4 or a substitution series between the yttrium and REE end members

WD1

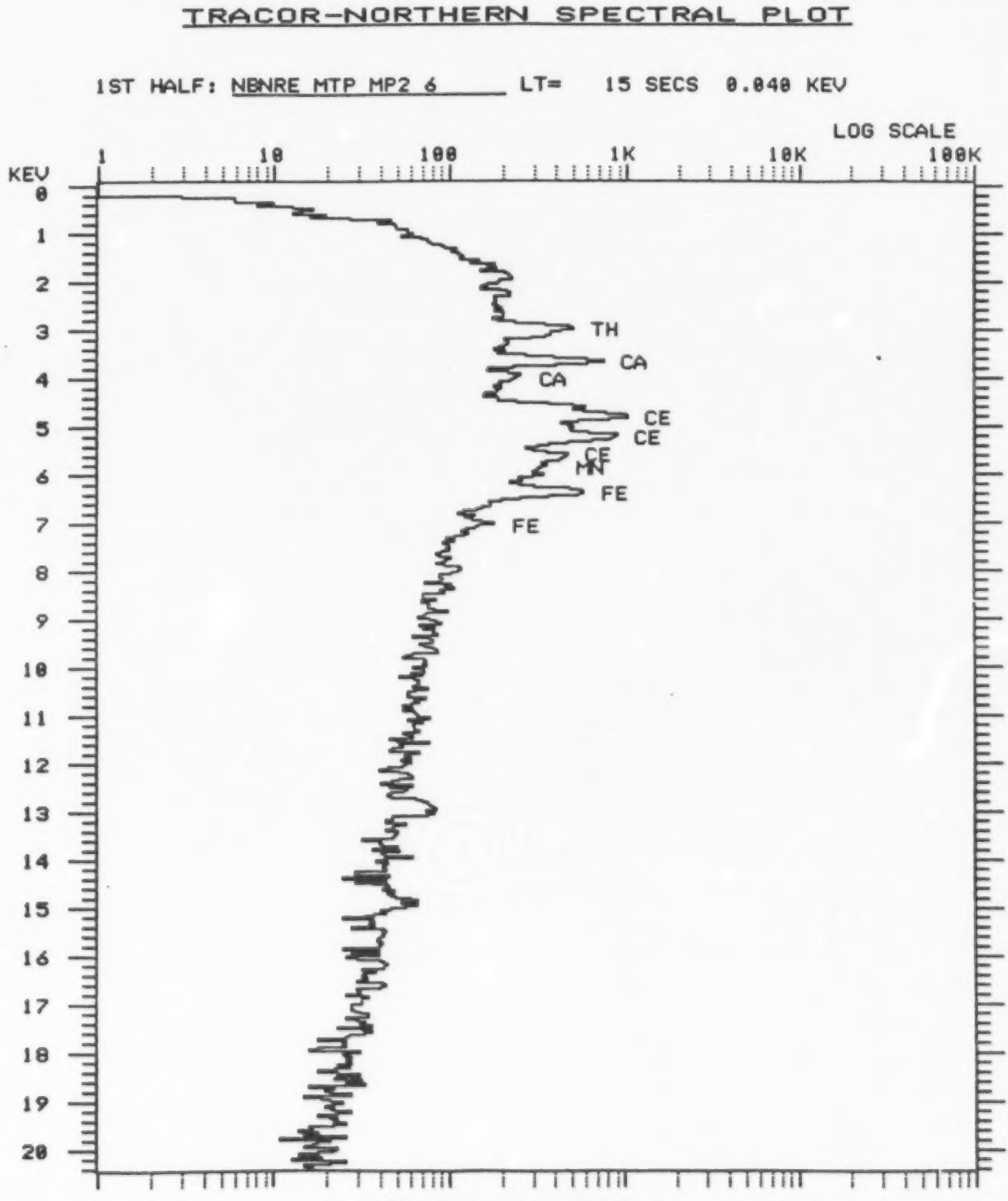

Photomicrograph 76 MP2,7
EDXA Spectral plot of thorian synchysite $(Ce,Ca,Th)(CO_3)_2F$, associated with Fe-Mn carbonates and/or oxides

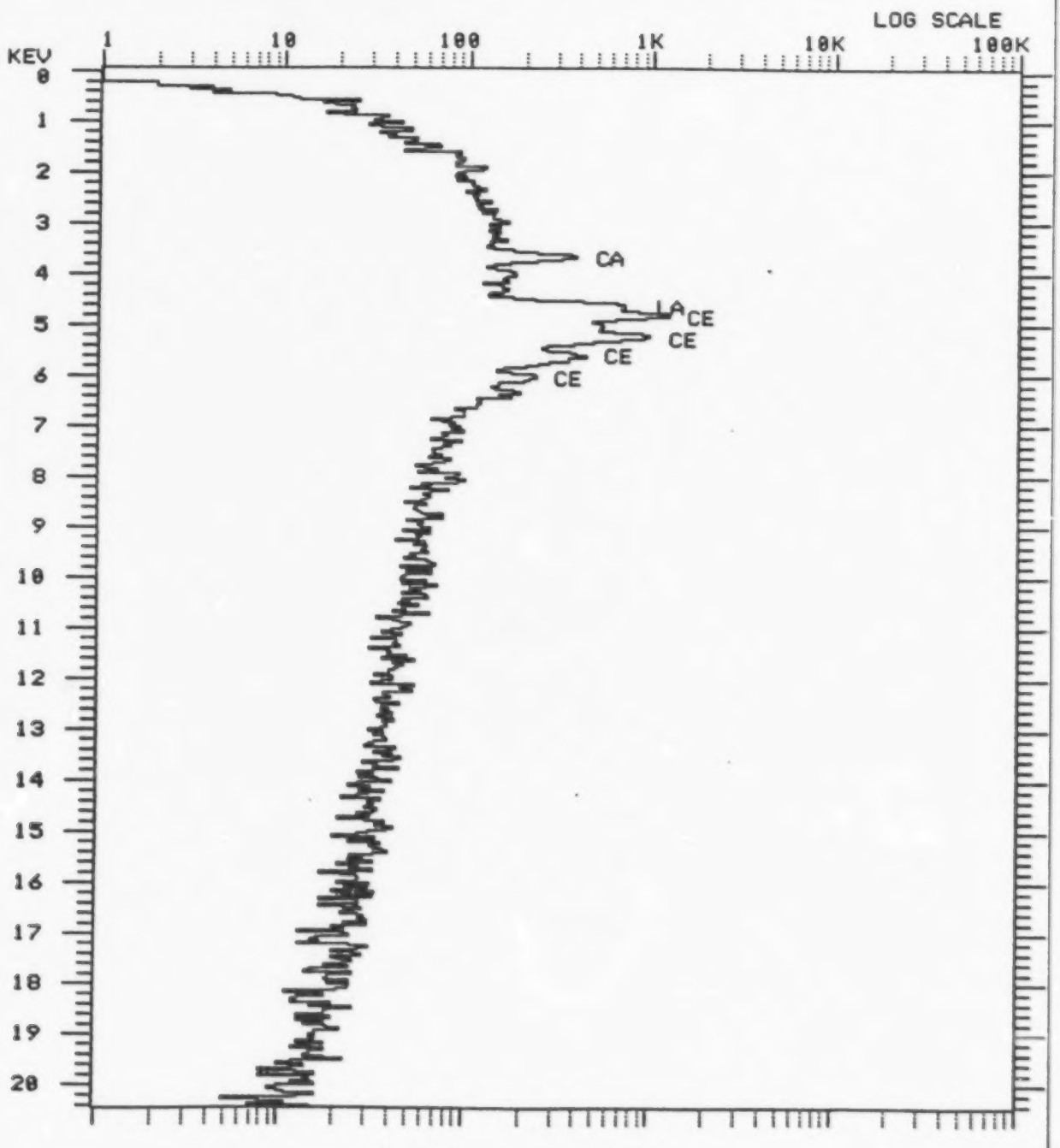

Photomicrograph 77 MP2,7
EDXA Spectral plot of Ce-La-Ca fluocarbonate, probably ranging in composition from parisite to roentgenite

WD1

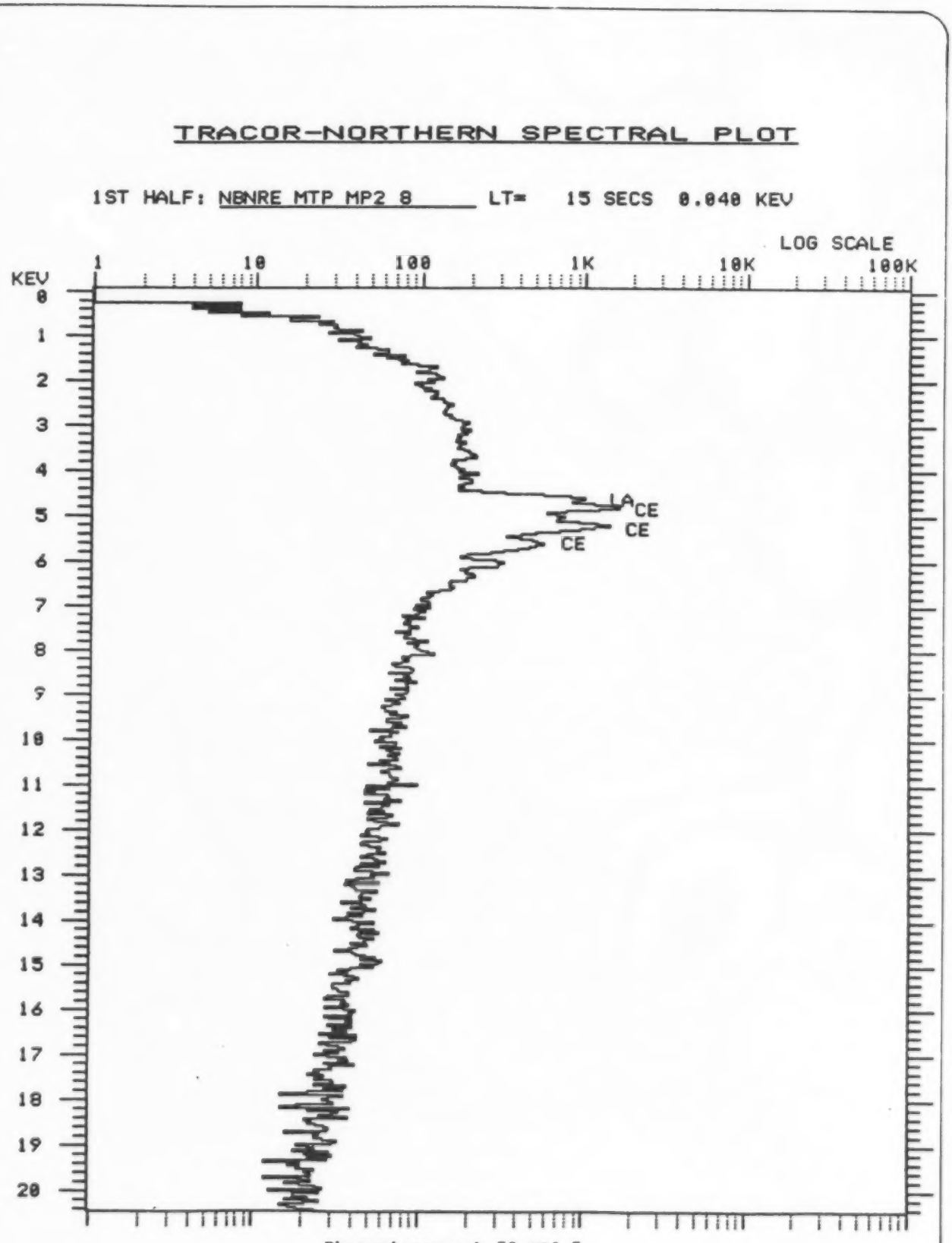

Photomicrograph 78 MP2,7
EDXA Spectral plot of Ce-La fluocarbonate, tentatively identified as bastnaesite, $(Ce,La)(CO_3)F$

WD1

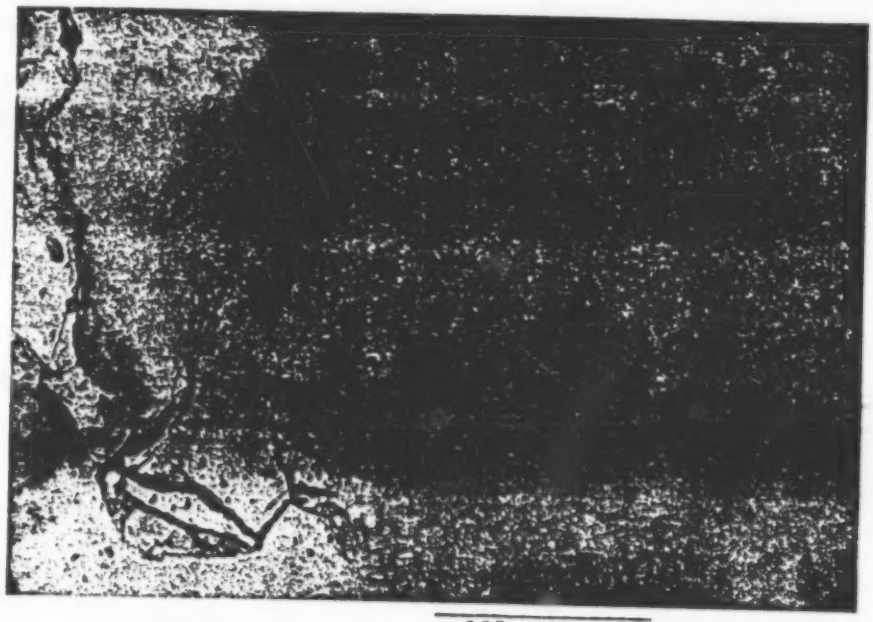

125 microns

Photomicrograph 79 - 200x T.L. MP1,6

Euhedral crystal of zircon, interstitial to quartz grains; also infilling interstices are ferroan and magnesium-calcium carbonates with minor clear fluorite

250 microns

Photomicrograph 80 - 100x T.L. MP2,7

Aggregate particle comprising hydrothermal brown biotite retrograded to chlorite and clay minerals hosted by quartz and minor carbonates

1187A

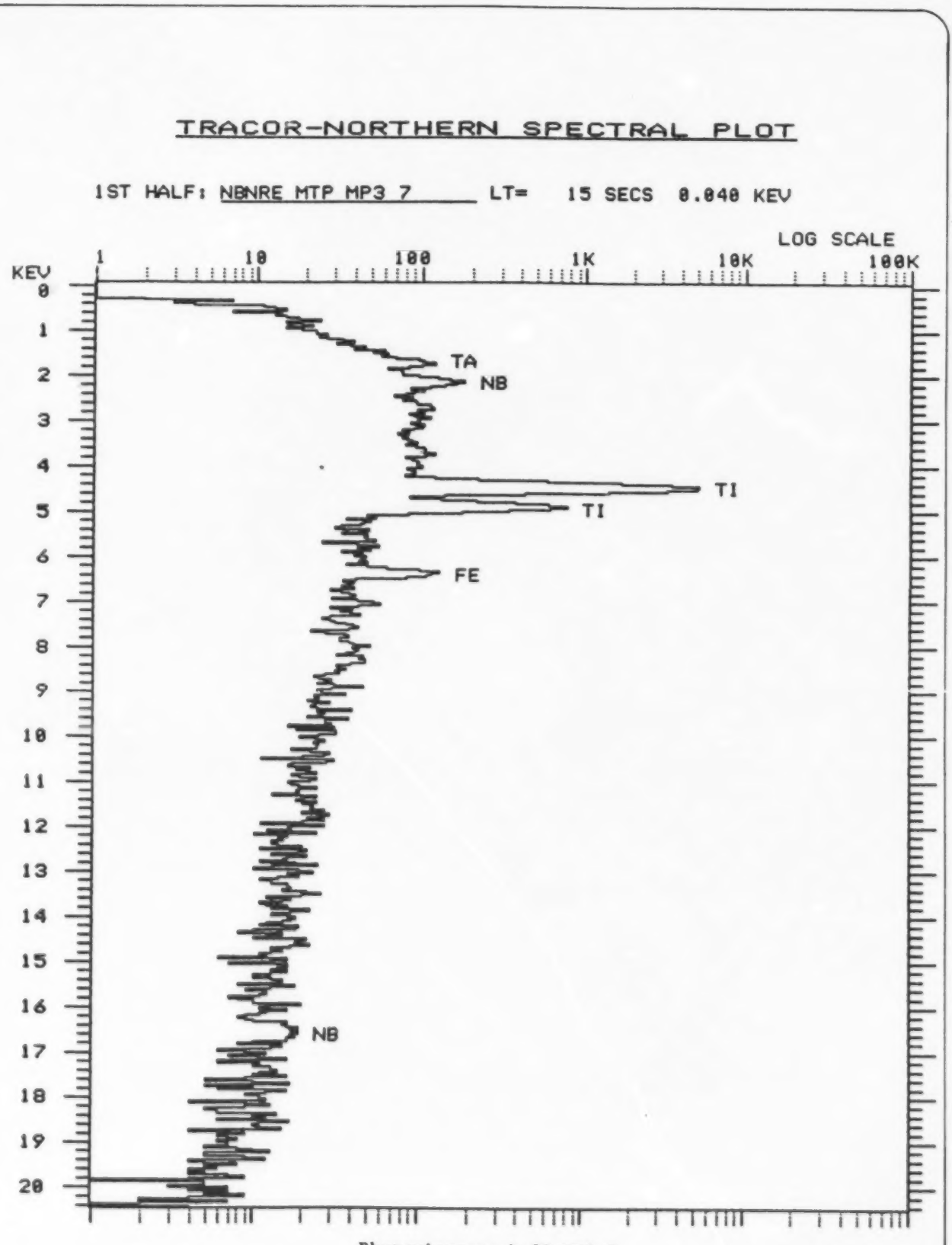

Photomicrograph 81 MP3,8
EDXA Spectral plot of rutile, TiO_2, containing minor Ta,Nb and Fe possibly microscopic intergrowths of columbite, $Fe(Nb,Ta)_2O_6$

WD1

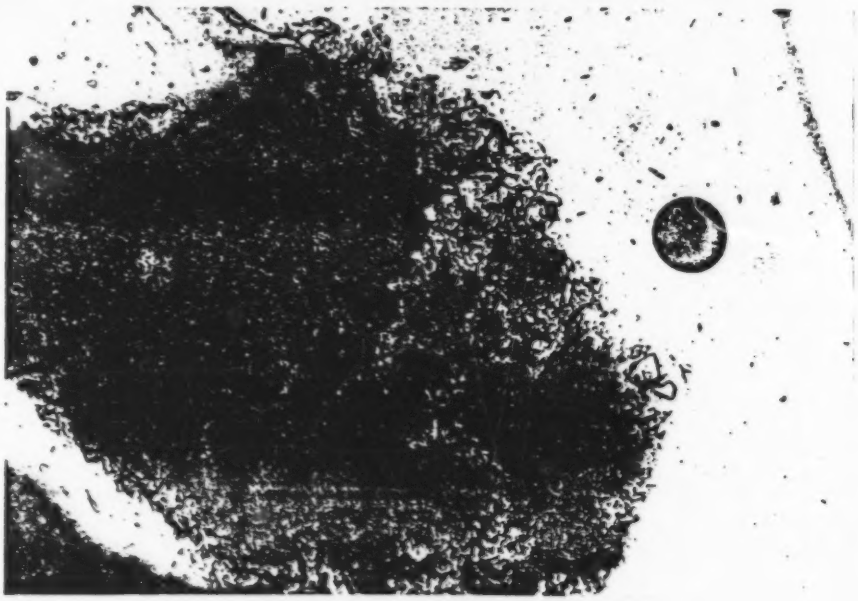

125 microns

Photomicrograph 82 - 200x T.L. MP3,8

Aggregate silicate gangue particle comprised of clear fluorite, pale brown biotite, chlorite, rutile and yellowish clays or micaceous sheet silicates

125 microns

Photomicrograph 83 - 200x T.L. MP3,8

Euhedral topaz prism partially enclosed by clear fluorite and quartz. Note abundance of fine ferroan carbonate inclusions in fluorite

1187A

WD1

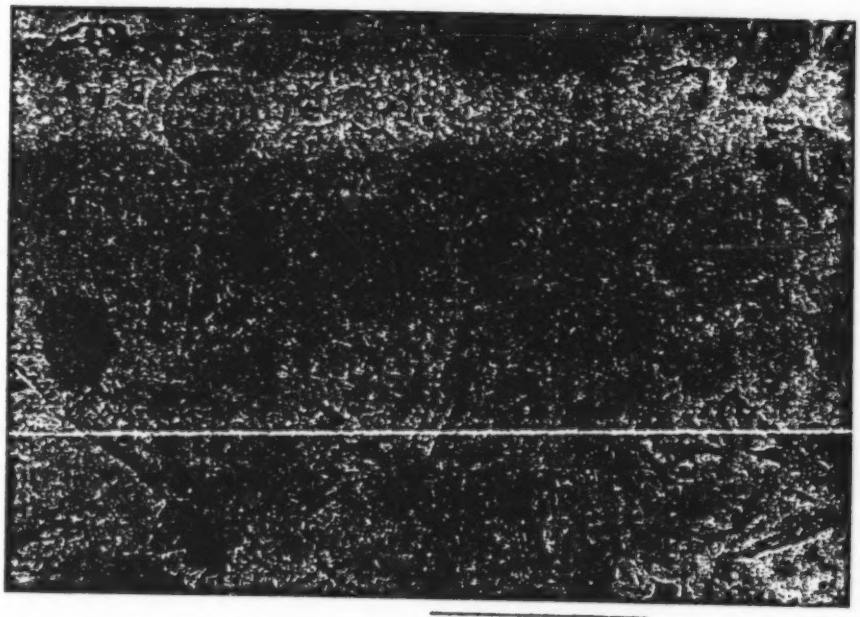

125 microns

Photomicrograph 84 - 200x T.L. MP5,10
Overview of silicate and fluorite mineral liberation exhibits quartz, clear fluorite, mauve fluorite, topaz and minor carbonates and clay minerals

1187A